



# This is to certify that the thesis entitled

# FLOW THROUGH COLLAPSIBLE VESSELS

presented by

Carol Kindermann Lyon

has been accepted towards fulfillment of the requirements for

M.S. degree in Physiology

Herry B. Devis

Major professor

Date November 3, 1978

**O**-7639

# FLOW THROUGH COLLAPSIBLE VESSELS

Ву

Carol Kindermann Lyon

# A THESIS

Submitted to
Michigan State University
in partial fulfillment of the requirements
for the degree of

MASTER OF SCIENCE

Department of Physiology

#### **ABSTRACT**

#### FLOW THROUGH COLLAPSIBLE VESSELS

Ву

### Carol Kindermann Lyon

These experiments examined the properties of flow through the classical physical model of collapsible blood vessels, the Starling resistor, and compared the results to the predictions of the mathematical "waterfall" model, and to the data generated from in vitro veins. The effects of increasing tissue pressure, outflow resistance, length, tension, stretch, and diameter were simulated. The pressure-flow relationships consisted of: first, an initial rising phase of high resistance at low flow rates; second, a plateau phase at moderate flow rates; and third, a late rising phase at high flow rates. Self-excited oscillations of the collapsible tubing were quantified, as was their effect of increasing the resistance of second and third phase pressure-flow relationships. The waterfall model predicts neither first phase, nor third phase pressure-flow relationships of the model or of in vitro veins. Simulation of the microcirculation using high viscosity fluids indicated a trend toward closer agreement with the waterfall model.

#### ACKNOWLEDGEMENTS

It has been a privilege and a pleasure to work with my research committee. I am very grateful to my committee chairman, Dr. J. B. Scott, for his encouragement and support throughout my graduate program. Dr. C. Y. Wang, my research advisor, has always been available for consultation and advice. I am indebted to him for his contribution of the three-dimensional pressure-flow surfaces. Dr. D. Anderson lent a sense of realism that was much appreciated. It was an honor to be able to work with this committee.

I would also like to acknowledge the invaluable support that I have received from my husband, Jim, my children, Stephen, Therese, Mark, and Paul, and from my colleagues, neighbors, former students, and many other friends.

# TABLE OF CONTENTS

		Page
LIST	OF TABLES	v
LIST	OF FIGURES	vi
I.	INTRODUCTION	1
II.	LITERATURE REVIEW	5
	Characteristics of Flow through Collapsible Blood vessels  Theories of Flow through Collapsible Blood Vessels Collapse of the Inferior Vena Cava	5 9 9 15
III.	REVIEW OF MODELING OF FLOW THROUGH COLLAPSIBLE VESSELS	20
	Physical Modeling of Pressure-flow Relationships Oscillatory Phenomena	20 28 30 31 33
IV.	STATEMENT OF OBJECTIVES	36
٧.	METHODS	37
VI.	RESULTS	45
	General Characteristics	45 47 48 50 50 52

TABLE OF	CONTENTScontinued	Page
	The Effect of Viscosity (0.5 Stokes)	58 60
	Effects of Diameter and Tubing Composition	62
	Pressure-flow Relationships of Veins	65
VII. D	ISCUSSION	69
	Comparison of Models	69
	The Waterfall Model	70
	The Starling Resistor Model	73
	General Characteristics	75
	The First Phase: The Early Rising Phase	75
	The Second Phase: The Plateau Phase	75
	The Third Phase: The Late Rising Phase The Effect of Outflow Resistance: Physiological	77
	Implications	80
	Physiological Implications	82
	Hysteresis	84
	The Effects of Viscosity: Physiological Implications	85
	In Vitro Venous Pressure-flow Relationships	88
VIII. S	UMMARY AND CONCLUSIONS	91
BIBLIOGR	АРНҮ	93
APPENDIX	SIMULTANEOUS MEASUREMENT OF REGIONAL INTRAMYOCARDIAL	
AI I ENDIA	PRESSURE AND BLOOD FLOW	103
	Introduction	103
	Intramyocardial Pressure Measurements	104
	Open Method	105
	Closed Method	106
	Perfusion Method	107
	Catheter-tip Micro-transducer Method	108
	Myocardial Blood Flow	109
	Methods	112
	Results and Discussion	116

# LIST OF TABLES

<b>TA</b> BLI		Page
1.	The Effect of P <sub>e</sub> -P <sub>o</sub> and Flow on Frequency and Pressure Amplitude of Oscillations	47
2.	Oscillatory Flow When P <sub>e</sub> -P <sub>o</sub> = 0	48
	The Effect of Outflow Resistance on Frequency and Pressure Amplitude of Oscillations	48
4.	The Effect of Length of Vessel on Frequency and Pressure Amplitude of Oscillations	52
5.	The Effect of Longitudinal Pre-stress on Frequency and Pressure Amplitude of Oscillations	54
6.	The Effect of Stretch on Resistance	55
7.	Analysis of Variance: The Effect of Stretch on Resistance.	57
8.	An Example of the Effect of Stretch on Frequency and Pressure Amplitude of Oscillations	57
9.	The Effect of Viscosity on Frequency and Pressure Amplitude of Oscillations	60
10.	Regional Intramyocardial Blood Flow and Simultaneously Recorded Intramyocardial Pressure	121

# LIST OF FIGURES

FIGURE	
l. Characterization of the pressure-flow relationship of the Starling resistor when $P_{\mathbf{e}}$ is held constant	25
2. Starling resistor model for perfusion with water	38
<ol> <li>Pressure-flow relationships of 7.5 cm Penrose tubing held at manufactured length during water perfusion</li> </ol>	46
4. The effect of outflow resistance on the pressure-flow relationships of Penrose tubing when $P_e-P_o=10$ mm Hg	49
5. The effect of length on the pressure-flow relationships of Penrose tubing when $P_e-P_o=16$ mm Hg	51
6. The effect of pre-stress on the pressure-flow relation- ships of Penrose tubing when $P_e-P_o=16$ mm Hg	53
7. The effect of stretch on the pressure-flow relationships of Penrose tubing when $P_e-P_o=16$ mm Hg	56
8. Pressure-flow relationships of 7.5 cm Penrose tubing during perfusion with 0.5 stokes fluid	59
9. Pressure-flow relationships of 7.5 cm tubing during perfusion with 10 stokes fluid	61
10. The effect of diameter: pressure-flow relationships of 0.635 cm diameter, 3.25 cm length Penrose tubing	63
11. Pressure-flow relationships of dialysis tubing, 1.5 cm diameter, 7.5 cm length	64
<ul><li>12. Pressure-flow relationships of the equine jugular vein,</li><li>7.5 cm length, during perfusion with equine blood</li></ul>	66
13. Pressure-flow relationships of the equine cephalic vein, 3.25 cm length, perfused with Ringer's bicarbonate solution	68

LIST OF FIGUREScontinued	Page
14. Three-dimensional surface of the pressure-flow relation- ships predicted by the mathematical waterfall model	71
15. Three-dimensional surface of the pressure-flow relation-ships of Penrose tubing	72
16. Simultaneously recorded intramyocardial pressure and regional blood flow of the maximally dilated left anterior descending coronary vascular bed during diastolic arrest	120

#### I. INTRODUCTION

This work investigates the phenomenon of vascular collapse which may occur when fluid pressure at some point within a vessel is exceeded by pressure external to that vessel. For blood vessels, external pressure includes all sources of tissue pressure, as defined by Guyton (1971): liquid, gel, and solid. The difference between intraluminal pressure and extraluminal pressure is defined as transmural pressure. When extraluminal pressure exceeds intraluminal pressure, transmural pressure is negative. Negative transmural pressure can cause a blood vessel to undergo partial to complete collapse, and consequently can alter the pressure-flow relationships of that vessel.

Examples of blood vessels that are normally subjected to collapse are: the cutaneous veins (Bates, 1974), myocardial blood vessels (Downey and Kirk, 1975) and those of skeletal muscle (Gray et al., 1967) and the liver (Mitzner, 1974), the placental circulation (Bissonette and Farrell, 1973), the renal venous system (Swann et al., 1952), interabdominal veins (Guyton and Adkins, 1954), and the microcirculation of the lung (Maloney et al., 1968). Pathophysiological collapse of blood vessels also occurs. As examples, cerebral capillaries have been shown to collapse when intracranial pressure is suddenly increased (Hekmatpanah, 1970), and the abdominal vena cava is known to collapse when abdominal pressure is increased by ascites (Vix and Payne, 1972).

Occasionally, external interventions are used to induce vascular collapse. Pressurized antigravity suits are used to increase tissue pressure of the extremities and induce collapse of the dependent veins and thereby prevent pooling of blood in the vessels of the extremities (Guyton, 1976). Pneumatic cuffs are used to collapse arteries to prevent hemorrhage during orthopedic surgery (Guyton, 1976), and to measure blood pressure by the production of the Korotkoff sounds heard with the stethoscope (Brooks, 1916).

The pressure-flow relationships of collapsible vessels have been modeled by use of a physical model that utilizes a "Starling resistor", and a mathematical "waterfall model". The physical model takes its name from the fact that the noted physiologist, E. H. Starling (Knowlton and Starling, 1912) devised a freely collapsible tube traversing a chamber in which pressure could be controlled, for use in his now famous heart-lung preparation. Vessels which are subject to passive collapse, whether experimental or physiological, have come to be known as "Starling resistors". Holt (1941) utilized such a physical model in an effort to understand and quantify the non-linear pressure-flow relationships of veins. Canine jugular veins and Penrose tubing were tested in the pressure chamber. Holt's data demonstrated that whenever the vein was partially collapsed, the relationship between flow and apparent driving pressure (inflow pressure minus outflow pressure,  $P_i - P_0$ ) became independent. Interestingly, Holt noted oscillations of these vessels when they were in a partially collapsed state. Many investigators have used a similar physical model to demonstrate the hemodynamics of

collapsible blood vessels (Swann <u>et al</u>., 1952; Brecher, 1952; Rodbard and Saiki, 1953; Katz <u>et al</u>., 1969; Fung and Sobin, 1973).

The "waterfall model" was described in simple quantitative terms by Permutt et al. (1962) and Lopez-Muniz et al. (1968). This model has been widely quoted to explain the pressure-flow relationships of both large and small blood vessels (Nakhjavan, 1966; Scharf et al., 1971; Downey and Kirk, 1974, 1975; Green, 1975; Mitzner, 1974). Just as flow over a waterfall is independent on the height of the falls, Permutt et al. (1962) proposed that flow through a blood vessel that is partially collapsed by tissue pressure is independent of outflow pressure. Other more sophisticated mathematical models of flow through collapsible vessels have been proposed (Kresch and Noordegraaf, 1969; Katz et al., 1969; Mahrenholtz, 1974; Oates, 1975a, 1975b), but the non-conventional cross-sectional geometry of the vessels and the non-linearity of fluid behavior present major theoretical difficulties. Therefore, none of the presently available mathematical models is sophisticated enough to encompass all of the phenomena of flow through collapsible vessels.

Recently, a revitalized interest in physical modeling of the dynamics of flow through collapsible vessels has been taken by biomedical engineers and physicists (Conrad, 1969; Katz et al., 1969; and Moreno et al., 1969). The families of pressure-flow relationships published by these investigators appeared to be radically different from any previously published curves. A most obvious difference was the presence of a "negative resistance" region of their curves where it appeared that a decrease in driving pressure was accompanied by increased flow.

The differences in apparatus, methods, experimental and extraneous variables has made comparison of published data extremely difficult. The continuing need for a reasonably simple expression describing pressure-flow relationships of collapsible vessels was answered in part by Brower and Noordergraaf (1973), who analyzed previous data for collapsible vessels, and made theoretical predictions for the flow ranges of zero to 14 cc/sec, conforming to the graphic form of  $P_i$ - $P_o$  as a function of flow (Q) and the difference between pressure external to the vessel and outflow pressure ( $P_e$ - $P_o$ ).

The pressure-flow relationships of the classical physical model of a collapsible vessel, the Penrose tubing Starling resistor, remain to be thoroughly quantified experimentally. Pressure-flow data for high flow rates, high viscosity flow, and comparable data for living vessels is not available, and consequently the appropriateness of the model is not known. An additional difficulty is the fact that the predictions of the "waterfall model" do not appear to be in agreement with the available data from physical modeling, especially in the low flow ranges. The present investigation studies in depth the properties of the Starling resistor, quantifies data for high and low Reynolds numbers, and compares these models to the data generated from experiments using in vitro equine jugular and cephalic veins.

#### II. LITERATURE REVIEW

# Characteristics of Flow through Collapsible Blood Vessels

In 1941, J. P. Holt used a Starling resistor\* model to demonstrate the non-linear pressure-flow relationships of collapsible veins. In doing so, he introduced into vascular research the use of a physical model to circumvent many of the experimental difficulties inherent to in vivo research. His prototype model has been used by many investigators (Brecher, 1952; Swann et al., 1952; Rodbard, 1955; Doppman et al., 1966; Katz et al., 1968; Fung and Sobin, 1972) for quantification of pressure-flow relationships of collapsible vessels.

Resort to the use of physical models to demonstrate vascular behavior underscores the difficulties inherent in the research of collapsible vessels <u>in vivo</u>. When vessels collapse to non-circular cross-section, they present paradoxical pressure-flow relationships: calculated resistance may fall greatly as flow increases (Permutt <u>et al.</u>, 1962); a rise in outflow resistance may be associated with a decrease in total calculated resistance (Rodbard, 1955); and absence of flow may exist in the presence of a measured inflow-outflow pressure difference (Nichol <u>et al.</u>, 1951).

Starling (Knowlton and Starling, 1912) used a collapsible tube encased within an airtight compartment in his heart-lung preparation.

Collapse of blood vessels is both common and normal. An example of vascular collapse can be seen when the hands or legs are elevated above the level of the heart. The visible cutaneous veins can be seen to flatten. In fact, if the jugular veins of the neck do not collapse when an indivudual is in the erect position, this is indicative of heart failure (Bates, 1974). Other examples of blood vessels that are normally subjected to collapse are: coronary vessels (Downey and Kirk, 1975), vessels of the skeletal muscle (Gray et al., 1967), and liver (Mitzner, 1974), the placental circulation (Bissonette and Farrell, 1973), the renal venous system (Swann et al., 1952), inter-abdominal veins (Norhagen, 1963) and the microvasculature of the lung (Maloney et al., 1968).

Collapse of blood vessels is not an all or none process. The cross-section of a collapsed vessel may be elliptical, or it may be flattened so that opposite sides are touching. The term "collapse" refers to any intermediate stage between circular cross-section and total closure.

Vascular collapse occurs because the cross-sectional shape of blood vessels with thin non-self supporting walls is markedly influenced by extravascular tissue pressure. The difference between intravascular blood pressure and extravascular tissue pressure is defined as transmural pressure. Vascular collapse can occur whenever the transmural pressure is negative.

Extravascular, or total tissue pressure, is influenced by the quantity of fluid and gel within the extravascular compartment, the

physical characteristics of the surrounding tissue, and location within the body. Increases in the fluid and gel content of the interstitial and intercellular compartments may be caused by an electrolyte imbalance, an increase in microvascular pressure, an increase in microvascular permeability, a decrease in plasma colloid osmotic pressure, or decreased efflux via the lymphatic system (Haddy et al., 1976).

The tension and visco-elastic properties of the tissue fibers surrounding the blood vessels influence the compliance of the extravascular compartment. The lower the tissue compliance, the greater the change in tissue pressure that will result from a given increase of extravascular volume. Some organs are enclosed within relatively non-compliant structures. For example, the brain is enclosed within the rigid cranium, and the kidney is enclosed within a fibrous encapsulating membrane. Tissue pressures within these organs are relatively sensitive to extravascular volume changes. Active contraction of muscle within the extravascular compartment also will decrease tissue compliance.

The level of tissue pressure varies from organ to organ. It is negative within the thorax and positive in the kidney. In some organs, the lungs and the heart for example, the level of tissue pressure changes cyclically. However, there is no general consensus regarding the magnitude of "normal" tissue pressure. The controversy arises largely because of differences in measurement techniques, but it is also related to the problem of defining "tissue pressure".

Intra-tissue "balloon" type methods (Gregg and Eckstein, 1941; Kjellmer, 1964; Kirk and Honig, 1964a) and needle or capillary pipette methods (Hinshaw et al., 1959, 1960; Gilmore, 1964; Gottschalk, 1952) measured pressures which were predominantly positive, and this generally was accepted as the correct value prior to 1960. However, Guyton (1963a) measured negative interstitial fluid pressure using implanted capsules. Other investigators, using cotton wick techniques that depend on fluid equillibration (Scholander et al., 1968; Stromberg and Wiederhielm, 1970; Stromme et al., 1969) have obtained pressures similar to those that Guyton measures.

The implanted capsule and the cotton wick techniques have been criticized (McDonald, 1968; Stromberg and Wiederhielm, 1970; Snashall et al., 1971) on the basis that osmotic forces exerted by proteins within the interstitial gel create artifactually negative pressures within the capsule and the cotton wick. Guyton (1971) has countered that the capsule method measures only true interstitial fluid pressure, but that the tissue balloon and needle techniques measure total tissue pressure, which is composed of the sum of "interstitial fluid pressure" and "solid tissue pressure". This difference is very important. Transmural pressures are affected by "total tissue pressure" since both solid and fluid phases are in direct physical contact with vascular walls.

In addition to extravascular tissue pressure, the other major determinant of transmural pressure is the lateral blood pressure exerted by the blood upon the walls of the blood vessels. Total blood volume, the pumping action of the heart, and vascular compliance and radius determine the blood pressure at any point in the vascular tree.

Within the capillaries, the hydrostatic pressure (blood pressure) depends on capillary volume which in turn depends on arterial pressure, venous pressure, and pre-capillary and post-capillary resistances. An increase in either arterial or venous pressure will result in an increase in capillary volume and hence pressure. An increase in post-capillary resistance will increase capillary volume and hence pressure; whereas, an increase in pre-capillary resistance will have the opposite effect. Just as tissue pressure varies from tissue to tissue, so too does capillary hydrostatic pressure (Berne and Levy, 1972). A final factor influencing lateral pressure of blood within large vessels is the velocity of blood flow. Blood flowing through a vessel of larger radius past a segment of smaller radius must accelerate to a higher velocity in the narrowed segment. By the Bernoulli effect, the increased velocity of blood flowing through the narrowed segment is accompanied by a decreased lateral pressure (White, 1974).

From the foregoing discussion, it can be seen that there are many factors which can produce a negative transmural pressure, either by increasing extramural tissue pressure or by decreasing intramural blood pressure. Whenever transmural pressure is negative, collapse of thin walled blood vessels becomes a possibility.

# Theories of Flow Through Collapsible Blood Vessels

# Collapse of the Inferior Vena Cava

Collapse of the inferior vena cava associated with respiratory activity has been the subject of a great deal of physiological research.

Early researchers of the venous system generally believed that negative intrathoracic pressure was an important factor in returning blood to the heart (Volkman, 1950; Donders, 1859; Ledderhose, 1906). Donders (1859) treated flow through the veins as if they were rigid tubes; he expected that flow should be proportional to the pressure gradient. He promoted the belief that the greater the inspiratory effort, the greater the blood flow into the thoracic cavity would be. Donders had completely ignored the fact that veins are non-self supporting structures that collapse when a critical transmural pressure is reached. Collapse of a vein greatly increases its resistance to flow, so that when collapse occurs, a non-linear pressure flow relationship results.

The extravascular pressure relationships along the length of the inferior vena cava subject it to conditions favoring collapse. When a vein transverses a chamber of higher pressure to enter one of lower pressure, collapse may occur at the downstream end of the higher pressure chamber. Tissue pressure within the abdominal cavity fluctuates with respiratory activity and is generally increased by descent of the diaphragm during respiration (Moreno et al., 1967; Katz, 1968). Pressure within the thorax is normally sub-atmospheric. With quiet breathing, pressure varies from about -8 mm Hg during inspiration to -4 mm Hg during expiration. Blood pressure of the intrathoracic inferior vena cava is approximately atmospheric. Therefore, a positive transmural pressure within the thorax holds the thoracic inferior vena cava open. However, the higher tissue pressure of the abdomen subjects the inferior vena cava to sub-diaphragmatic collapse.

There is ample evidence of sub-diaphragmatic collapse of the inferior vena cava. The collapse has been visualized radiographically during normal respiration (Katz, 1968; Norhagen, 1963; Nordenstrom and Norhagen, 1965), and during conditions of increased abdominal pressure (Ranniger and Switz, 1965; Vix and Payne, 1972; Doppman et al., 1966). Pressures recorded from a pressure catheter being pulled across the diaphragmatic region of the inferior vena cava demonstrate the drop in pressure that occurs across a collapsed vascular segment (Guyton and Adkins, 1954; Duomarco and Rimini, 1954; Lawrence and Myerson, 1973). Finally, catheter tip flow velocity meters have recorded flow acceleration during inspiration when collapse is most likely to occur (Wexler et al., 1968; Yokota and Kreuzer, 1973).

When the veins entering the thorax collapse, flow becomes independent of the pressure gradient from the peripheral veins to the right atrium, and peripheral venous pressure is independent of pressure in the right atrium. Under these circumstances, decreasing right atrial pressure to lower levels has no effect on extrathoracic venous pressures (Holt, 1941). In experiments when thoracic pressure was decreased by breathing air under negative pressure, venous return remained essentially constant, even though the usual pressure drop from peripheral veins to right atrium was increased many fold (Holt, 1944; Lenfant and Howell, 1960).

Duomarco <u>et al</u>. (1944) supported the concept of Holt (1944) that venous collapse concommitant to negative intra-thoracic pressures would prevent an inspiratory increase in venous return. Dumarco <u>et al</u>. (1944)

measured pressures in the canine inferior vena cava and the jugular-vena cava venous system and they noted a drop in pressure wherever a vein entered the thorax. They considered the cause of this pressure drop to be collapse of the venous segment. This pressure gradient was likened to the hydraulic gradient of a waterfall, where upper level, lower level, and flow constitute mutually independent factors: the downstream level has no effect on flow falling over the falls. This analogy was later presented in mathematical form by Permutt et al. (1962) and has become known as the "waterfall model" of flow through collapsible vessels.

In the years following Holt's original experiment (1941), further studies have led to conflicting views concerning the effect of respiration on venous return. Contrary to the predictions of Holt (1941) and Dumarco et al. (1944), many studies report a phasic increase in blood flow into the heart during inspiration (Yokota and Kreuzer, 1973; Tafur and Guntheroth, 1966; Morgan et al., 1966; Moreno et al., 1967; Katz, 1968). But it is generally conceded that a decrease in pressure within the thorax, below the level at which the veins entering the chest collapse, can cause no further increase in the rate of venous return (Holt, 1941, 1944; Brecher, 1956; Guyton and Adkins, 1954; Guyton, 1962). And it is also well documented that an increase in thoracic pressure to the point that right atrial pressure exceeds atmospheric pressure will cause a decrease in the rate of venous return to the heart (Holt, 1944; Brecher and Mixter, 1954; Brecher, 1956; Guyton, 1963b). However, the effects of normal respiratory pressure fluctuations on

inferior vena cava pressure flow relationships remain controversial.

Brecher (1952, 1956; Brecher et al., 1952) claims that normal respiration augments venous return. Measurements of flow in the superior and the thoracic inferior vena cava in the closed-chest dog, using the bristle flowmeter, showed that the rate of flow to the right atrium increased during inspiration and decreased during expiration. The increased flow during inspiration was attributed to the emptying of blood from the extrathoracic veins into the thoracic veins and to the increased intra-abdominal pressure compressing the abdominal veins. Brecher referred to this phenomenon as a "time dependent depletion stage" of venous collapse. Brecher suggested that the time required for vena cava collapse was of the same order of magnitude as the events of the respiratory cycle. This time dependency was said to prevent vena cava collapse from reaching the flow limiting stage during a normal inspiration. Brecher et al. (1953) simulated the pressure changes within the vena cava which accompany the respiratory cycle, and as a result of this simulation, claimed that the algebraic summation of the increased flow during inspiration, and the decreased flow during expiration, would cause a net increase in the return of blood to the heart.

Guyton (1962, 1963b) has taken the position that increases and decreases in central venous pressure resulting from respiration are harmful rather than helpful to venous return. He showed that when right atrial pressure became more negative than -4 mm Hg, venous collapse occurred, and a further increase in negativity of right atrial pressure did not cause a further increase in venous return (Guyton and Adkins,

1954). However, as right atrial pressure was increased from zero to the level of mean circulatory filling pressure, venous collapse did not occur, so that venous return decreased linearly to zero. Guyton (1962) reasoned that if increasingly negative right atrial pressures could not increase venous return, but positive right atrial pressures could decrease it, the net effect of such pressure pulsations would be to decrease venous return. He called this phenomenon "venous rectification". To test this premise, varying quantities of blood were injected and withdrawn from the canine right atrium at frequencies varying from between 60 to 160 cycles per minute and of zero to 64 ml volume per cycle. This procedure never increased venous return. Instead, even the smallest experimental right atrial pulsation decreased venous return when right atrial pressure was in the range of zero to -4 mm Hg. Intense pulsations reduced venous return to as low as 50% of normal. The fact that venous return decreased, even at rapid pulsation frequencies, tended to refute the claim of Brecher et al. (1953) that a "time dependent depletion stage" causes respiratory enhancement of venous return. However, the apparently conflicting findings might be explained by differences in collapsibility of the right atrium and the vena cava.

The effects of respiration upon the pressure-flow relationships of the vena cava remain controversial. Because venous researchers have been unable to agree even on the directional changes of flow effected by inferior vena cava collapse during normal respiration, much less on qualitative or quantitative changes, physical modeling continues to be an important means of discovering the underlying mechanisms and principles of venous collapse.

# Vascular Collapse in the Microcirculation

The non-linear pressure-flow relationships of the pulmonary circulation have been studied extensively by use of the isolated perfused lung technique (Permutt et al., 1962; West et al., 1964; West and Dollery, 1965; Lopez-Muniz et al., 1968; Maloney et al., 1968). By use of this method, perfusion pressure can be modified at will, and tissue pressure can also be easily modified simply by changing bronchial ventilatory pressure. Because pulmonary capillaries are in direct contact with the alveolar wall, they are subjected to alveolar air pressures. Therefore, ventilatory pressure is generally assumed to be directly transmitted through the alveoli to the pulmonary capillary walls.

Normal pulmonary capillary pressure is very low, somewhere between 8 and 12 mm Hg (West, 1974). This means that a slight decrease in pulmonary capillary pressure, or an increase of alveolar pressure such as that which results from expiration, can lower transmural pressure sufficiently to cause vascular collapse of the pulmonary microvasculature, resulting in a non-linear pressure-flow relationship. In an effort to explain the dynamics of this non-linear pressure-flow relationship, Permutt et al. (1962) adopted Duomarco and Rimini's (1954) waterfall analogy. They presented a mathematical analysis of flow through the microcirculation of the lung which is now called the "waterfall model". Permutt et al. (1962) proposed that flow through a blood vessel which is partially collapsed by tissue pressure is independent of outflow pressure, just as flow over a waterfall is independent of the height of the falls. According to the waterfall model, if  $P_i$ ,  $P_o$ , and  $P_e$  are inflow,

outflow, and exterior tissue pressures, then the pressures, flow Q, and resistance R, can be described by the following statements:

When 
$$P_i > P_o > P_e$$
,  $Q = \frac{P_i - P_o}{R}$ , and the vessel is open. (1)

When 
$$P_i > P_e > P_o$$
,  $Q = \frac{P_i - P_e}{R}$ , and the vessel is partially collapsed and the flow is independent of  $P_o$ . (2)

When 
$$P_e > P_i > P_o$$
, Q = 0, and the vessel is closed. (3)

West <u>et al</u>. (1964) presented evidence that vascular collapse in different parts of the lung was a function of pulmonary capillary hydrostatic level, and that on this basis, the lungs can be divided into three zones. If  $P_A$ ,  $P_a$ , and  $P_v$  are alveolar pressure, pulmonary arterial pressure, and pulmonary venous pressure, respectively, then for:

Zone I, the apex,  $P_A > P_a > P_v$ , and  $P_e > P_i > P_o$  (vessels closed);

Zone II, the mid-portion,  $P_a > P_A > P_v$ , and  $P_i > P_e > P_o$  (vessels partially closed); and in

Zone III, the base,  $P_a > P_v > P_A$ , and  $P_i > P_o > P_e$  (vessels open).

These zones have been shown to move up and down the lungs as alveolar pressure and pulmonary artery and vein pressures fluctuate (Maloney et al., 1968).

Another theory proposed to explain non-linear pressure-flow relationships of the microvasculature is that of "critical closure".

Burton (1951) and Nichol et al. (1951) showed that when the perfusion pressure of a vascular bed was gradually decreased, flow ceased before

the arteriovenous pressure gradient reached zero. When extravascular tissue pressure was progressively increased, flow ceased when tissue pressure was less than arterial pressure. This phenomenon was most likely to occur under conditions of high vasomotor tone. Burton (1951, 1962) theorized that when transmural pressure falls to a critically low value, the presence of active tension within the wall of a vessel could overcome even a positive transmural pressure and collapse the vessel. Burton called this pressure the "critical closing pressure". He concluded that the arteriole, because it has a minimal radius and high levels of active tension, was the most likely anatomical location for critical closing.

Permutt and Riley (1965) applied the waterfall model to the phenomenon of critical closure. They assumed that active tension is additive to exterior tissue pressure ( $P_e$ ), to give a critical closing pressure ( $P_c$ ). Under these circumstances, the pressure-flow relationship of a vascular bed would depend upon the gradient between inflow pressure and the critical closing pressure:

$$Q = \frac{P_i - P_c}{R} \tag{4}$$

The mechanism responsible for the lack of flow in the presence of an inflow-outflow pressure difference remains controversial. The vascular wall of the small arteriole has a wall thickness to radius ratio of  $\frac{20}{15}$  (30  $\mu$  diameter, 20  $\mu$  wall thickness) and is composed of a moderate amount of elastin fibers and a relatively large amount of muscle (Strandness and Sumner, 1975). This elastic tissue would tend

to resist the deformation required for complete closure (Alexander, 1977).

Histological studies have been equivocal regarding the role of the arteriole in vascular collapse. The anatomical site of vascular collapse in the microcirculation has been investigated in skeletal muscle (Gray et al., 1967) and in the pulmonary circulation (Maloney et al., 1968).

Gray et al. (1967) investigated this phenomenon in rat and dog calf muscles during isometric muscle contraction. Radiographs showed "nipped" and narrowed arterial segments during contraction. Rapidly frozen histological preparations showed kinking and pinching of arteries as they entered the muscle, and of arteries and veins as they passed between muscle fasciculi. The appearance of the capillaries suggested that they were at least as wide as when the muscle was relaxed. Their findings suggested that compression of the larger supplying vessels, not collapse of the microvasculature, was responsible for increased vascular resistance during strong muscular contraction.

Maloney et al. (1968) found different vessels responsible for vascular collapse in the pulmonary circulation. They showed that wherever pulmonary artery pressure was less than pericapillary tissue pressure (Zone I), most of the vessels of less than 30  $\mu$  diameter were closed. Small arterioles, pre-capillary sphincters, pre-capillary arterio-venous anastomoses, capillaries and venules are all less than 30  $\mu$  diameter, and would fall into this category.

Presently, the mathematical waterfall model (Permutt et al., 1962) is cited frequently to explain non-linear pressure-flow relationships of the microcirculation (Scharf et al., 1971; Downey and Kirk, 1974, 1975; Green, 1975; Mitzner, 1974). The "critical closure" theory of Burton (1951) remains controversial (Alexander, 1977). One of the goals of the present experimental research is to measure pressure-flow relationships in a Starling resistor model of the microcirculation. The data will be compared to the theoretical models of flow through the microvasculature, especially the "waterfall model".

# III. REVIEW OF MODELING OF FLOW THROUGH COLLAPSIBLE VESSELS

# Physical Modeling of Pressure-flow Relationships

The use of thin-walled collapsible tubing as a physical analogue of blood vessels dates back to 1912, when Starling (Knowlton and Starling, 1912) devised this method to simulate peripheral resistance in the heart-lung preparation. It consisted of a freely collapsible tube traversing a chamber in which pressure could be controlled. The term "Starling resistor" is now generally applied to vessels that collapse passively, whether experimental or physiological. The first pressure-flow data was published by Holt (1941). His prototype experimental apparatus has since been modified and used to model flow through the lungs (Lopez-Muniz et al., 1968), kidney (Swann et al., 1952), arterioles (Rodbard et al., 1971), single segments of vein (Brecher, 1952), segments of vein in series (Doppman, et al., 1966), and the entire length of the inferior vena cava (Katz, 1968).

The purpose of the use of a Starling resistor model was to circumvent, via an hydraulic analog, the experimental inconveniences encountered during <u>in vivo</u> research of collapsible blood vessels: the experimental animal must be kept in a physiological steady state for a reasonably long period of time; perfusion pressure, outflow pressure, and blood flow must be controlled; and tissue pressure outside of the

vessels must be accurately measured, modified, and/or maintained constant. Because flow rates and experimental pressures, especially tissue pressure, are extremely difficult to reproduce from one animal experiment to the next, only a statistical quantification of these relationships can be established <u>in vivo</u>. Therefore, it has been much more convenient to conduct experiments on a Starling resistor model to quantify pressure-flow relationships during collapse in order to better understand the underlying physical principles.

The experimental set-up has consisted of a flexible latex tube (Penrose drain) mounted between two rigid tubes within an airtight box in which pressure can be controlled. There are variable resistances both upstream ( $R_i$ ) and downstream ( $R_0$ ) to the flexible tubing, and an upstream source of flow. The pressure external to the tubing within the box ( $P_e$ ) and pressures immediately upstream and downstream to the flexible tube ( $P_i$  and  $P_0$  respectively) and flow (Q) are monitored.

Although the use of Penrose tubing as a model collapsible vessel circumvented many of the experimental difficulties of <u>in vivo</u> research, a state of confusion still remained concerning even qualitative pressure-flow relationships. This can be accounted for by the variety of experimental conditions used by different investigators. The reason for this is that there are more independent variables for the pressure-flow relationships of a collapsible vessel than for the simple pressure-flow relationship of a long, round, cylindrical tube. During steady, laminar flow through the latter tube, the driving pressure,  $\Delta P$ ,  $(P_i - P_o)$  is proportional to flow, so that

$$\Delta P = RQ$$
 (5)

R is given by Poiseuille's Law:

$$R = \frac{8 \eta 1}{\pi r^4} \tag{6}$$

where  $\underline{r}$  is the radius of the tube,  $\eta$  is the viscosity, and  $\underline{l}$  is the length of the vessel. For a collapsible vessel, transmural pressure also must be considered because it affects the cross-section of the vessel and therefore, the resistance to flow. This factor increased the number of variables to be measured during experiments on collapsible tubing. Flow was sometimes measured as a function of variations in any one of the three variables,  $P_i$ ,  $P_o$ , or  $P_e$ , while the other two were held constant; occasionally flow was held constant while one or two of the pressures were varied. This resulted in a wide variety of pressure-flow graphs, each with different variables and parameters.

To document the confusion that existed in 1969, Conrad (1969) plotted the experimental results described in four publications (Holt, 1941, 1959; Rodbard, 1955; Rodbard and Saiki, 1953) on a single pressure-flow graph. It does not appear that the four curves agree even qualitatively without the expenditure of considerable time and effort to understand the graph. In an effort to clarify these relationships, Conrad (1969) proposed a three-dimensional surface to encompass  $P_i$ ,  $P_o$ , and Q, with  $P_e$  fixed. Brower and Noordergraaf (1973) found that this three-dimensional surface was difficult to interpret, saw the need for a uniform treatment of variables, and suggested the use of Q for the independent variable;  $P_i$ - $P_o$  for the dependent variable, and  $P_e$ - $P_o$  for the parameter. The rationale for the use of these variables will be discussed subsequently.

Let us take a closer look at the results of the aforementioned experimental studies. The earliest data on pressure-flow relationships in a collapsible vessel were obtained by Holt (1941) using thin walled rubber tubes and also a canine jugular vein. He showed that when the partially collapsed tube was being perfused, increasing inflow pressure, P<sub>i</sub>, increased the rate of flow through the collapsible segment and decreased its resistance to flow. Under the same circumstances of partial collapse, lowering the pressure on the downstream side of the collapsible segment,  $\mathbf{P}_{_{\boldsymbol{O}}}\text{, increased the resistance to flow through the}$ collapsible segment and either did not change the rate of flow, or decreased it slightly. Increasing the chamber pressure,  $P_{\rho}$ , around the collapsible tube decreased the rate of flow and increased flow resistance. In these experiments, the tube opened and closed periodically when partially collapsed. This oscillatory phenomenon will be discussed in another section, but it must be noted that these oscillations affect the pressure-flow relationships of the collapsible vessels.

Although the data obtained by Rodbard (1953) with the one tube model generally confirmed the findings of Holt (1941), he further added to the confusing number of variables when he devised an elaborate system of tubes and resistances which he called a "capillaron" (Rodbard, 1963). In his capillaron model, a collapsible tube was mounted within a chamber in which the pressure was regulated by varying the resistance of a shunt flow from the inflow tubing. In this system, as upstream pressure was increased, it tended to increase the flow through the collapsible segment, but the pressure in the chamber increased also,

and the increased chamber pressure tended to collapse the tubing and thus limit flow. This experimental set-up was designed to explain autoregulation of organs within non-compliant enclosing capsules, such as the kidney. Rodbard suggested that increased filtration due to increased capillary pressure may increase tissue pressure surrounding capillaries and collapse them. His experiments established the fact that flow through a collapsible vessel can be regulated by a passive hydraulic device with the proper selection of pressures and resistances, but they also increased the number of variables used for the pressure-flow graphs.

In 1969, <u>IEEE Transactions on Bio-Medical Engineering</u> published a symposium on veins, reflecting a revitalized interest in the phenomenon of flow through collapsible vessels being taken by bio-medical engineers and physicists. The detailed experiments of Conrad (1969), Moreno <u>et al.</u> (1969), and Katz <u>et al.</u> (1969), all of whom published similar pressure-flow data, exemplify this renewed interest. Conrad (1969) generated three families of curves using the parameters  $P_e$  held constant, down-stream resistance ( $P_o = \frac{P_o}{Q^2}$ ) held constant, and the ratio  $P_e = \frac{P_o}{R_o}$  held constant. By systematic variation of these parameters, he was able to elucidate some of the underlying mechanisms of flow through collapsible tubes. The curves were plots of  $P_i$ - $P_o$  as a dependent variable of Q and were of the general form of Figure 1.

Photographs (Conrad, 1969) of the tube showed the following:

In Region I, the tube was collapsed flat except for two small channels which remained open at either side of the tube. In Region II, the

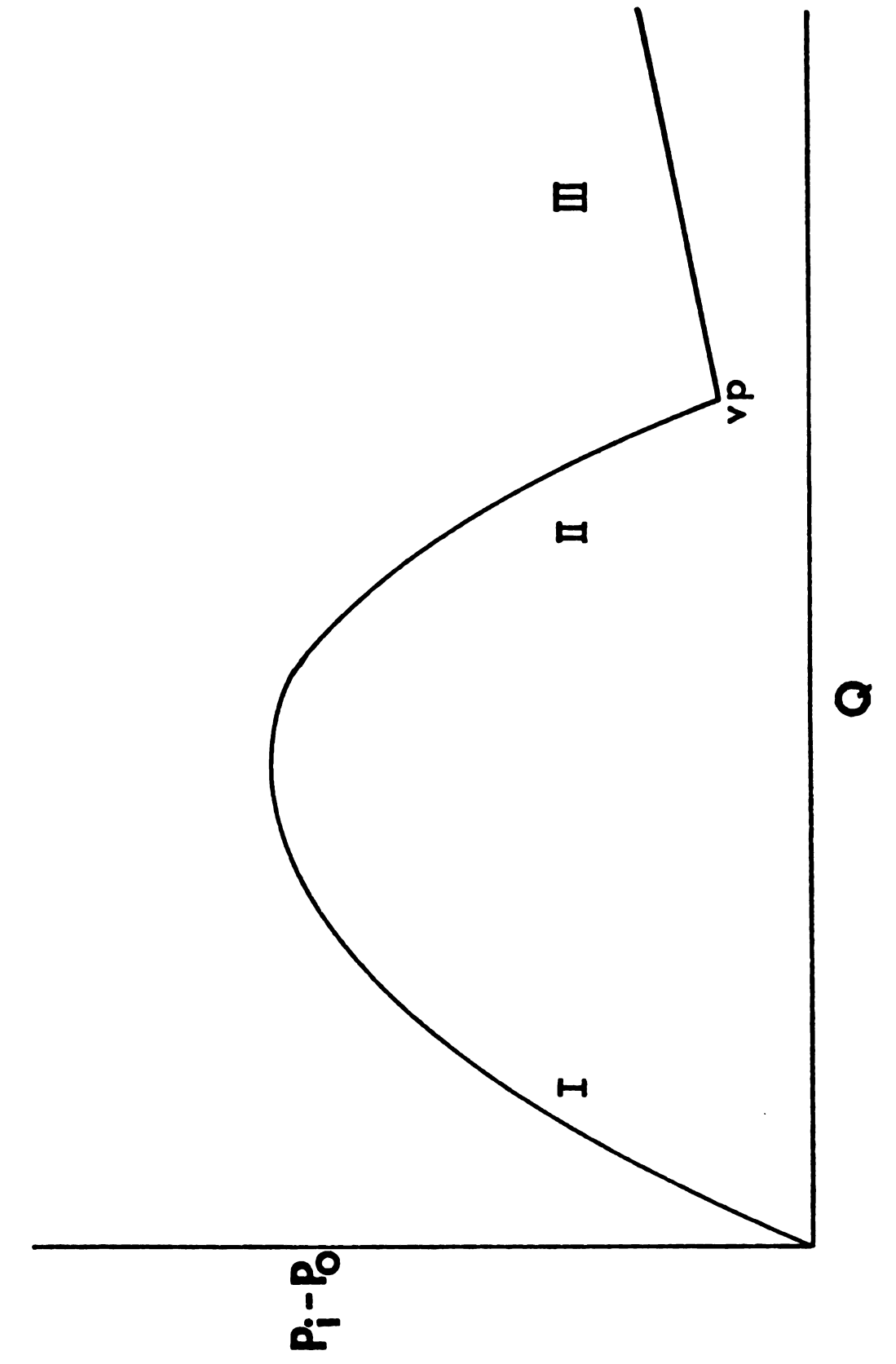


Figure 1. Characterization of the pressure-flow relationship of the Starling resistor when  $P_{\rm e}$  is held constant.

collapse was asymetric along its length; the greater collapse was at the downstream portion of the tube. In Region III, the tube was completely open.

The steep slope of Region I resulted from flow through the side channels of the tube which was collapsed sufficiently to cause the sides to come into contact with one another. As the parameter  $P_e$  was increased, the initial slope and the maximum pressure difference,  $P_i^{-P}_0$ , increased also.

In Region II,  $P_i > P_e > P_o$ , and the slope was negative, implying that the driving pressure decreased as flow was increased. Conrad called this a "negative resistance region", and showed that the negative slope of this region was proportional to outflow resistance  $R_o$ . Katz et al. (1969) further showed that when flow increased,  $P_i$  remained nearly constant, but  $P_o$  increased rapidly, as could be expected with the use of high outflow resistance. A little consideration of these facts reveals that by holding  $P_e$  constant, and allowing  $P_o$  to increase, that  $P_e - P_o$ , and thus transmural pressure was allowed to vary. Use of the parameter  $P_e - P_o$  held constant by Brower and Noordergraaf (1973) thus eliminated this apparent contradiction of the negative resistance region.

The valley point (vp), which is the transition from Region II to Region III, occurs at higher flow rates when  $P_e$  is increased and/or  $R_o$  is decreased. Using Conrad's (1969) definition of  $P_o = R_o Q^2$ , and the data which he supplied, it can be shown that flow at the valley point is equal to the flow at which  $P_o$  approximates  $P_e$ . Therefore, in Region III,

the tube is open and the slope of the curve is similar to that of an open rigid tube, much lower than that of Region I. The curves of Conrad (1969), Katz et al. (1969), and Moreno et al. (1969) were drastically different from any previously presented for pressure-flow relationships of a collapsible tube.

Obviously, the presentation of data for direct comparison of experimental results suffered from the presence of so many experimental and extraneous variables. The continuing need for a reasonably simple expression describing pressure-flow relationships for a collapsible tube was answered in part by Brower and Noordergraaf (1973), who took advantage of the fact that although there are three different pressures  $(P_i, P_o, and P_e)$ , each independent, and three pressure differences  $(P_i-P_o, P_i-P_e, and P_e-P_o)$ , only two of these pressure differences are independent. Brower and Noordergraaf (1973) chose the flow Q as the independent variable and the parameters  $P_i - P_o$ ,  $P_e - P_o$  as independent They recalculated the data of Conrad (1969), Katz et al. variables. (1969), and Moreno et al. (1969) to conform to the graphic form of  $P_i-P_o$ as a function of Q and  $P_e-P_o$ . This eliminated the negative resistance region of their curves. Brower and Noordergraaf (1973) then replotted the data of Holt (1941, 1959), Rodbard (1955), and Rodbard and Saiki (1953) using these new parameters, and were able to combine their data into the same set of curves. Thus, Brower and Noordergraaf (1973) were able to reconcile the apparently contradictory results of many earlier reports of pressure-flow experiments. However, they stated that for flow rates greater than 14 cc/sec, the pressure-flow relationships were

uncertain due to lack of data. It is our intention to investigate these higher flow rates because they in fact represent physiological flow ranges.

#### Oscillatory Phenomena

A fascinating property of a collapsible tube is that when  $P_i > P_e > P_o$ , pulsatile flow may occur under steady state conditions. A possible mechanism of this phenomenon can be explained as follows. Consider a segment of the tube at the downstream end, where  $P_e > P_o$ , that is completely collapsed instantaneously by  $P_e$ . Then Q = 0 out of the tube. When flow stops, continued inflow into the tube from the upstream pressure source causes the pressure within the whole tube to rise toward the level of  $P_i$ . This forces the tube open because  $P_i > P_e$ . When the tube opens and flow commences, the pressure immediately drops, and the cycle begins again. This principle also operates in the musical vibrations of reed instruments, and probably in the vocalizations of the larynx also (Rodbard, 1953).

Early investigators have noted these oscillations (Brooks and Luckhardt, 1916; Holt, 1941; Brecher, 1952; Rodbard, 1953, 1955), but quantification under controlled experimental conditions remained elusive. Brecher (1956) reported oscillations of frequencies as low as 1 per 20 seconds and as high as a few hundred per second when using Penrose tubing, and from 3 to 20 per second in animal experiments. Rodbard (1953) speculated that these oscillations may be the cause of a variety of cardiovascular vibrations: those associated with coarctation of the

aorta; murmurs of arteriovenous anastomoses, patent ductus arteriosus and aortic stenosis; and the Korotkoff sounds heard when arteries are compressed during the measurement of blood pressure.

Conrad (1969) recorded oscillations which he found in the negative resistance region of the pressure-flow curves that he plotted, and Katz  $\underline{\text{et al}}$ . (1969) programmed into their mathematical model a facsimile of the oscillations of the negative resistance region. Since these curves were plotted at constant  $P_e$  rather than constant transmural pressure, these results apply to specific cases and are not generalizable.

Other mathematical treatments of oscillatory phenomena have suggested that the cause may be that mean flow velocity has exceeded the sonic velocity, i.e., the velocity of pressure waves on the tube (Griffiths, 1971; Oates, 1975a; Brower and Scholten, 1975), but Conrad et al. (1978) refute this mechanism as a cause of oscillations. Whether or not oscillations may exist in the vessels of the microcirculation remains controversial. Conrad's (1973) calculations show that under the flow conditions of the microcirculation (low Reynolds number flow oscillations may be present, while Fung (1973) calculates that such oscillations cannot exist in the vessels of the microcirculation. Our intention is to provide quantification of these oscillations under controlled experimental conditions at both high and low Reynolds number flow, and under conditions simulating a variety of physiological stresses to which blood vessels are subjected.

#### Modeling of the Cross-sectional Shapes of Collapse

When a segment of a blood vessel collapses to an elliptical cross-sectional shape, i.e., buckles, resistance to flow through that segment increases more than might be predicted by the change in cross-sectional area alone. For a vessel of elliptical cross-section, resistance is a complex function of both area and cross-sectional shape (Langlois, 1964). For mathematical modeling of pressure-flow relationships of collapsing vessels, it has therefore been necessary to know their cross-sectional dimensions at varying transmural pressures. Measurements of the cross-sectional dimensions of Penrose tubing have been obtained (Brooks and Luckhardt, 1916; Reddy et al., 1970), and recently, Attinger (1969) and Reddy et al. (1970) have measured the cross-sectional dimensions of veins in vitro. This data has not always been applied to the development of the mathematical models.

Mathematical models of the collapse phenomenon, or buckling, have been developed by Katz and Chen (1970) and Moreno  $\underline{et}$   $\underline{al}$ . (1970), Kresch and Noordergraaf (1972) and Flaherty  $\underline{et}$   $\underline{al}$ . (1972). Katz and Chen (1970) and Moreno  $\underline{et}$   $\underline{al}$ . (1970) developed programmable equations for the collapse phenomenon by applying the mathematical theory of bending movements. Their assumption of constant perimeter, with bending as the only mechanism for increase in cross-section, is contrary to the finding of Reddy  $\underline{et}$   $\underline{al}$ . (1970) who noted that stretching as well as bending is an important mechanism for increases in cross-sectional area of veins.

Kresch and Noordergraaf (1972) reduced the problem to determining the shape of a uniformly collapsed isotropic tube with zero longitudinal

stress. The condition of constant cross-sectional shape along the length of the tube is severely restrictive, and the assumption of zero longitudinal pre-stress is not in keeping with physiological data (Yates, 1969; Moreno et al., 1970).

Flaherty et al. (1972) also formulated programmable equations for a wide range of transmural pressures, taking into account the fact that vascular collapse may be multi-lobular. A multi-lobed collapse due to anatomical tethering appears to be possible because Reddy et al. (1970) noted a three-lobed collapse in vitro that was caused by the end constraints on the vein. They further calculated flow conductance of an incompressible fluid through a collapsed vessel as a function of transmural pressure and number of lobes of collapse.

While knowledge of cross-sectional shape is necessary for mathematical modeling, it is not needed for physical modeling. The experimental transmural pressures and flow rates determine the cross-sectional dimensions of the tube. For this reason, data for cross-sectional dimensions need not be collected.

# Mathematical Modeling of Pressure-flow Relationships in Collapsible Vessels

Perhaps the earliest and simplest mathematical model of flow through collapsible vessels was the "waterfall model" formulated by Permutt et al. (1962). However, the use of digital and analog computers has led to more sophisticated models. Attempts to use these computers to model and analyze the entire cardiovascular system have led to the

realization that the constituents of the system require more accurate representation (Moreno et al., 1969).

In keeping with this need for definition and understanding of specific components of the system, investigators of hemodynamics of the venous system have formulated mathematical models of an individual segment of vein (Kresch and Noordergraaf, 1969) and a collapsible tube (Oates, 1975a, 1975b; Mahrenholtz, 1974; Katz et al., 1969). The purpose of this modeling is to gain insight into the behavior of interconnected segments of veins, and then the entire venous system.

Kresch and Noordergraaf (1969) were the first to base their analysis on the linearized Navier-Stokes equations of incompressible viscous fluid flow, which they modified by a cross-sectional shape factor developed from wave transmission theory. The resulting model considered fluid inertia, resistance to flow, and vascular compliance.

Another recent theory for flow through collapsible tubes, proposed by Katz et al. (1969), was based on empirically derived laws of fluid mechanics for nozzle flow, and it included a nonlinear convective acceleration term. In this model, cross-sectional area was based on experimentally determined transmural pressure versus area relationships for Penrose tubing. In computer simulation of this mathematical model, the connecting elements used in series with the Penrose tubing of the physical model were also simulated, resulting in curves similar to those of Conrad (1969), Katz et al. (1969), and Moreno et al. (1969), that show a region of apparent negative resistance, which Brower and Noordergraaf (1973) later showed was not a property of the collapsible tube itself, but of the connecting elements in series with the tube.

The major difficulties of mathematical modeling flow through collapsible vessels are the non-conventional cross-sectional geometry of the tube and the non-linearity of fluid behavior. The use of 9 variables and ten system parameters by Katz et al. (1969) for their model was not adequate to describe the myriad of additional phenomena to which flow through collapsible vessels is subjected. In this regard, no presently available model can without additional data.

Brower (1970) attempted a mathematical model encompassing changes in tension or longitudinal pre-stress, length and diameter of tubing, and viscosity. He used for his mathematical model short lengths of tubing of rectangular cross-section and assumed boundary layer separation in the divergent portion of the immediate post-collapse segment of the collapsible tubing. Except for changes due to fluid viscosity, the changes that Brower attempted to model mathematically have been generally ignored by both theoretical and experimental investigators even though they represent important physiological phenomena. Our plan is to utilize the physical model to generate quantitative data for the effects of length, longitudinal pre-stress, and stretch.

## Physical Modeling of the Microcirculation

When Permutt (1962) applied his Starling resistor model to the microcirculation, he assumed that pressure-flow data obtained from water perfusion of large diameter tubing applied equally well to miniature blood perfused vessels. The non-linear Navier-Stokes equations for viscous flow indicate that the instabilities observed with flow through

large collapsible vessels may disappear as the diameter of the vessel becomes so small that viscous effects dominate inertial effects.

Whether or not flow is stable (laminar) or turbulent can be predicted from vessel diameter, mean flow velocity, and the density and viscosity of the fluid. These parameters can be expressed by a dimensionless quantity, the Reynolds number:

$$Re = \frac{\overline{V} D}{v} = \frac{\rho \overline{V} D}{n}$$
 (7)

where Re = Reynolds number (unitless)

 $\overline{V}$  = average velocity in cm/sec

D = diameter of the tube in cm

 $\rho$  = fluid density in Gm/cc

 $\eta$  = viscosity in poises

 $v = \frac{\eta}{\rho} = \text{kinematic viscosity in stokes.}$ 

Modeling theory states that flows with the same Reynolds number demonstrate the same flow characteristics. Therefore, if the diameter of the vessels of the microvasculature cannot be utilized for physical modeling, the Reynolds number corresponding to microvascular blood flow still can be estimated and approximated by increasing the viscosity of the perfusing fluid. In this way, the pressure-flow relationship for a given Reynolds number can be measured and applied to flow of the same Reynolds number in the microcirculation.

Physical modeling with high viscosity fluids has been minimal.

Holt (1969) perfused Penrose tubing with 0.125 stokes fluid and achieved a Reynolds number of 130 at low flow rates. He reported only that

increasing viscosity resulted in an increased cross-sectional area of the tubing at any given flow rate. In an effort to model pulmonary alveolar blood flow, Fung and Sobin (1972) perfused 2 cm diameter tubing with 300 poise fluid at a flow velocity of 3 cm/sec and thereby achieved a Reynolds number of 0.02, which is comparable to that in the pulmonary capillary bed. Photographs of the tube taken over extended periods of time revealed no flutter but a slight constriction at the outflow end of the tube. Because quantitative pressure-flow data for low Reynolds number flow is entirely lacking from the literature, we expect that the data we will generate from physical modeling with high viscosity fluids will supply much needed information for the development of theory of pressure-flow patterns of the microcirculation.

#### IV. STATEMENT OF OBJECTIVES

From the preceding discussion, it is apparent that further experimentation is needed in the following areas:

- Pressure-flow relationships for flow ranges above 4 cc/sec during water perfusion to simulate venous blood flow.
- 2) Pressure-flow relationships simulating the effect of increasing tissue pressure, outflow resistance, length, tension, stretch, diameter and changes in composition of blood vessels.
- 3) Pressure-flow relationships during perfusion with high viscosity fluid that simulate the flow in the microcirculation.
- 4) Quantification of the oscillatory phenomenon and its effect on pressure-flow relationships under the above controlled experimental conditions.
- 5) In vitro pressure-flow relationships of large and small veins.

The goal of this experimental research is to provide such information.

#### V. METHODS

The physical model (Figure 2) used in the present study consisted of flexible latex Penrose tubing (American Hospital Supply, McGaw Park, IL) enclosed in an air-tight transparent Plexiglas box. The Penrose tubing was 1.27 cm in diameter when expanded, 7.5 cm long, and had a wall thickness of 0.032 cm. Within the box, the tube was mounted at both ends on rigid cylindrical metal tubes of 1.27 cm inner diameter, having a wall thickness of 0.05 cm. The tubing was mounted horizontally and was strain free longitudinally unless otherwise noted. The plane of collapse due to residual strains of the manufacturing process was positioned horizontally. Pressure ports, for the measurement of inflow pressure ( $P_i$ ) and outflow pressure ( $P_o$ ) were located outside the box on the metal tubing, 8.5 cm from either end of the collapsible tube. The pressure in the box  $(P_p)$  was modified by the use of a hand-held rubber bulb pump connected by latex tubing to a port in the box. The  $P_{\mbox{e}}$  pressure cannula was inserted into the box through an air-tight needle hole in this latex tubing.  $P_e$ ,  $P_i$ , and  $P_o$  pressure measuring cannulae were polyethylene tubing (PE 60), 80 cm long, filled with distilled water, connected to Statham low volume displacement transducers (P23Gb) (Hato Rey, Puerto Rico) and coupled to a Hewlett-Packard (7796 Model 1065C) (Waltham, MA) direct writing oscillograph and an Esterline Angus-XY recorder (Model 575, Indianapolis, IN). All pressure transducers

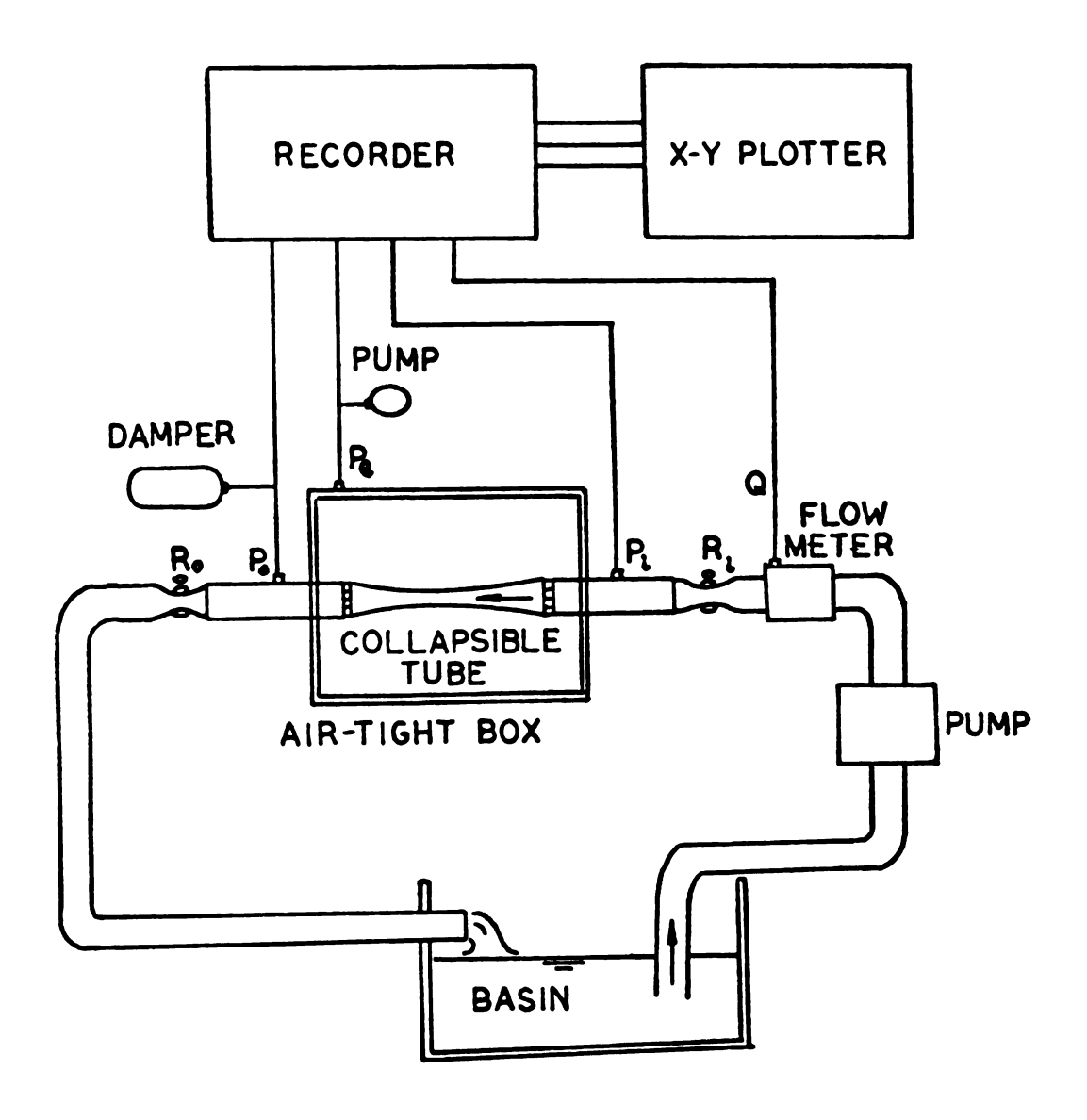


Figure 2. Starling resistor model for perfusion with water. Pressure ports for the measurement of inflow pressure  $(P_0)$ , outflow pressure  $(P_0)$ , and the pressure in the box  $(P_e)$ , are located outside of the air-tight box. Upstream resistance  $(R_i)$  and downstream resistance  $(R_i)$  consist of screw-clamps on latex tubing. Q represents flow measured by the flow-meter.

were calibrated with a mercury manometer using fluid pressure during zero flow as the zero reference point. The Hewlett-Packard electronic mean was used for all pressure-flow measurements. Oscillations of the tubing were quantified for pressure amplitude and frequency by use of the Hewlett-Packard electronic <u>low</u> filter setting and expansion of the time scale.

Resistances upstream to the  $P_i$  pressure port  $(R_i)$  and downstream to the  $P_o$  pressure port  $(R_o)$  were controlled by screw clamps on latex tubing, 1.2 cm inner diameter. This latex tubing extended 8.5 cm from the  $P_o$  pressure port to an outflow reservoir and it produced minimal outflow resistance (approximately 1 mmHg/80 cc water/sec.). Unless otherwise stated,  $R_o$  is non-constrictive. Outflow resistance  $(R_o)$  downstream to the  $P_o$  pressure port was applied when stated by tightening the screw clamp of the outflow tubing so that it formed a near elliptical cross-section, the size of which was measured by the size of its minor axis.

Markings were etched into the sides of the rigid mounting tubes at 1 cm intervals so that either the length or the amount of longitudinal strain of the Penrose tubing could be controlled and modified. To study the effects of vessel length, a section of tubing was cut shorter in 1 centimeter decrements and the distance between the mounting tubes was shortened accordingly. The effects of pre-stress and stretch were studied by taking  $4\frac{1}{2}$ ,  $7\frac{1}{2}$ , and  $10\frac{1}{2}$  cm lengths of tubing and pre-stressing them to 3 cm longer than manufactured length. The effects of stretch were also studied by mounting a  $4\frac{1}{2}$  cm section of tubing and increasing

the distance between the mounts by 0.5 to 1 cm increments, and securing them in place.

For water perfusion experiments, a pressure-dependent centrifugal pump (Little Giant Pump Company, Okalhoma City, OK) capable of delivering from less than 1 cc/sec up to 80 cc/sec of non-pulsatile flow was employed to recirculate room temperature water through the system.  $\mathbf{R}_{\mathbf{i}}$  served to modify the flow rate. Flow rate was measured upstream to  $P_i$  by a flow-through flow probe (3/16 inch diameter) (BLC-2048) connected to a BL-610 Pulsed Logic Flowmeter (Biotronex Laboratory, Inc., Silver Springs, MD), also coupled to the oscillograph and XY recorder. The zero flow setting was obtained by stopping the pump, clamping the latex tubing in front of the flowmeter, and waiting for stabilization; calibration was obtained from fifteen second timed collections which demonstrated that the flow meter output was linear. Zero drift was less than 0.1 cc/sec during the time necessary to plot a curve and the zero flow setting was checked immediately before initiating flow. Calibration checked at the end of the experiments was found to vary less than 1%.

Because there were high amplitude fluctuations of  $P_0$  when the Penrose tube oscillated, a "windkessel" chamber was used during water perfusion experiments to dampen the pulse of the  $P_0$  measurements. It consisted of a 1.5 cc water filled latex bulb chamber connected in series by a T-tube to the pressure transducer at its junction with the  $P_0$  cannula. This compliance chamber was tested at low amplitude fluctuations (+ 10 mmHg) and produced the same mean pressure as when the

Hewlett-Packard electronic mean was used without the compliance chamber.

The method of experimentation used in this study was to initiate a low flow rate through the system. Pressure in the box was adjusted to a predetermined level of  $P_e$ - $P_o$  for each curve. As flow was increased in small step-wise increments, slight changes of  $P_e$  were necessary to maintain  $P_e$ - $P_o$  at a constant level. With Q as the independent variable,  $P_i$ - $P_o$  was chosen as the dependent variable to allow comparison with data obtained from physiological experimentation. This method was used by Brower and Noordergraaf (1973) and it allows a more compact presentation of data because it makes use of the fact that although there are three different pressures, there are only two independent pressure differences. All data points were graphed immediately via the XY recorder, which also served as an analog computer of  $P_i$ - $P_o$  and  $P_e$ - $P_o$ . Data points were then recalculated and replotted when necessary.

Dow Corning Series 200 silicone fluid (0.5 stokes and 10 stokes) was used to study the effects of viscosity. The experimental setup was modified to consist of a reservoir filled with fluid which was pumped by a powerful Sigma-motor positive displacement pump designed to deliver constant flow against high back pressure (35# torque, 1-400 rpm). Tubing from the pump led to an inverted 1 quart Ball glass jar with a rubber stopper held by a bail top. Inflow and outflow tubing were inserted through the metal stopper. This jar served as a pressure chamber which effectively extinguished the pulse of the pump and drove flow through the experimental tubing. As it passed through the experimental apparatus, fluid dropped from the outflow tube of the model into

a reservoir atop a Toledo scale counterbalance. The counterbalance served to quantify flow. Changes in weight during a timed collecting period were optically recorded\* and then the necessary adjustment for specific gravity of the silicone fluid was calculated. Both the Sigma motor pump and the centrifugal pump were used and comparable data resulted from both methods of pumping fluid, therefore data resulting from both pumping methods were combined for the representative 0.5 stoke graph.

The elements in series with the collapsible tubing furnished considerable resistance to high viscosity flow, and it was necessary to adjust for this. The resistance of the elements exclusive of the collapsible tube was determined experimentally and found to be within 2% of that determined theoretically. Therefore, for any given flow rate, the level of  $P_e$ - $P_o$  was increased to take into account the theoretical pressure drop across the metal mounting tube from the end of the collapsible tube to the point at which  $P_o$  was measured. The true  $P_i$ - $P_o$  was computed by subtracting the theoretical pressure drop across the rigid mounting tubing from the recorded  $P_i$ - $P_o$ .

Penrose tubing of 0.633 cm diameter, and dialysis tubing (Arthur H. Thomas Co., Philadelphia, Pa.) of 1.58 cm diameter were used to determine the effect of different quality and diameter of tubing.

Reliability of timing and reading of the Toledo counterbalance was tested with the lowest, highest and medium constant flow rates of the pump. Readings were accurate to within 10%. When data was being collected, two readings were taken at each experimental flow rate. If the readings differed by more than 10%, a third reading was taken.

The 1.58 cm diameter tube was mounted on the 1.27 cm rigid tubes. The 0.635 cm tubing was mounted on 0.635 cm internal diameter rigid tubing. To maintain the length-diameter ratio that was used for the general characteristics of the 1.27 cm diameter tubing, the 0.635 cm tubing was of 3.25 cm length. The distance from the flowmeter to the  $P_i$  pressure port was 10 cm, and from the pressure ports to collapsible tubing was 2 cm. The outflow tubing was 10 cm long and 0.635 cm internal diameter.

For the study of veins, equine jugular veins of 7.5 cm length, and equine cephalic veins of 3.5 cm length were used. These veins were free of valves and side branches, exhibited very little taper, and were approximately 1.3 cm and 0.64 cm respectively in diameter when the horse was in the lateral recumbent position. Before the vein was dissected free from its connective tissue sheath, it was catheterized with polyethylene tubing and then carefully tied to the tubing so that the physiological length-tension relationship of the vein was maintained. Immediately after removal from the horse, the vein was mounted on the corresponding size of rigid tubing within the warm, humidified box, the catheterizing tubing was removed, and the vein was perfused in the physiological direction of flow. A gas mixture of 95%  $\rm O_2$ , 5%  $\rm CO_2$  was bubbled through the perfusate of either Ringer's bicarbonate\* solution

<sup>\*</sup>Ringer's Bicarbonate Solution

<sup>46.5</sup> Gm. Sodium Chloride 128 meq.

<sup>11.4</sup> Gm. Sodium Bicarbonate 22 meg.

<sup>0.85</sup> Gm. Magnesium Chloride 2 meq.

<sup>1.8</sup> Gm. Potassium Chloride 4.2 meq.

<sup>5.0</sup> Gm. Calcium Gluconate 5 meq.

Distilled water quantity sufficient to make 6 liters.

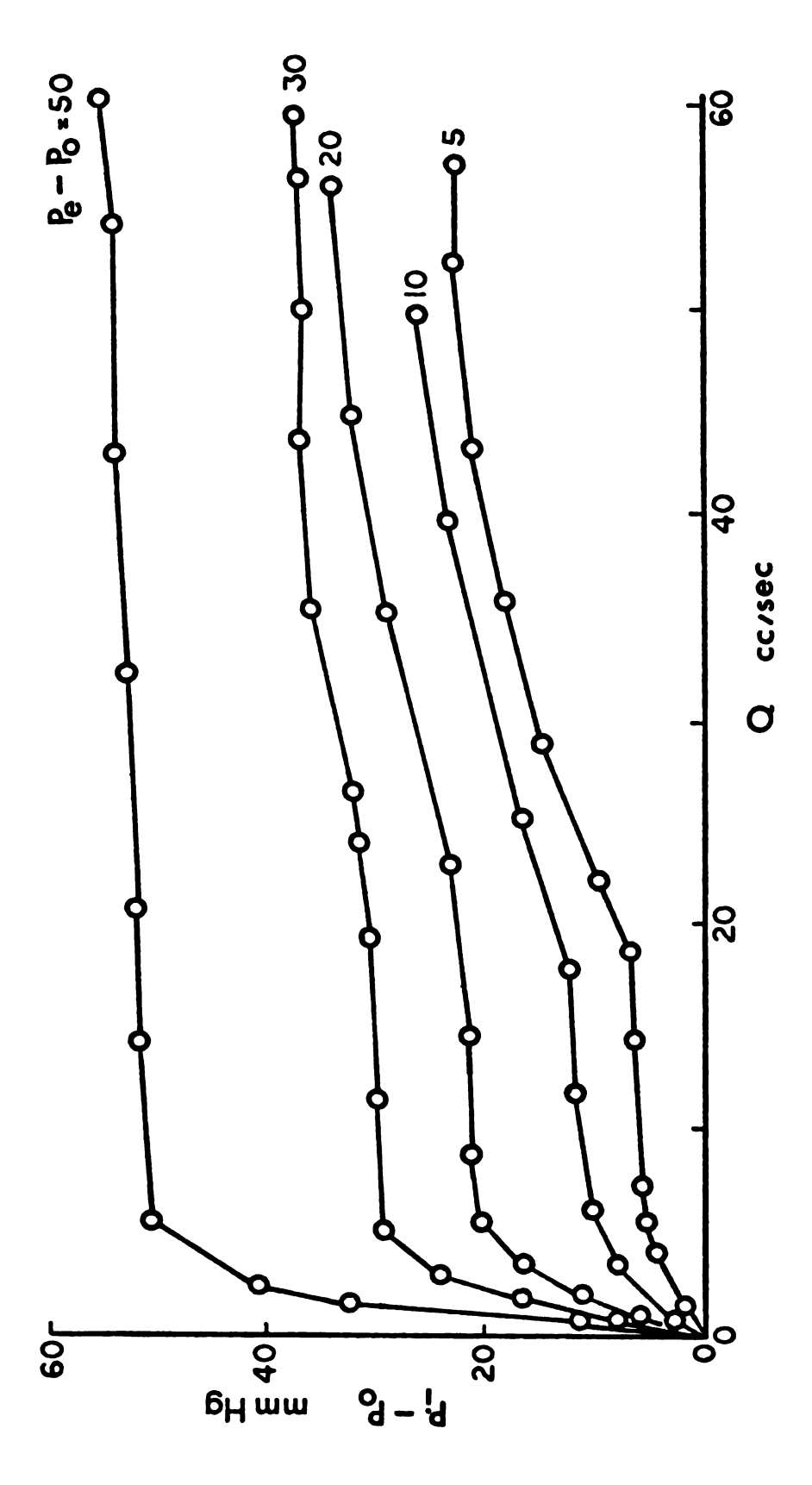
or stirred equine blood with 5,000 units Sodium Heparin added per liter. Both fluids were kept at  $37^{\circ}\text{C}$ .

#### VI. RESULTS

#### General Characteristics

A representative graph of the pressure-flow relationships of 1.27 cm diameter Penrose tubing held at manufactured length (7.5 cm) during water perfusion, is presented in Figure 3. For many of these curves, there are three distinct phases: an initial sharply rising phase, a plateau phase, and a late rising phase, of lower slope than the initial rising phase.

The slope of the initial rising phase increased as the parameter  $P_e^-P_O^-$  was increased. During the initial rising phase, at flows less than 6 cc/sec, the tube had the appearance of a flattened tube with small round side channels. As flow approached 6 to 8 cc/sec., the length of the flattened area gradually decreased until, at the beginning of the plateau phase, only the outflow region of the tube appeared to be "pinched" closed and the tube began to open and close intermittently. When  $P_e^-P_O^-$  was held constant at low levels, these self-excited oscillations (flutter) became increasingly more vigorous as flow was increased (Table 1).  $P_i^-P_O^-$  stabilized during the plateau phase at approximately the level of  $P_e^-P_O^-$ . At flows greater than 20 cc/sec the curves again began to rise. This late rising phase appeared at higher flow rates for higher  $P_e^-P_O^-$  and was not noted at all when  $P_e^-P_O^-$  was held at 50 mm Hg.



Pressure-flow relationships of 7.5 cm Penrose tubing held at manufactured length during water perfusion. Figure 3.

Table 1. The Effect of  $P_e$ - $P_o$  and Flow on Frequency and Pressure Amplitude of Oscillations

Pe-Po	Flow Amplitude Frequency P <sub>i</sub> -P <sub>o</sub>				Flow Amplitude Frequency			P <sub>i</sub> -P <sub>o</sub>
mm Hg	cc/sec	mm Hg	Hz	mm Hg	cc/sec	mm Hg	Hz	mm Hg
0	16			1.4	50	31	5.25	11
10	16	1	5.5	11.0	50	16	7.0	16.8
30	16	1	10.5	31.5	50	1	10.25	33.6
50	16	1	14.5	50.7	50	1	13.0	52.9

It was also noted that the amplitude of the flutter-caused pressure fluctuations increased during the late rising phase. Reynolds number for this data based on tubing diameter, maximum flow rate, and average velocity of flow ranges from zero to 6,000.

# The Effect of Oscillations when $P_e-P_0 = 0$

When  $P_e^-P_o$  was held at zero, oscillations of the tube occurred at flow rates greater than 20 cc/sec. These oscillations were sustained as flow was incrementally increased, but they could easily be discontinued by a slight temporary increase in  $R_o$ . The effect of these oscillations (Table 2) was to greatly increase the required inflow pressure  $(P_i^-P_o^-)$ , for any given flow rate.

Table 2. Oscillatory Flow When  $P_e-P_o = 0$ 

Flow cc/sec	Amplitude mm Hg	Oscillatory Frequency Hz	Pi-Po mm Hg	Non-Oscillatory Pi-P i o mm Hg
16				1.4
23	12	3.0	4.5	2.5
50	31	5.25	11.0	4.0

#### The Effect of Outflow Resistance

Raising outflow resistance ( $R_0$ ) downstream to the  $P_0$  pressure port, had the effect of increasing the value of all pressure measurements. However, with  $P_e$ - $P_0$  held constant, this outflow resistance effectively reduced the frequency and the pressure amplitude of the flutter, and consequently decreased the slope of the late rising phase. Table 3 summarizes the flutter data of a representative experiment at  $P_e$ - $P_0$  = 16 mm Hg. A graph of a representative experiment at  $P_e$ - $P_0$  = 10 mm Hg is shown in Figure 4.

Table 3. The Effect of Outflow Resistance on Frequency and Pressure Amplitude of Oscillations

$P_e - P_o = 16 \text{ mm}$	. Hg. Flow	rate = 75 cc/se	С	
Inner Minor Axis (mm.)	Po mm. Hg.	Frequency Hz.	Amplitude mm. Hg.	PP mm.Hg.
12.7 (round)	1	15	19-24	26
1.5	6	14	5	18
0.5	42	12	3	18
Minimum	58	11	1	16.5

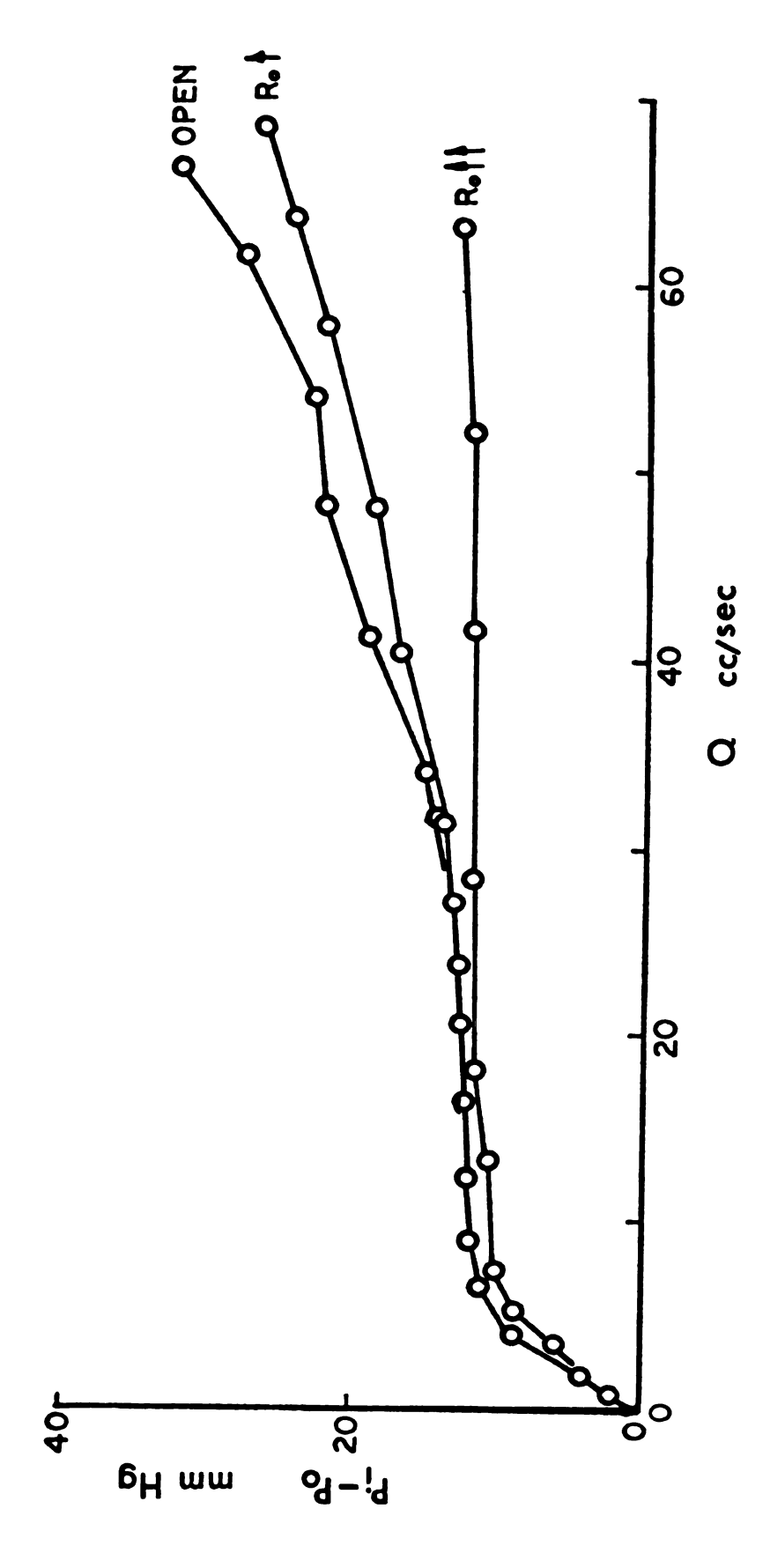


Figure 4. The effect of outflow resistance on the pressure-flow relationships of Penrose tubing when P  $_{e}^{-P}$  = 10 mm Hg.

# The Effects of Length, Longitudinal Pre-stress, and Stretch

The effects of length, longitudinal pre-stress, and stretch were tested at  $P_e$ - $P_o$  = 16 mm Hg because the changes in the slope of the late rising phase of the curves seemed to be maximal at low levels of  $P_e$ - $P_o$ .

#### Length

An experiment with different lengths of tubing with no stretch resulted in the graph of Figure 5. Changes in length affected both the initial and late rising phases. During the initial rising phase, the 2.5 cm length of tubing was held partially open by the end constraints, resulting in a very low pressure gradient at flows less than 25 cc/sec. For the 2.5 cm length, no flutter, only a four-lobed constriction, was noted at all flow rates. This effect of the end constraints was also apparent in the initial rising phase of the curve for the 3.5 cm segment of tubing. The pressure difference of the late rising phase reached a maximum at a length of 5.5 cm. At lengths greater than 5.5 cm, the slope of the late rising phase decreased with length. Representative flutter data for lengths greater than 4.5 cm is presented in Table 4.

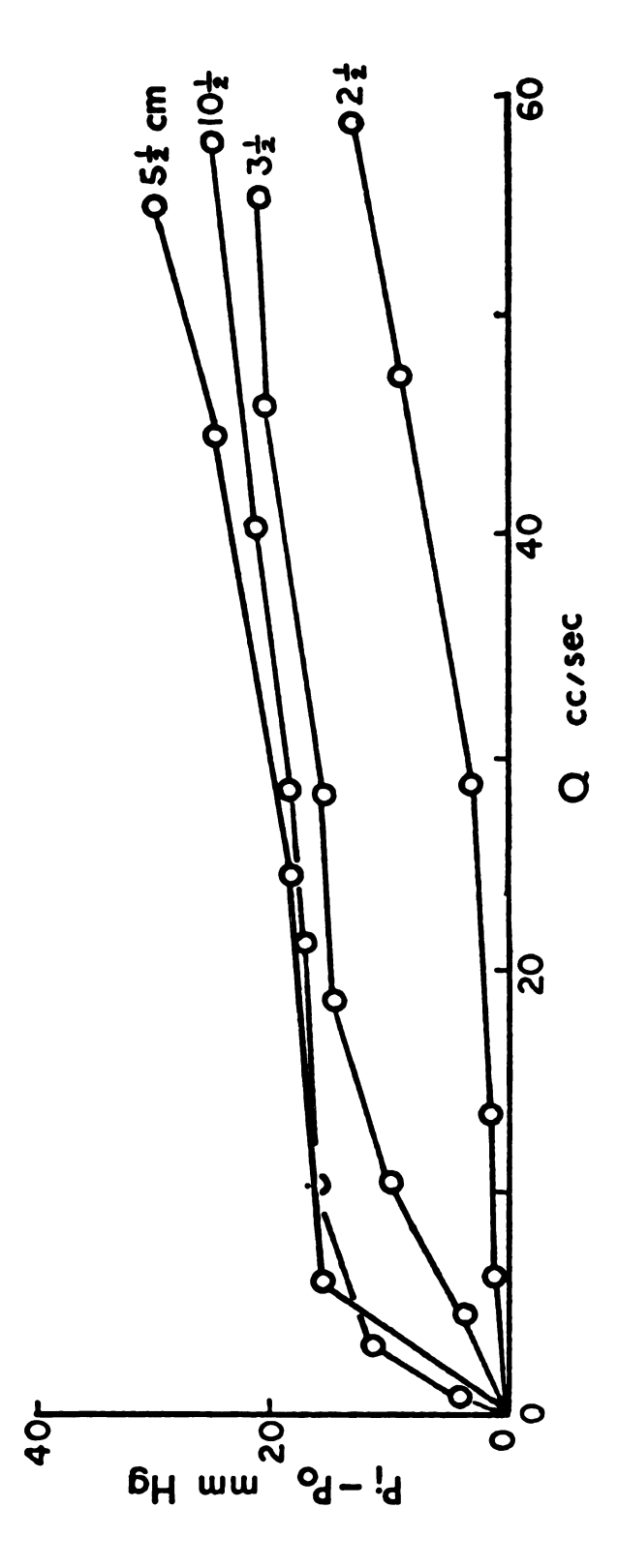


Figure 5. The effect of length on the pressure-flow relationships of Penrose tubing when  $P_{e}$  -  $P_{o}$  = 16 mm Hg.

Table 4. The Effect of Length of Vessel on Frequency and Pressure Amplitude of Oscillations

P <sub>e</sub> -P <sub>o</sub> =	16 mm Hg.					
	27 cc/sec			75 cc/sec		
Length Cm.	Frequency Hz.	Amplitude mm Hg.	PP mm Hg.	Frequency Hz.	Amplitude mm Hg.	PP. mm Hg.
2.5	0	0	2	0	0	16
4.5	0	0	16	11	7	24
5.5	0	0	18	12	26	43
6.5	8	1	18.5	12	24	41
7.5	8	3	19	11.5	25	39
10.5	8	1.5	18	8	28	31.5
13.5	8	2	17.5	9	16	27

#### Longitudinal Pre-stress

A representative graph demonstrating the effect of longitudinal changes in pre-stress (tension) while length is held constant, is presented in Figure 6. Longitudinal pre-stress decreased the slope of the initial rising phase as compared to the same length unstressed.

Increased longitudinal tension, which resulted from pre-stress probably decreased the compliance of the tube for cross-sectional changes and so the end constraints tended to keep the tubing open, and this decreased the slope of the initial rising phase. This effect was more marked with shorter lengths. Longitudinal pre-stress increased the pressure amplitude of the flutter and increased the slope of the late rising phase when compared to the same length unstressed. The effect of longitudinal pre-stress on flutter is presented in Table 5.

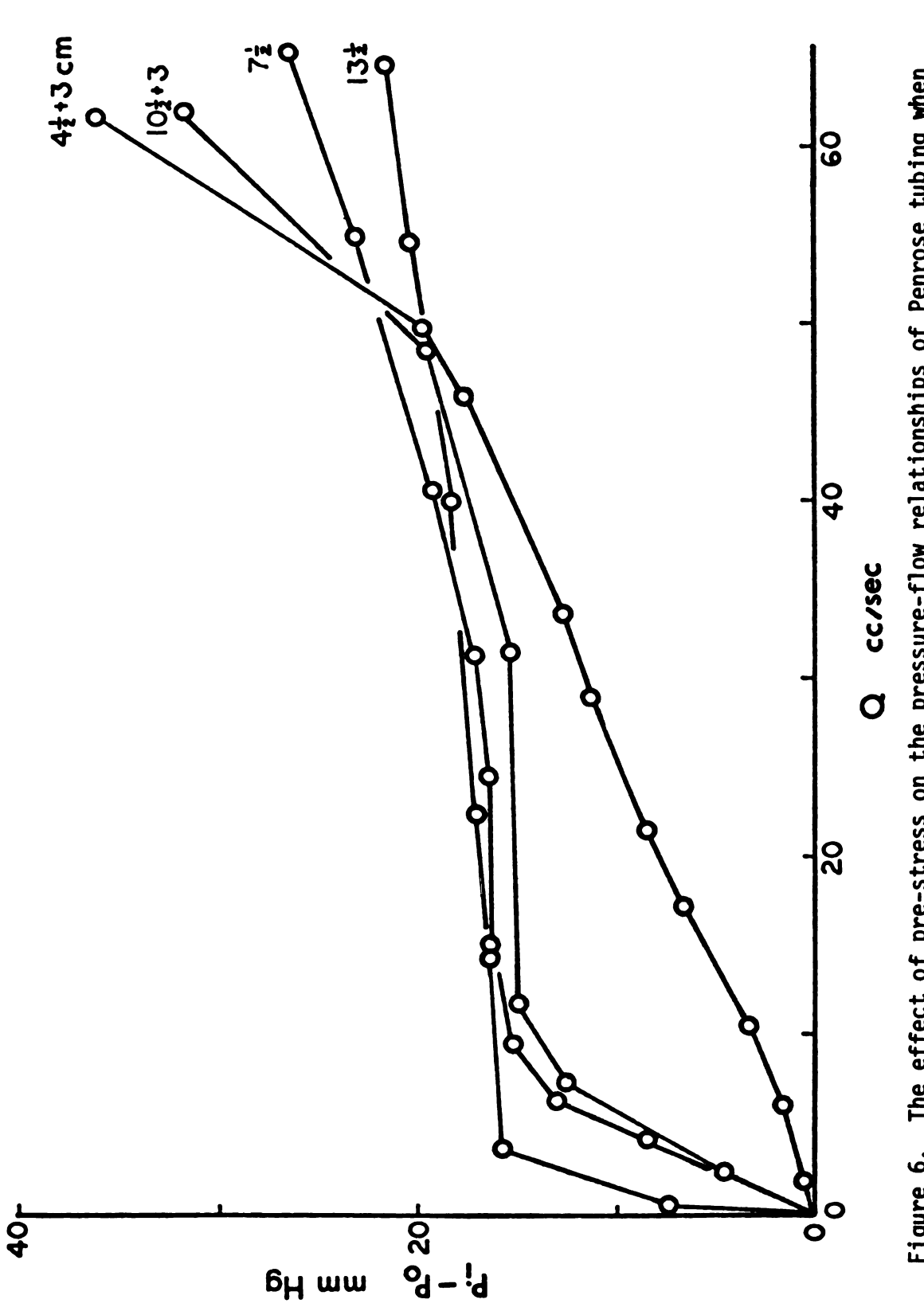


Figure 6. The effect of pre-stress on the pressure-flow relationships of Penrose tubing when  $P_e-P_0=16~\text{mm}$  Hg.

Table 5. The Effect of Longitudinal Pre-stress on Frequency and Pressure Amplitude of Oscillations

$P_e-P_o = 16 \text{ mm Hg.}$ Flow rate = 75 cc/sec					
Manufactured Length cm	Experimental Length cm	Frequency Hz	Amplitude mm Hg.	P <sub>i</sub> -P <sub>o</sub> mm Hg.	
13.5	13.5	8.8	29	27	
10.5	13.5	8.5	63	39	
10.5	10.5	9.3	38	31	
7.5	10.5	10.1	43-58	41.5	
7.5	7.5	10.8	20-30	33	
4.5	7.5	11.2	52-54	54.5	

#### Stretch

The effect of stretch was quantified by taking a 4.5 cm. length of tubing and recording the characteristics when it was stretched to 5.5, 6.5, 7.5, 8.5, and 9 centimeters length. In this manner, both longitudinal stress and stretched length were increased concommitantly. Whereas for the previous experiments, the changes were reasonably consistent, the results obtained for stretch, which is a combination of longitudinal stress and length, were less so. Therefore, a statistical analysis of the pressure gradient at a flow rate of 74 cc/sec was undertaken (Table 6). This analysis demonstrated that at this high flow rate, the pressure gradient increased as the tube was stretched from 4.5 to 7.5 cm. When stretched to 7.5 cm., the tube existed in either one or

Table 6. The Effect of Stretch on Resistance. (n = 25)

$P_e - P_o = 16 \text{ mm} \text{ F}$	lg. Flow rate	= 74 cc/sec		
Manufactured Length	Experimental Length	Pi-P mean	PP s.d.	Resistance
Cm.	Cm.	mm Hg.	mm Hg.	mm Hg/cc/sec
4.5	4.5	25.9*	2.4	0.35
4.5	5.5	38.5*	2.5	0.52
4.5	6.5	56.1*	3.2	0.76
4.5	8.5	42.0*	1.6	0.57
4.5	9.0	43.9*	0.9	0.59

<sup>\*</sup>P < 0.05

the other of two distinct states: a high resistance state of vigorous flutter (mean  $P_i-P_0=52.6$  mm Hg), or a lower resistance state of less vigorous flutter (mean  $P_i-P_0=36.5$  mm Hg). Stretched to 8.5 cm. and 9 cm., the resistance of the tube increased incrementally from its lower resistance state at 7.5 cm. As can be seen from Figure 7, stretch also decreased the slope of the initial rising phase. The effect of shortening the tube shorter than manufactured length was to cause either kinking or intussusception. When the tube kinked, either a partial or complete blockage of flow resulted. Intussusception decreased flutter and decreased the slope of the late rising phase, probably by the mechanism of increased outflow resistance.

Analysis of variance (Table 7) was performed on the raw data of the stable stretched lengths. Tukey's multiple comparisons between all

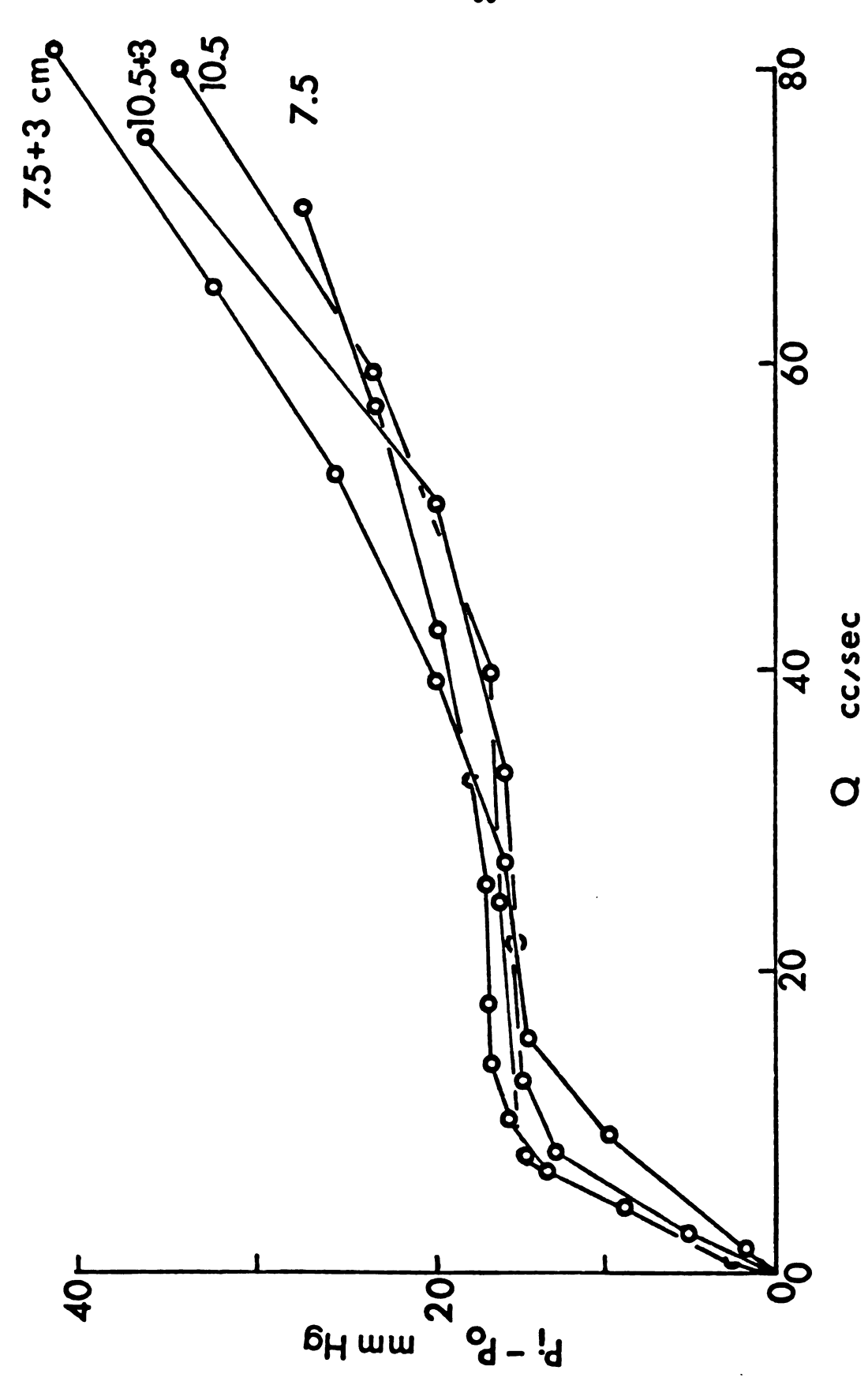


Figure 7. The effect of stretch on the pressure-flow relationships of Penrose tubing when  $P_{e}$  -  $P_{o}$  = 16 mm Hg.

Table 7. Analysis of Variance: The Effect of Stretch on Resistance.  $P_e^{-P_o} = 16 \text{ mm Hg}$ , Flow Rate of 74 cc/sec.

ANOVA		Cum of		
Source	df	Sum of squares	Mean square	F
Treatment	4	89,101.2	22,275.5	586.8*
Error	120	4,555.3	38.0	
Total	124	93,656.6		

<sup>\*</sup>P<0.005

stable means proved significant (p<0.05). Table 8 summarizes the data obtained from a representative experiment to elucidate the effect of stretch on frequency and pressure amplitude of flutter. It shows that the pressure amplitude of the flutter of the stretched tubing was always greater than that for the unstretched tubing.

Table 8. An Example of the Effect of Stretch on Frequency and Pressure Amplitude of Oscillations

$P_e - P_o = 16 \text{ mm H}$	g. Flow rate =	75 cc/sec		
Manufactured Length Cm	Experimental Length Cm	Frequency Hz	Amplitude mm Hg.	P <sub>i</sub> -P mm Hg.
4.5	4.5	11	6-8	26.8
4.5	5.5	10.25	24-30	33.5
4.5	6.5	12.25	58	63
4.5	7.5	11.25	47	51.8
4.5	7.5	9.7	9-26	33.3
4.5	8.5	11	12-47	40
4.5	9.0	4.1	7-50	44.3

#### The Effect of Viscosity (0.5 Stokes)

A representative graph of the pressure-flow relationships of 7.5 cm Penrose tubing held at manufactured length, during perfusion with 0.5 stokes fluid is presented in Figure 8. Note the continued presence of the initial rising phase with zero pressure intercept, for flow rates less than 3 cc/sec. Although flows up to 60 cc/sec were measured, the results are not presented in the graph because an increase of slope at high flow rates (third phase) was never observed. Flutter was initiated precipitously at 20 to 30 cc/sec and was of comparable frequency, but much lower pressure amplitude at any given flow rate when compared with the flutter observed during water perfusion (Table 9). Linear regression for the slopes of these curves at flow rates greater than 10 cc/sec yielded these slopes:

 $P_e - P_o = 10 \text{ mm Hg}, 0.118 \text{ mm Hg/cc/sec}.$   $P_e - P_o = 15 \text{ mm Hg}, 0.155 \text{ mm Hg/cc/sec}.$   $P_e - P_o = 30 \text{ mm Hg}, 0.105 \text{ mm Hg/cc/sec}.$   $P_e - P_o = 60 \text{ mm Hg}, 0.181 \text{ mm Hg/cc/sec}.$ 

These slopes are two to four times the slope calculated from Poiseuille's law for the open Penrose tube (0.041 mm Hg/cc/sec) perfused with 0.5 stokes fluid. The resistance of the open tube to this fluid determined experimentally was 0.0537 mm Hg/cc/sec. Neither outlet resistance nor removal of the end piece distal to the  $P_{\rm O}$  port caused any apparent change in this slope. The cross-sectional shape of the tube during the early rising phase of the curves varied from round at the inflow end,

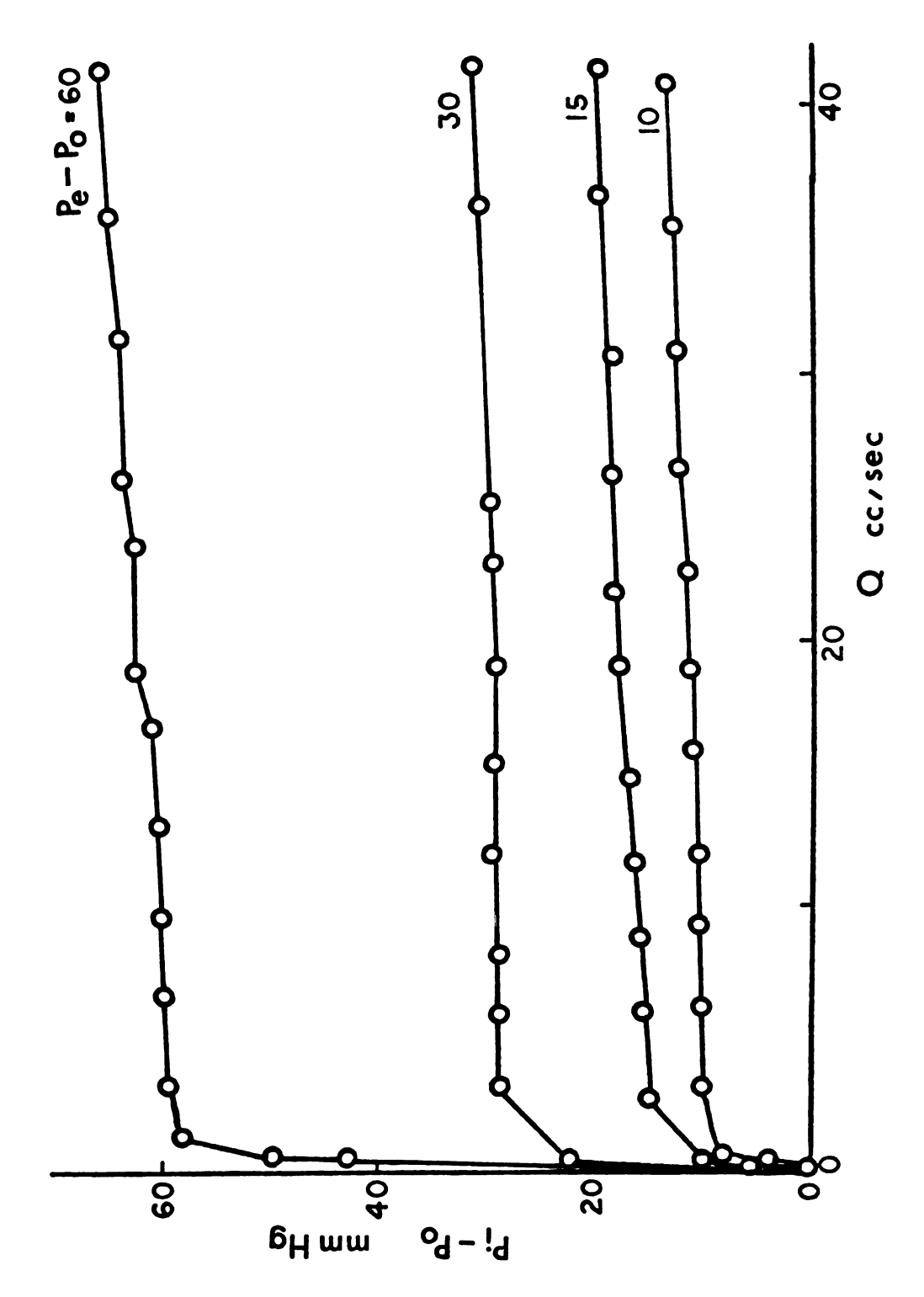


Figure 8. Pressure-flow relationships of 7.5 cm tubing during perfusion with 0.5 stokes fluid.

Table 9. The Effect of Viscosity on Frequency and Pressure Amplitude of Oscillations

Viscosity in stokes	Flow cc/sec.	Amplitude mm Hg.		Frequency Hz	PP mm Hg.
		P <sub>i</sub>	Po		
0.01	16	1	*	5.5	11
0.50	14.5	0	12	6.0	10.8
10.	14.5	0	0	0	
0.01	50	16	*	7	16.8
				I	I

 $<sup>^{*}</sup>P_{\Omega}$  amplitude too great to measure.

52

0.50

to oval in the center, and flattened at the outlet. As flow was gradually increased from 3 cc/sec up to the flow at which flutter was initiated, a construction of the tubing at the outlet was observed. Maximum Reynolds number based on tubing diameter, maximum flow rate, and average velocity of flow for this data was 110.

15.5

8.2

### The Effect of Viscosity (10 Stokes)

A representative graph of the pressure-flow relationships of 7.5 cm Penrose tubing held at manufactured length, perfused with 10 stokes fluid is presented in Figure 9. Both the initial rising phase and the late rising phase are absent. No flutter of the tubing was ever observed during these experiments. When the tube was empty and collapsed

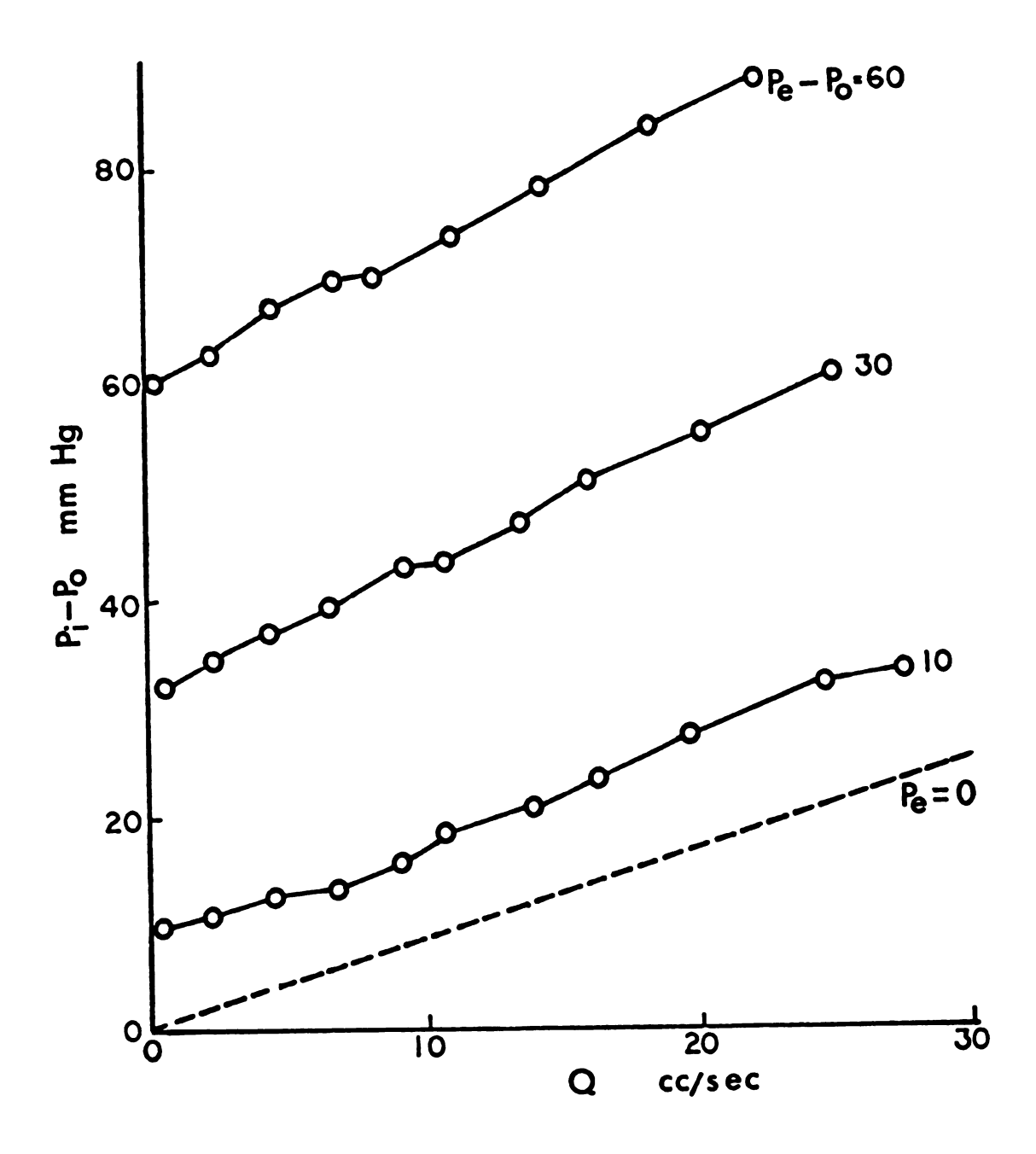


Figure 9. Pressure-flow relationships of 7.5 cm Penrose tubing during perfusion with 10 stokes fluid.

by the pre-set  $P_e$ , and fluid was pumped into the tube at a very low flow rate, the tube gradually opened from the inflow end toward the outflow end, and it was not until then that fluid began to exit from the outflow tubing. Throughout the entire flow range, the outflow end of the tube remained somewhat constricted. Linear regression yielded the following results:

For 
$$P_e - P_o = 60$$
 mm Hg.,  $Y = (1.26X + 60.03)$  mm Hg.  
For  $P_e - P_o = 30$  mm Hg.,  $Y = (1.16X + 31.42)$  mm Hg.  
For  $P_e - P_o = 10$  mm Hg.,  $Y = (0.92X + 8.16)$  mm Hg.  
(Y is the level of  $P_i - P_o$ , X is the flow rate)

These slopes are somewhat higher than the slope calculated from Poiseuille's law for the open Penrose tube perfused with this fluid, 0.829 mm Hg/cc/sec. The resistance of the open tube to this fluid, determined experimentally, was 0.848 mm Hg/cc/sec. Maximum Reynolds number based on tubing diameter, maximum flow rate, and average velocity of flow for this data was 2.6.

### Effects of Diameter and Tubing Composition

The pressure-flow relationships of the water perfused 0.635 cm diameter, 3.25 cm length Penrose tubing, mounted upon 0.635 cm internal diameter rigid tubing demonstrated an interesting effect of tubing diameter (Figure 10). The initial rising phase of the curves was steeper, and the plateau phase began earlier, at approximately 5 cc per second, at  $P_i$ - $P_0$  always lower than  $P_e$ - $P_0$ . Flutter of the tubing was

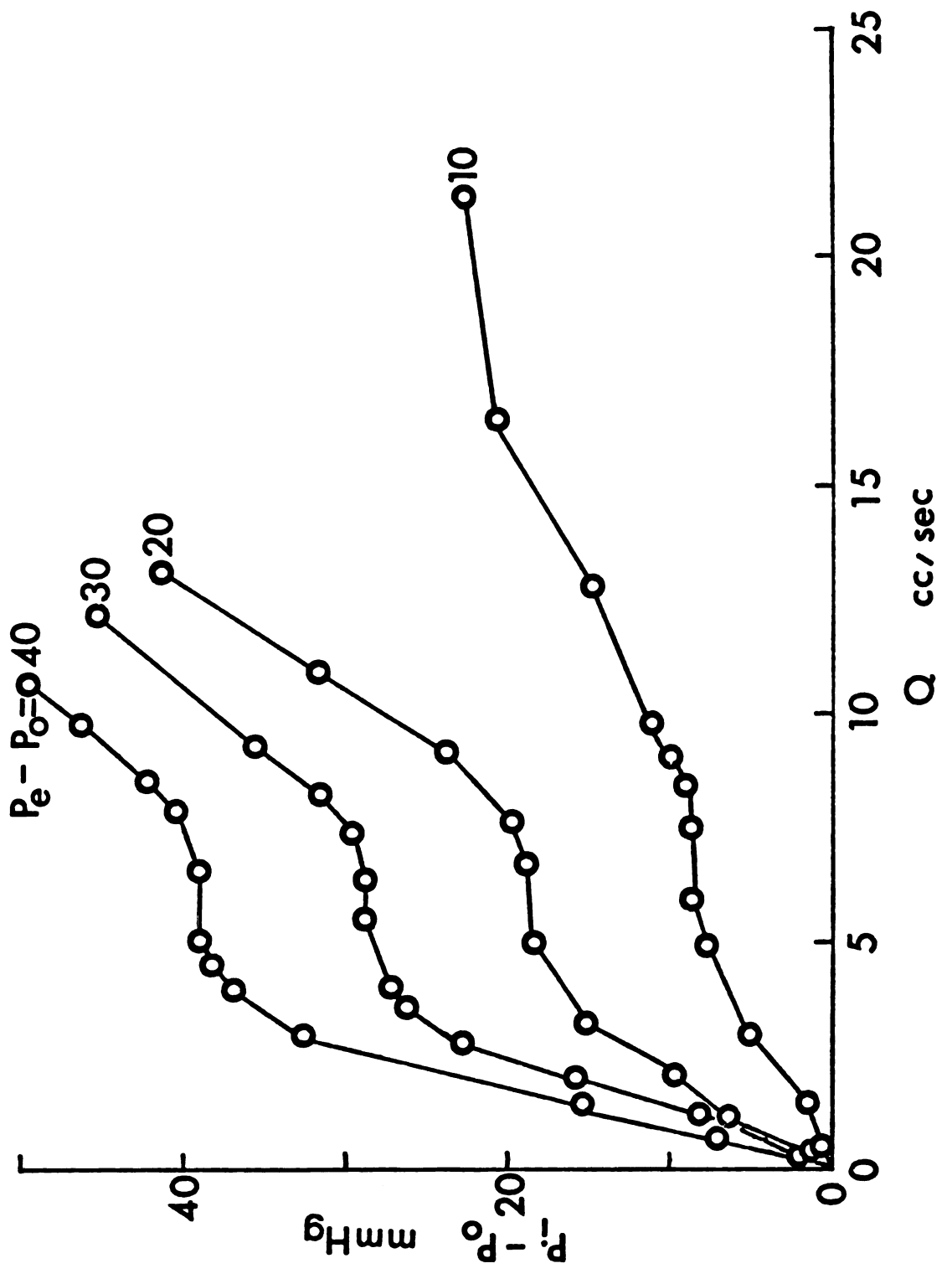


Figure 10. The effect of diameter: pressure-flow relationships of 0.635 cm diameter, 3.25 cm length Penrose tubing.

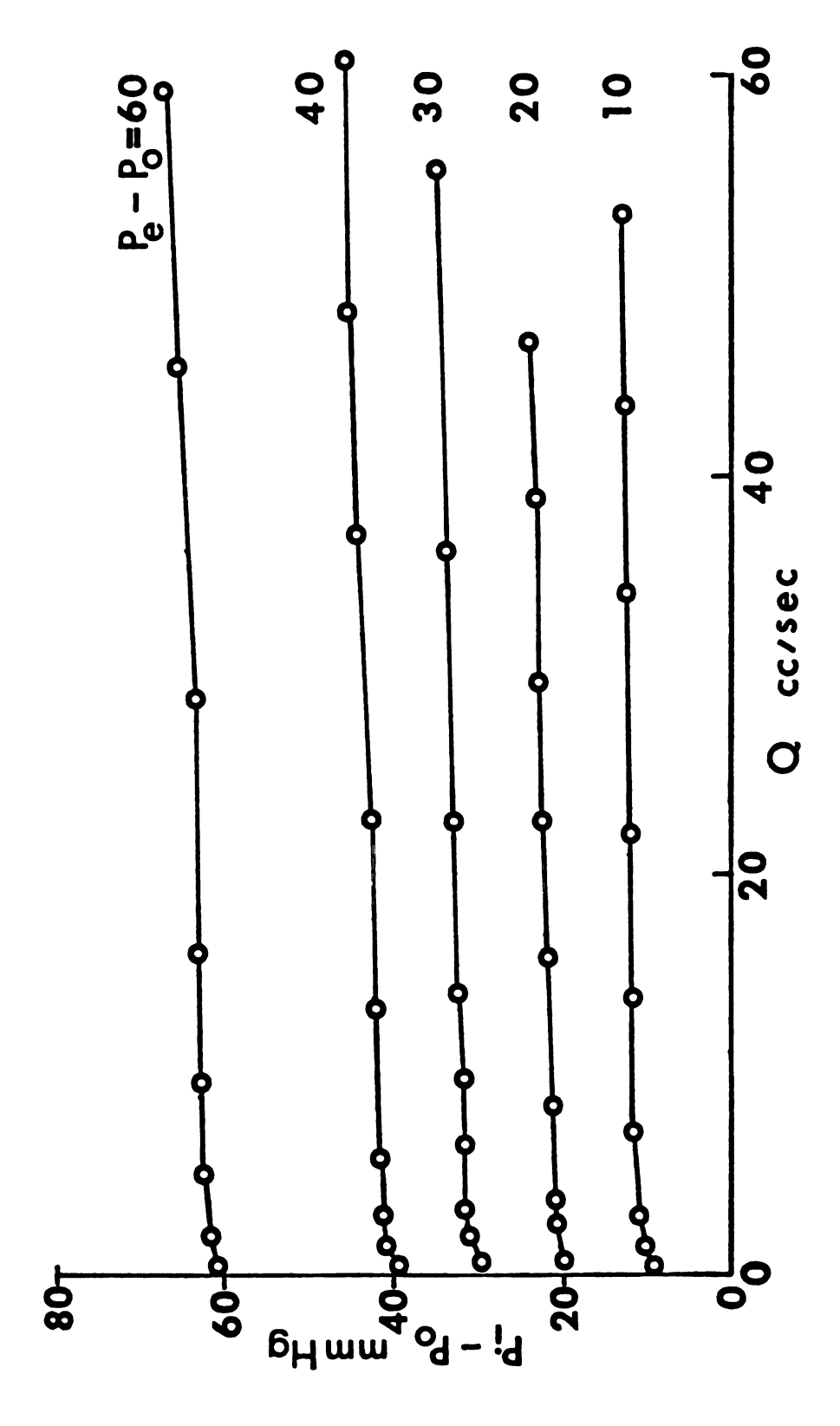


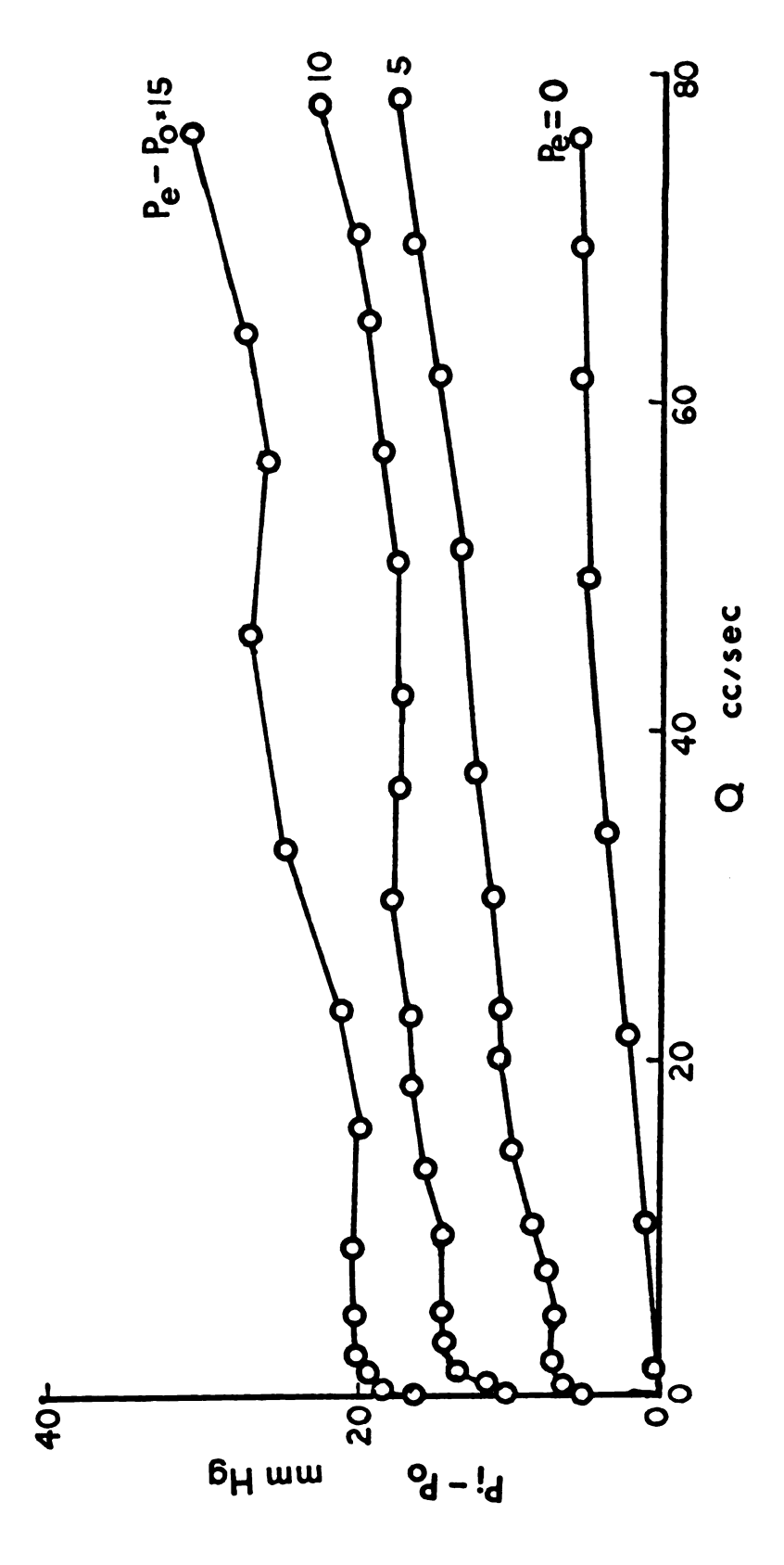
Table 11. Pressure-flow relationships of dialysis tubing, 1.5 cm diameter, 7.5 cm length.

noted at the beginning of the plateau phase and continued as flow was increased. The steep curve of the late rising phase also began at lower flow rates than when 1.27 cm diameter tubing was used, at a flow rate of approximately 8 cc/sec, while  $P_i-P_o$  was still less than  $P_e-P_o$ . The Reynolds number for water perfusion at 20 cc/sec of the 0.635 cm diameter tubing is 4,000.

Water perfusion of dialysis tubing, 1.58 cm diameter, 7.5 cm length resulted in the graph presented in Figure 11. The zero flow pressure intercept was approximately at  $P_i - P_o = P_e - P_o$ . The curve at flow rates less than 5 cc/sec was slightly convex to the pressure axis; at higher flow rates up to 77 cc/sec, the pressure-flow relationship appeared to be linear. At all flow rates above 5 cc/sec, a low intensity flutter of the tubing was apparent.

## Pressure-flow Relationships of Veins

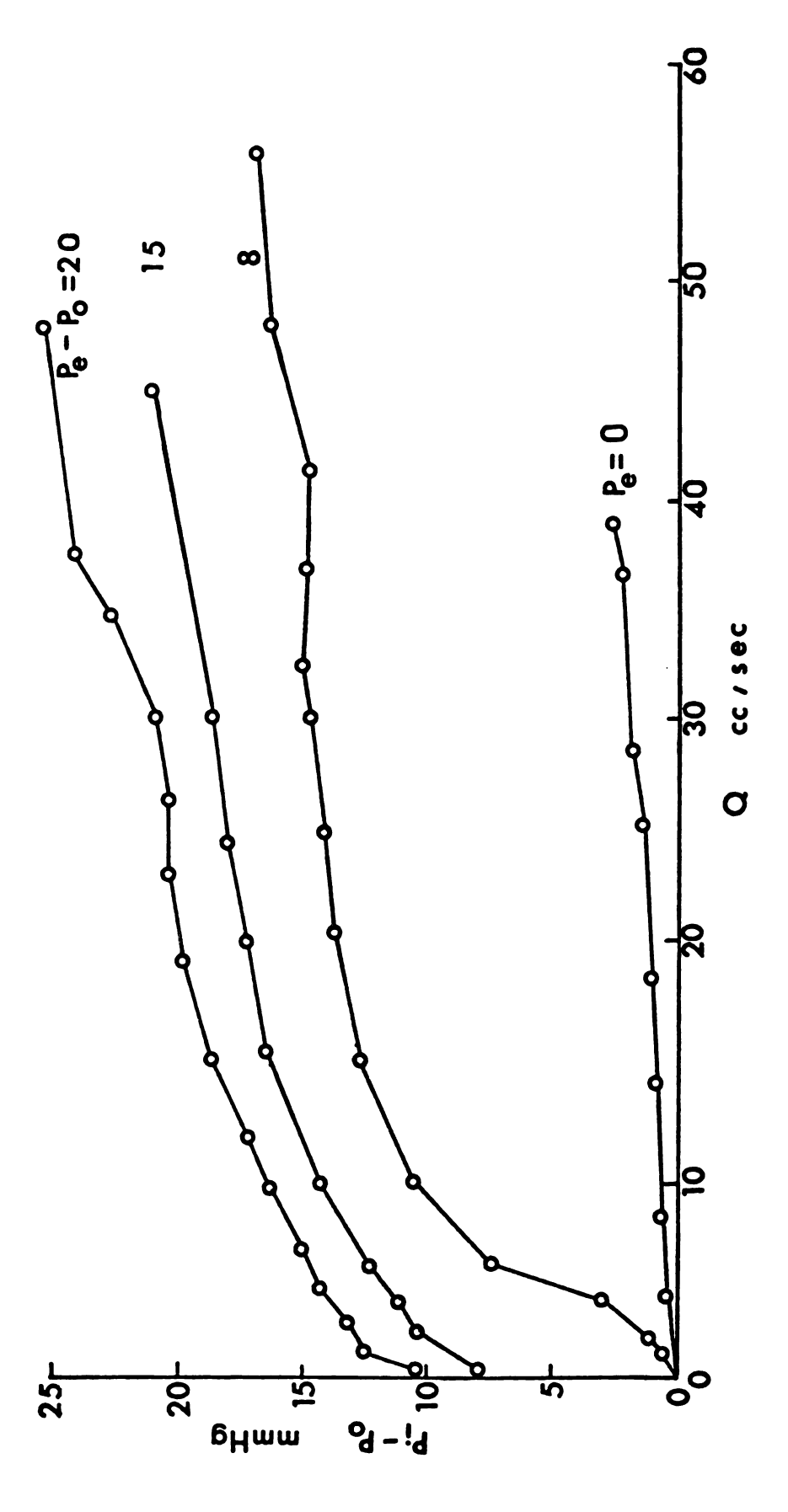
The pressure-flow relationships of an equine jugular vein, 7.5 cm in length, 1.3 cm diameter, perfused with blood, are presented in Figure 12. The graphs of the jugular veins perfused with blood and those perfused with Ringer's bicarbonate solution were qualitatively identical. Neither the Ringer's perfused, nor the blood perfused veins demonstrated a zero pressure-flow intercept for  $P_e-P_o$  greater than zero. The graph demonstrates that there was total closure of the vein at  $P_i-P_o < P_e-P_o$ , when  $P_i < P_e$ . At  $P_i < P_e$ , and in the very low flow ranges (less than 5 cc/sec), a three lobed collapse was observed. At flow



Pressure-flow relationships of the equine jugular vein, 7.5 cm length, during perfusion with equine blood. Figure 12.

rates greater than 5 cc/sec, the vein was seen to undergo a relatively weak flutter.

Perfusion of equine cephalic veins, 3.5 cm length, 0.64 cm diameter, with Ringer's bicarbonate solution resulted in the graph of Figure 13. When  $P_e^-P_0^-$  was held at 8 mm Hg, there was a zero pressureflow intercept. The curve showed an initial rising phase, convex to the pressure axis for flows less than 10 cc/sec. When  $P_e^-P_0^-$  was held at 15 mm Hg, the zero flow intercept was approximately 7.5 mm Hg; at  $P_e^-P_0^- = 20$  mm Hg, the zero flow intercept was approximately 11 mm Hg. In other words, flow began when  $P_i^-$  was from 7.5 to 9 mm Hg less than  $P_e^-$ . All three curves demonstrated a relatively steep initial rising phase, followed by a plateau phase, the slope of which is slightly greater than the slope of the pressure-flow relationship when  $P_e^- = 0$ . At flow rates greater than 30 cc/sec, there was a tendency for the slopes to increase, suggesting the presence of a third phase of pressure-flow relationships. A three lobed collapse was noted in the low flow ranges (zero to 5 cc/sec) and flutter was noted at all flow rates above 10 cc/sec.



Pressure-flow relationships of the equine cephalic vein,  $3.25\ \mathrm{cm}$  length, perfused with Ringer's bicarbonate solution. Figure 13.

#### VII. DISCUSSION

The non-linear pressure-flow relationships of collapsible vessels have been described by both a mathematical waterfall model (Permutt et al., 1962) and a physical model using a Starling resistor. Unfortunately, the predictions of pressure-flow relationships based on the two models do not seem to be in agreement with each other. The present work studies in depth the properties of flow through the Starling resistor model and compares the results to the waterfall model. For these experiments, blood flow through collapsible blood vessels was simulated by pumping fluid through a segment of Penrose tubing inside a pressurized box, and the relationship between external pressure  $(P_e)$ , inflow pressure  $(P_i)$ , outflow pressure  $(P_o)$ , and flow (Q) was investigated. The pressure gradient  $(P_i-P_0)$  was plotted as a function of Q at various constant values for  $P_e-P_o$ . An objective of this present study was to determine which model more closely approximates venous behavior, and toward this end, pressure-flow relationships of in vitro veins were also measured.

### Comparison of Models

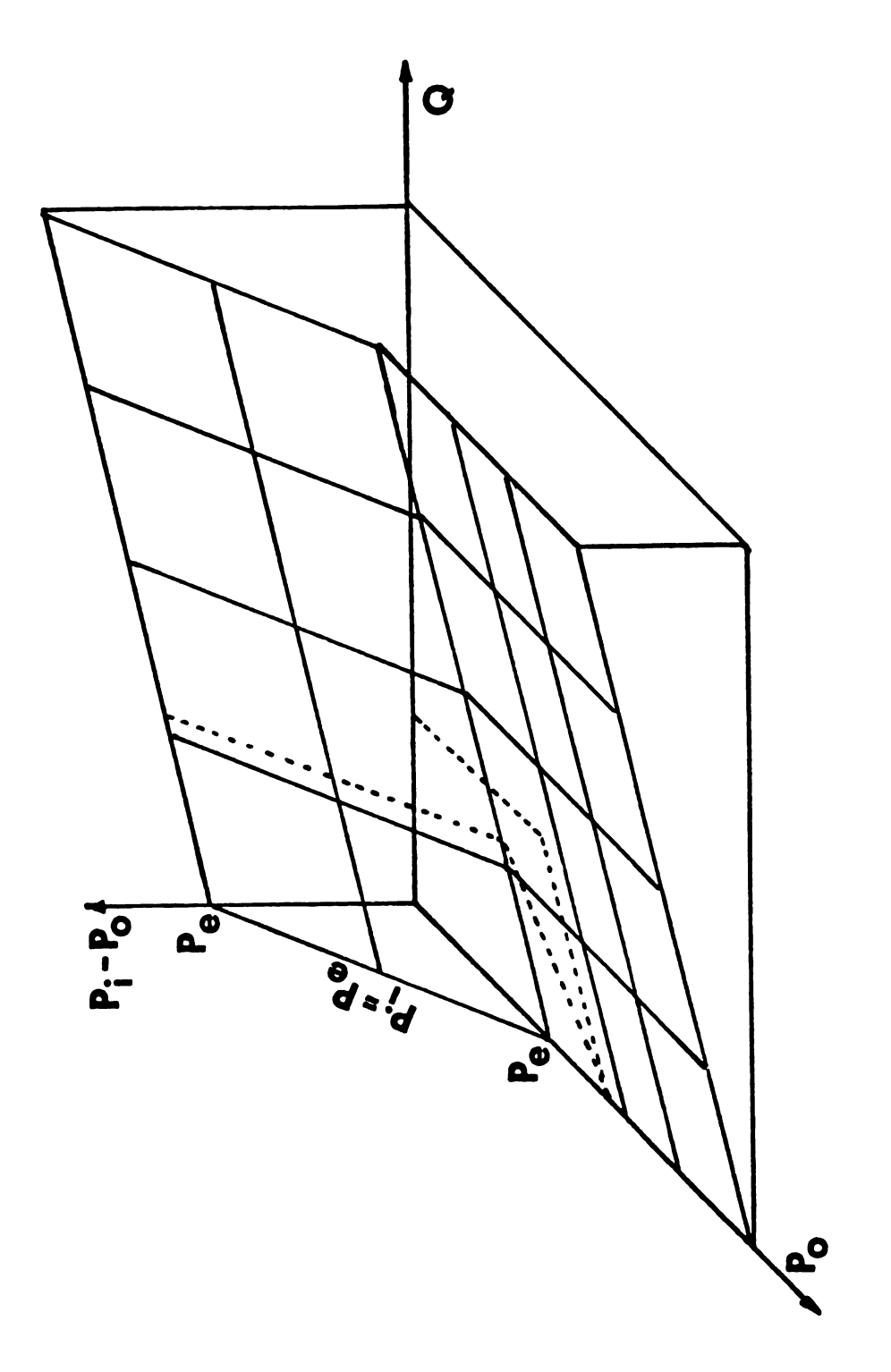
The pressure-flow relationships of the Penrose rubing Starling resistor model show that at low flow rates, where  $P_e > P_i > P_o$ , the initial steep slope of the curves increased as the parameter  $P_e - P_o$ 

increased. This data confirms the predictions of Brower and Noordergraff (1973). In this flow range, the pressure-flow relationships were also similar to those reported by Conrad (1969), Katz et al. (1969), and Moreno et al. (1969). This might be expected even though the aforementioned investigators held  $P_e$  constant, while  $P_e^-P_o$  was held constant for this investigation. This similarity is accounted for by the fact that in this flow range  $P_o$  is low, so the difference between  $P_e$  and  $P_e^-P_o$  is minimal. This early rising phase is not predicted at all by the waterfall model, and reasons for this will be discussed subsequently.

At flow rates of approximately 6 to 8 cc/sec, the curves leveled off to a plateau, the second phase. As the parameter  $P_e$ - $P_o$  was increased, this second phase began at lower flow rates. Although the pressure-flow relationships in these flow ranges are similar to the theoretical curves of Brower and Noordergraaf (1973) and those of the waterfall model, they are strikingly different from those of Conrad (1969), Katz et al. (1969), and Moreno et al. (1969). Three dimensional pressure-flow surfaces for both the mathematical waterfall model (Figure 14) and the Starling resistor physical model (Figure 15) will serve to clarify the differences between the two models at these flow rates.

#### The Waterfall Model

On the axes of this three dimensional graph are Q extending across the page,  $P_i$ - $P_o$  extending upward, and  $P_o$  coming out of the page. The parameter  $P_e$  is held constant. Note that there are sharp transitions



Three-dimensional surface of the pressure-flow relationships predicted by the mathematical waterfall model. Figure 14.

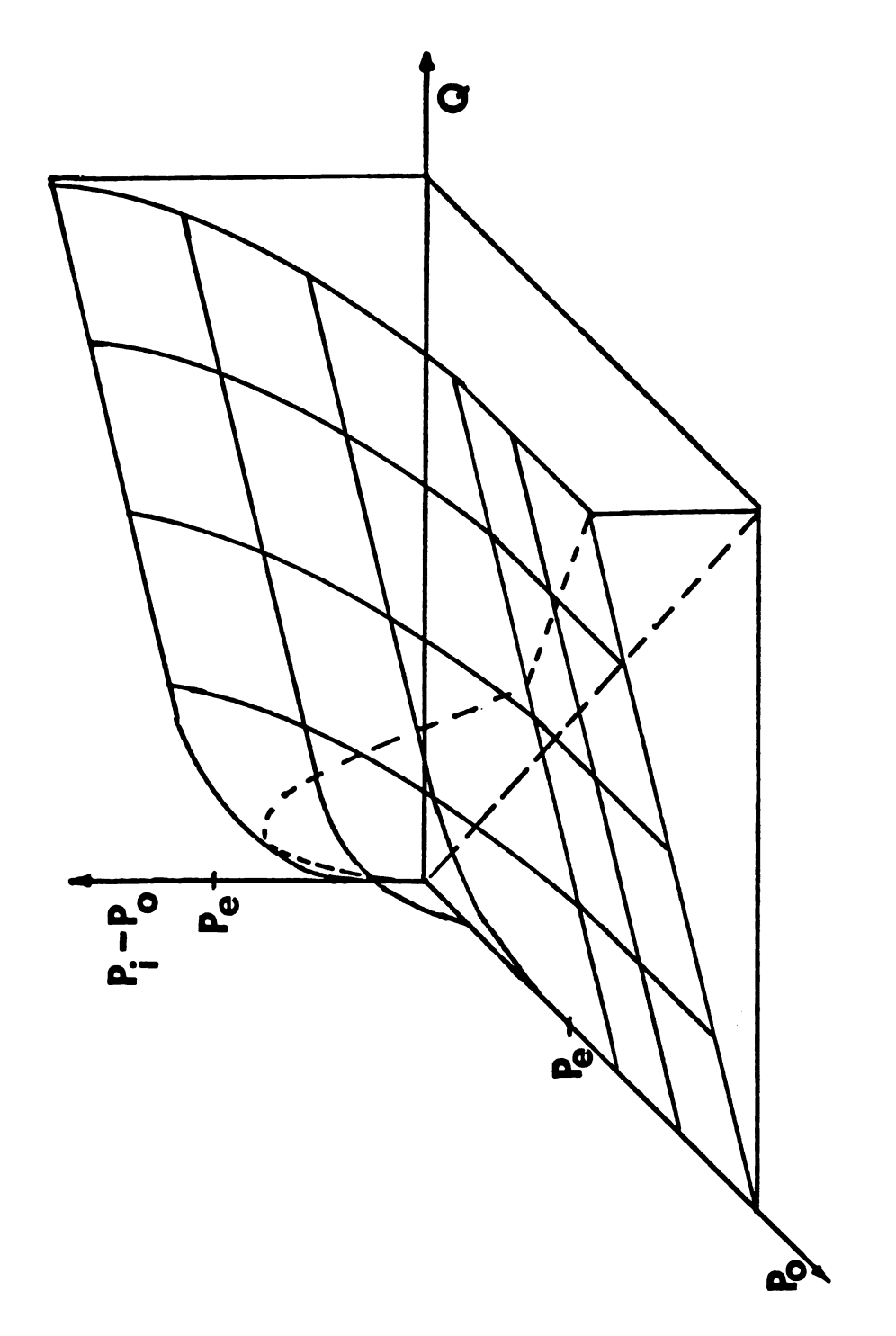


Figure 15. Three-dimensional surface of the pressure-flow relationships of Penrose tubing.

between the three flow regimes proposed by Permutt et al. (1962). The lower portion of the figure represents the flow regime of the fully expanded tube, when  $P_i > P_o > P_e$  and

$$Q = \frac{P_i - P_o}{R} . (1)$$

The no flow regime corresponds to  $P_e > P_i > P_o$  and is represented by the small triangle bounded by the  $P_i - P_o$  axis, and  $P_o$  axis, and the line  $P_i = P_e$ . Q = 0 unless  $P_i$  exceeds  $P_e(P_i - P_o > P_e - P_o)$ , and when inflow is suddenly stopped,  $P_i$  drops to the level of  $P_e$ . The upper portion of the figure depicts flow when  $P_i > P_e > P_o$  and

$$Q = \frac{P_i - P_e}{R} , \qquad (2)$$

hence

$$P_i - P_o = R Q + P_e - P_o$$
 (8)

The dashed lines represent Permutt's original formulation of the waterfall model (1963), as it was presented in graphic form: Q as a function of  $P_{\Omega}$ .

# The Starling Resistor Model

Pressure-flow relationships of a Penrose Starling resistor are depicted in Figure 15. Note that while the curves in the regime of  $P_i > P_e > P_o$  are similar to the above graph, the curves become rounded when  $P_e > P_i > P_o$ , due to the fact that under these conditions, flow persists through small side channels of the collapsed tube.

The curves emanating from the  $P_0$  axis, where  $P_e > P_0$ , represent the pressure-flow relationships which were recorded during this present

study, using minimal outflow resistance and holding  $P_e^-P_o$  constant. If  $P_e$  rather than  $P_e^-P_o$  is held constant and there is a high level of outflow resistance, then as  $P_o$  increases linearly with Q,  $P_o$  approaches and then exceeds  $P_e$ . The resulting curve cuts diagonally across the surface along the dashed line. Such a curve is typical of those generated by Conrad (1969), Katz <u>et al</u>. (1969), and Moreno <u>et al</u>. (1969), when they experimented with high outflow resistance and plotted  $P_i^-P_o$  as a function of constant  $P_e$ , but greatly decreasing  $P_e^-P_o$ .

The three-dimensional graphs serve to illustrate that the so-called "negative resistance" region in the curves of Conrad (1969), Katz et al. (1969), and Moreno et al. (1969) results from their particular method of experimentation. In fact, by drawing a similar curve diagonally across the pressure-flow surface of the waterfall model, a region of negative slope can be demonstrated.

One of the major differences between the two models appears to be the presence of an early rising phase of the curves in the Starling resistor model, and its absence in the waterfall model. In pilot experiments, we found that the mechanical properties of Penrose tubing changed when it was exposed to air, heat, and light for an extended period of time. Under these circumstances, perfusion of the deteriorated Penrose tubing did not yield an early rising phase of pressureflow relationships. Nor did water perfusion of dialysis tubing (Figure 9). This indicates that a different type of tubing may have been used by Permutt et al. (1962) for their physical model from which they derived their mathematical model of flow through collapsible vessels.

### General Characteristics

#### The First Phase: The Early Rising Phase

In our experiments with water perfusion, we found that the slope of the early rising phase was increased by increasing  $P_e^-P_o^-$ , increasing length of tubing, and decreasing diameter of the tubing. Increasing viscosity also increased the slope of the first phase. Pre-stress and stretch decreased the slope.

These results indicate that the greater the rigidity of the vessel wall opposing bending and complete closure of the lumen, the lower will be the slope of the initial rising phase. This is confirmed by the fact that the dialysis tubing, which is extremely compliant at low transmural pressures, collapsed completely and did not present an initial rising phase of pressure-flow relationships.

#### The Second Phase: The Plateau Phase

During water perfusion, a second phase of the pressure-flow relationships, the plateau phase, began at flow rates of 6 to 8 cc/sec, when  $P_i$ - $P_o$  was almost equal to  $P_e$ - $P_o$ . At these pressures, a critical transmural pressure was achieved at which the sides of the collapsed tube were no longer in contact with each other. Oscillations of low pressure amplitude developed in the tubing at the beginning of the plateau phase and continued throughout this phase. In this flow range, the frequency of the oscillations increased as the level of  $P_e$ - $P_o$  was increased.

Other investigators (Katz <u>et al.</u>, 1969; Moreno <u>et al.</u>, 1969; Conrad, 1969) have noted the appearance and then gradual disappearance of this oscillatory phenomenon. One reason for the disappearance of the oscillations is that these investigators held  $P_e$  constant, and used high outflow resistance. As  $P_o$  approximated  $P_e$ , the relationship  $P_i > P_e > P_o$ , upon which the oscillatory mechanism is dependent, became  $P_i > P_o > P_e$ . Under these conditions, the tube does not flutter, but remains fully open to flow.

During water perfusion, the slope of the curves of the second phase for  $P_e^-P_o^-$  greater than zero, was consistently slightly higher than the slope of the open Penrose tube at  $P_e^-=0$ . The slope predicted by the waterfall model in the region of  $P_i^->P_e^->P_o^-$  is identical to that of the open tube of circular cross-section. The slightly higher slopes of this experimental study can be attributed to the low amplitude oscillations of the tubing during the second phase of pressure flow relationships.

Brower and Noordergraaf (1973) predicted in their theoretical treatment of characteristics of collapsible tubes that  $P_i^-P_o$  would reach an asymptotic value near  $P_e^-P_o^-$ . The curves measured in the laboratory of Brower and Noordergraaf showed that  $P_i^-P_o^-$  rose above the level of  $P_e^-P_o^-$ , but they concluded that this was due to systematic error in data collection. However, they did not measure pressure-flow relationships at Q>14 cc/sec, and therefore did not foresee  $P_i^-P_o^->P_e^-P_o^-$ .

### The Third Phase: The Late Rising Phase

In the present study, pressure-flow relationships were measured at Q>14 cc/sec. These higher flow rates represent physiological flow ranges for this reason. A peak blood flow velocity of 146.7 cm/sec has been measured in the inferior vena cava below the confluence of the hepatic veins following two and a half minutes of moderate exercise by unasthetized male volunteers (Wexler et al., 1968). This flow velocity represents a Reynolds number of 6,400 to 8,000, as calculated by use of their data for inferior vena cava diameter (2.2 cm) and a blood viscosity of 0.04 to 0.05 stokes (Strandness and Sumner, 1975). This Reynolds number corresponds to a flow rate of 64 to 80 cc/sec when the physical model employed in this present study is used to model flow. For this reason, flow rates much higher than 14 cc/sec are required to model physiological flow ranges.

At these higher flow rates, the curves demonstrated a late rising phase. As the parameter  $P_e$ - $P_o$  was increased, this late rising phase was less pronounced and occurred at higher flow rates. On the representative graph (Figure 2), a late rising phase was not seen at all for  $P_e$ - $P_o$  = 50 mm Hg. Decreasing the diameter of the tubing by one half caused the late rising phase to appear at approximately one half the flow rate of the larger diameter tubing.

The following evidence indicates that this late rising phase is related to the pressure amplitude of the oscillatory phenomenon:

1) At low levels of  $P_e^-P_o^-$ , during the third phase, the frequency of oscillations was relatively unaffected, but the pressure amplitude

was greatly increased, and a pronounced third phase was present (Table 1).

- 2) At high flow rates, the frequency of the oscillations increased as  $P_e^-P_o^-$  was increased but the pressure amplitude was lower, and the third phase was less apparent at higher  $P_e^-P_o^-$  (Table 1).
- 3) Outflow resistance applied beyond the  $P_0$  pressure port had the effect of decreasing oscillatory pressure amplitude greatly, and frequency only somewhat, but decreased the slope of the third phase appreciably (Table 3).
- 4) For those other manuevers which changed the slope of the third phase (i.e., length, stress, stretch), the maximum pressure difference of the third phase consistently reflected the pressure amplitude of the oscillations. (The 10.5 cm length of tubing was the one exception.) (Tables 4, 5 and 8.)
- 5) When  $P_e^-P_o$  was held at zero and the tube was perfused at high flow rates, the tube existed in either an oscillatory state or non-oscillatory state.  $P_i^-P_o^-$  for the oscillatory state was much greater than for the non-oscillatory state (Table 2).
- 6) For the experiments in which the tube was perfused with 0.5 stokes fluid, no late rising phase was ever seen; at high flow rates comparable to those of water perfusion, the amplitude of the oscillations was lower for the 0.5 stokes perfusion, but their frequency was not (Table 9).

The preceding analysis indicates that the late rising phase is directionally related to the pressure amplitude of the oscillations.

However, the direction of change in the slope of the third phase was not always consistent for a given factor. For example, length and stretch both increased the slope of the third phase, but beyond a given increment, further increases in length and stretch decreased the slope of the third phase. It is tempting to speculate about the possibility of some phenomenon common to all these factors being the cause of the late rising phase of pressure-flow relationships.

A possible cause of third phase pressure-flow relationships could be the occurrence of turbulent flow. Several factors tend to diminish this possibility. First, the Reynolds number at which the onset of the third phase was noted was approximately 1,900, and it is unusual for turbulence to occur in a long straight tube at Reynolds numbers less than 2,000. Second, our experimental apparatus consisted of a straight smooth inflow tube of length ten times the diameter of the collapsible tube, and a steady, non-pulsatile inflow. Neither of these conditions favor the development of turbulence. In addition, a test was conducted to determine if turbulent flow was the cause of the third phase. A glass tube of 1.27 cm internal diameter was used for an end-piece, and a constant infusion pump (Harvard Apparatus Infusion Pump, Dover, Mass.) was used to inject dye into the flowing stream of water as it exited the collapsible tubing. At low flows, the dye streamed in a thin thread. During the second phase, when flutter occurred, the dye began to show a periodic variation in density along the length of the glass outflow tubing. At third phase pressure-flow conditions, the periodic changes in density of dye became more intense and the length

between two periods of intense color became smaller. The expectation for the appearance of the dye, if turbulent flow were present, would be that of total diffusion and uniform color, but the steady transition of the appearance of the dye, from diffuse to well differentiated waves of color, argues against the onset of turbulence as a cause for the high resistance of the third phase. Consequently, it is concluded that turbulent flow can be ruled out as the cause of the late rising phase.

The wide variety of factors that influence the magnitude of the third phase, as well as the biphasic pattern brought about by some of those factors (length and stretch), indicate that this late increase in driving pressure probably arises from a complex interaction of factors. However, the possibility of some unknown single causative phenomenon common to all of the factors which influence the third phase cannot be completely ruled out.

# The Effect of Outflow Resistance: Physiological Implications

The experiments of Rodbard (1955) and Conrad (1969) demonstrated that when  $P_e$  was held constant, an increase in outflow resistance decreased the frequency of the oscillations of the tubing. One purpose of my experiments was to determine if outflow resistance would affect the oscillations when  $P_e^-P_o^-$ , and hence transmural pressure at the outflow end of the tube, was held constant. At constant  $P_e^-P_o^-$ , increased outflow resistance did decrease the frequency and pressure amplitude of the oscillation, and thereby decreased the magnitude of the third phase pressure-flow relationship.

It has been suggested (Rodbard and Saiki, 1953) that oscillations of collapsible blood vessels are responsible for the vibrations commonly found in the arterial system. Whether or not these arterial sounds result from turbulent flow, per se, or from vibrations of the arterial walls remains controversial (McDonald, 1968). However, there are venous sounds associated with palpable vibrations, e.g., the cervical venous hum, that is frequently found during high cardiac output states. This sound increases with inspiration, when resistance in the thoracic vessels is decreased (decreased  $R_0$ ), and it is suggested that pericardial tamponade, constrictive pericarditis, and right heart failure (all of which increase  $R_0$ ) would decrease the incidence of the cervical venous hum (Hardison, 1975). A venous hum has been experimentally produced over the femoral vein in individuals by tilting them head down at a 45° angle. Under these conditions, the femoral vein is not subject to its normal distending pressure, and is partially collapsed (Cutforth, 1970). These two examples of venous vibrations that are responsive to changes in outflow resistance appear to conform to the predictions of the model for oscillations in collapsible vessels. One final example of palpable, audible venous vibrations are those of the arteriovenous shunts of hemodialysis patients. Arteriovenous anastomoses also occur pathologically post-surgically. When blood of high flow velocity passes directly from a narrow segment of artery into a segment of vein, outflow pressure may be sufficiently low to cause the more compliant vein to undergo partial collapse and then flutter. The mechanism responsible for all of these venous vibrations is probably similar to that of the model:  $P_i > P_e > P_o$ .

# The Effects of Length, Pre-stress, and Stretch: Physiological Implications

Obviously, the length of a vessel is anatomically determined, and there is a great diversity of vascular lengths. There is also evidence that veins are continuously subjected to longitudinal stress (Yates, 1970; Moreno et al., 1970) associated with anatomical tethering of the vein to various structures within the body. Stretch can be viewed as a dynamic combination of an increase in both length and longitudinal stress. Both small and large vessels are subjected to stretch. For example, cyclical increases in volume subject the microcirculation of the lungs and heart to stretch, whereas the veins of the extremities are stretched by gross body movements. Brower's (1970) mathematical modeling of length and pre-stress serves to predict qualitative changes only, so the purpose of my experiments was to provide quantitative data regarding the effect of length, tension, and stretch upon vascular collapse.

The results of the tests of these various factors were similar in several ways. Short lengths of tubing, whether subjected to longitudinal tension or not, demonstrated longer, lower first phase pressure-flow relationships. This effect on the first phase was also noted when greater lengths were subjected to pre-stress and stretch. The collapsible tubing was held partially open by the rigid mounting tubing, thus creating an unfavorable condition for collapse. The rigid metal mounting tubing may be considered to represent anatomical tethering that tends to hold vessels open. Examples of anatomical tethering are the

junctions of the inferior vena cava with the right atrium and with the diaphragm. Because the venous sinuses of the brain and blood vessels within the bones are non-collapsible vessels, they too serve as anatomical tethering which tends to hold open the veins that lead away from them. From the results of this modeling experiment, then, it appears that short tethered vessels, and vessels under longitudinal stress tend to resist compression from external pressure during low flow states, when  $P_i$  falls below  $P_{\rho}$ .

At times, the first phase was so prolonged as to completely obliterate the second phase. The slope of the third phase was always increased by pre-stress and stretch over that of the unstressed tubing, but the effects of stretch and length were complex. The maximum  $\Delta P$  of the third phase was noted for 5.5 cm tubing. At greater lengths, the pressure amplitude of the oscillations and the maximum  $\Delta P$  of the third phase decreased consistently. For the longer segments, the appearance of the oscillating tube was that of a heavy bounding tube, and it appeared as if the weight of the perfusing water within the tubing was preventing the complete closure of the bottom half of the tubing. Therefore, long segments of tubing presented a decreased slope of the third phase of the pressure-flow relationships.

The multi-directional effect of stretch on the late rising phase may reflect the effects of increasing length. As stretch, and hence length, was increased, the maximum  $\Delta P$  of the third phase was achieved when the tubing was stretched to 6.5 cm. Beyond this, a slight increment of stretch caused instability of the pressure-flow relationship.

However, the resistance of the stretched tubing was always higher than that of the unstretched tubing.

Stretch of blood vessels occurs when anatomical structures increase in length. The circumference of the left ventricle has been shown to increase during the cardiac cycle by about 10 to 12 percent (Ninomiya et al., 1965). In contrast, bronchial segments have been shown to increase in length by 60 percent as the lung expands from residual volume to total lung capacity (Hughes et al., 1972). For this degree of stretch of blood vessels, the model predicts greatly increased resistance to blood flow.

### Hysteresis

When the 4.5 cm length of tubing was stretched to 7.5 cm, a hysteresis loop was noted. When the tube was stretched from 6.5 to 7.5 cm, a high  $\Delta P$  was obtained (52.6 mm Hg.). When the stretch of the tubing was decreased from 8.5 cm to 7.5 cm,  $\Delta P$  was reduced to 36.5 mm Hg. Hysteresis of venous pressure-volume curves has been noted (Alexander, 1963), and the phenomenon has been called stress relaxation. A similar mechanism may have occurred here. This finding with the physical model indicates that when a vessel is stretched, it may have a higher resistance than if the same degree of stretch occurred as a result of relaxation from a higher state of stretch.

During the course of the present investigations, a second hysteresis loop was noted: the oscillatory and non-oscillatory states when external pressure was held at  $P_e-P_o=0$ . The non-oscillatory state was

present when flow was gradually increased from 0 to 80 cc/sec. The oscillatory state occurred when  $P_e-P_o=0$  was approached from  $P_e-P_o>0$  at moderate flow rates. This state could be converted to a non-oscillatory state by a slight increase in outflow resistance.

In their discussion of the effects of outflow resistance on the oscillatory phenomenon, Rodbard and Saiki (1953) report that slight outflow resistance from a surgeon's finger is often enough to cause "stenotic" heart valve leaflets to fall away from each other and to return to normal functioning. A similar hysteresis loop may account for this effect.

# The Effects of Viscosity: Physiological Implications

A controversy exists regarding the possibility of tissue pressure induced self-excited oscillations of the blood vessels of the microvasculature (Conrad, 1973; Fung, 1973), but no quantitative data from modeling experiments is available. The waterfall model was originally proposed to explain pressure-flow relationships of the vessels of the microcirculation (Permutt et al., 1962), but if self-excited oscillations exist in the microcirculation, the pressure-flow relationships will differ from those of the waterfall model. In order to obtain quantitative data, high viscosity fluid was used to model pressure-flow relationships of the microcirculation. In this way, Reynolds numbers approaching those of the microcirculation could be achieved. Under such circumstances, modeling theory predicts that similar pressure-flow

relationships will be obtained. Ten stokes fluid was chosen because it was the highest viscosity that could practically be pumped through the physical model. This viscosity is considerably higher than that of water, which is approximately 0.01 stokes at room temperature; and that of blood, which, when corrected for shear rate, demonstrates an apparent viscosity of 0.05 stokes in the vena cava (Strandness and Sumner, 1975), and 0.04 stokes in the pulmonary microcirculation (Fung and Sobin, 1972).

When the pressure-flow relationships achieved by perfusion with low, moderate, and high viscosity solutions are compared, a progressive transition between each is noted. High Reynolds number flow, achieved with water perfusion, resulted in pressure-flow relationships with a high third phase. When 0.5 stokes fluid was used to achieve moderate Reynolds number flow, the third phase of the pressure-flow relationships did not appear, and a long straight second phase was evident. At the low Reynolds numbers achieved with 10 stokes perfusion, only the second phase of the pressure-flow relationships remained.

There was a very steep slope to the early rising phase of the pressure-flow relationships during perfusion with 0.5 stokes fluid; consequently, the plateau phase occurred at considerably lower flow rates than for water perfusion. The absence of an initial rising phase during 10 stokes perfusion seems to be an extension of this trend. The non-zero pressure intercept was very close to the level of Pe. This data indicates that a part of the non-zero pressure intercept noted during <u>in vivo</u> perfusion of vascular beds (Burton, 1951; Nichol <u>et al.</u>, 1951) is caused by and is approximately equal to total tissue pressure.

Compared with water perfusion, perfusion with 0.5 stokes viscosity fluid resulted in amplitude modulation of the oscillations. Instead of the high rising third phase seen with water perfusion, the slope of the plateau of the second phase remained low and ranged between two to four times that predicted by the waterfall model. Perfusion with 10 stokes fluid resulted in no perceptible oscillations of the tube, but a constriction similar to that reported by Fung and Sobin (1972) was always present at the downstream end of the tube. The slopes of these curves were only slightly higher than those predicted by the waterfall model. These higher slopes are accounted for by oscillations of the tubing when perfused with 0.5 stokes fluid, and constriction of the tubing when perfused with 10 stokes fluid. However, the trend is clear: the higher the viscosity of the perfusing fluid, and hence the lower the Reynolds number flow, the more closely the pressure-flow relationships approximate those of the waterfall model.

The Reynolds number achieved with 10 stokes fluid ranged from 0 to 2.6, while that of the pulmonary microcirculation lies in the range of  $10^{-1}$  to  $10^{-4}$  (Fung and Sobin, 1972). Therefore, we predict that pressure-flow relationships of the microcirculation may be very nearly those of the waterfall model. Because there were no oscillations of the tube at low Reynolds number flow, this experiment provides quantitative evidence to support Fung's (1973) contention that when tissue pressure is stable, self-excited oscillations of the blood vessels of the microcirculation do not occur.

The Reynolds number for flow through veins of 1 mm radius or wider is greater than 6 (data from Brower, 1970). Since the pressure-flow relationships become more unlike those predicted by the waterfall model as the Reynolds number increases, it is apparent that one needs to be very cautious about applying the waterfall model to venous flow.

### In <u>Vitro</u> Venous Pressure-flow Relationships

The pressure-flow relationships of collapsible veins have been described by both a mathematical waterfall model (Nakhjavan et al., 1966) and a physical model using a Starling resistor (Holt, 1941; Conrad, 1969; Katz, 1968; Brower and Noordergraaf, 1973). The pressure-flow relationships of in vitro veins were tested to see which model more closely predicts the pressure-flow relationships of veins. For the equine jugular vein, the pressure-flow relationships demonstrated total closure until  $P_i$ - $P_o$  approximated  $P_e$ - $P_o$ . Although the waterfall model predicted this total closure, it did not predict the effects of oscillations which increased the resistance at higher flow rates. Because the presence of the initial rising phase is dependent on the rigidity of the walls of the vessel, its absence is probably due to the quality of the composition of the walls of the veins. This may result in differences between the mechanical properties of veins and Penrose tubing.

Attinger (1969) measured wall thickness to radius ratios and elastic moduli of veins <u>in vitro</u>. For veins, Attinger found that the wall thickness to radius ratio is highly dependent upon transmural pressure. At 10 cm water transmural pressure, the ratios are: jugular

vein, 0.035; superior vena cava, 0.021; inferior vena cava, 0.018, and portal vein, 0.022. These ratios more than double at a transmural pressure of zero. Attinger also showed that the elastic modulus is dependent on transmural pressure. He calculated a range of elastic moduli of  $0.4 \times 10^6$  to  $5.0 \times 10^6$  dynes/cm<sup>2</sup> for transmural pressures of 2 and 10 cm of water respectively for the inferior and superior venae cavae. Penrose tubing, 1.27 cm diameter, has a measured wall thickness to radius ratio of 0.050, and an elastic modulus of  $18 \times 10^6$  dynes/cm<sup>2</sup> (Brower, 1970).

The relatively low thickness to radius ratio and lower elastic modulus of equine jugular veins may have accounted for the total closure, therefore the equine cephalic vein, a more muscular dependent vein with a larger wall thickness to lumen radius ratio (Strandness and Sumner, 1975) was also tested. At low  $P_e$ - $P_o$ , the pressure-flow relationship at low  $P_e$ - $P_o$  demonstrated a zero flow intercept, an early rising phase, and a plateau phase similar to that of the Penrose tube. For higher  $P_e$ - $P_o$ , the zero flow intercept was approximately 7.5 to 9 mm Hg less than the preset level of  $P_e$ - $P_o$ . This demonstrates that there is not total closure whenever  $P_e$  >  $P_i$ .

When Holt (1941) inserted a canine jugular vein into his Starling resistor model, he did not experiment with  $P_e > P_i > P_o$ , which is a necessary condition for early rising phase pressure-flow relationships. Although comparison of Holt's data to that of the present investigation suffers from the use of differing variables, the data appear to be compatible.

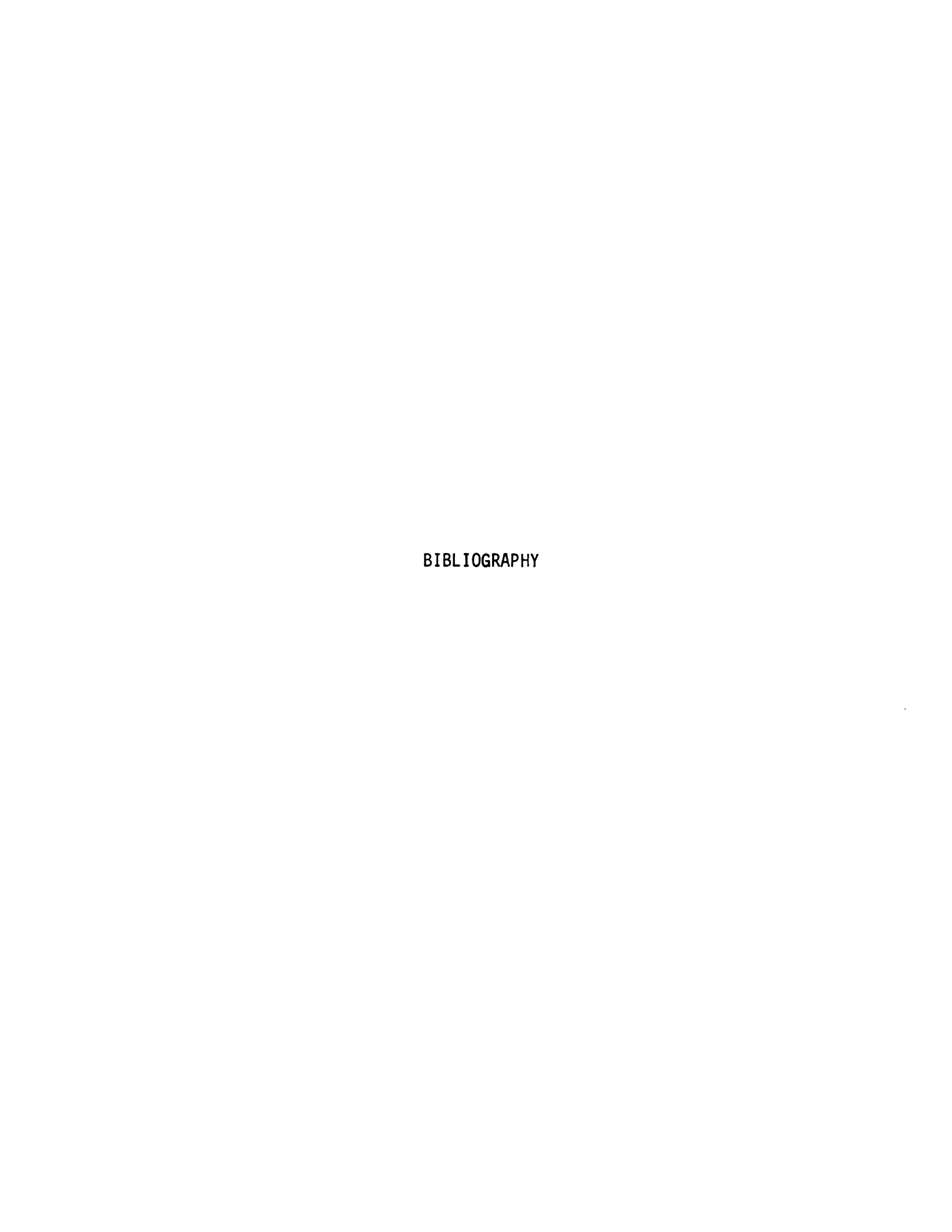
Since the cephalic vein demonstrates an early rising phase, followed by a plateau phase, and a late rising phase, it appears that the best physical analogue for the small dependent vein is the Penrose tube, perfused with water. Comparison of graphs, however, shows that the pressure-flow relationships of the larger vein are most similar to those of dialysis tubing. It therefore seems that the Penrose tube serves as a better physical model of pressure-flow relationships of small muscular veins <u>in vitro</u>, and that dialysis tubing is a better physical analogue for large veins <u>in vitro</u>. It must be emphasized that these results are restricted to excised veins, and any extension to veins <u>in vivo</u> in the living subject must await further experimental proof.

#### VIII. SUMMARY AND CONCLUSIONS

The present experimental research studied in depth the pressureflow relationships of the Penrose Starling resistor model and compared the results to those predicted by the mathematical waterfall model, as well as those measured with in vitro veins. The results indicate that:

- 1. At high Reynolds numbers, simulating venous flow, the pressure-flow relationships of the Starling resistor consisted of an early sharply rising phase at low flow rates, a plateau phase where  $P_i P_o \stackrel{\sim}{=} P_e P_o$  at moderate flow rates, and a late rising phase at high flow rates. Both the initial slope and the length of the plateau phase increased when the parameter  $P_e P_o$  was increased. The waterfall model predicts neither the early rising phase nor the late rising phase of these pressure-flow relationships.
- 2. Increasing the length of the tubing increased the slope of the early rising phase. Increasing length increased the magnitude of the late rising phase ΔP to a maximum at 5½ cm length. At greater lengths, the slope and ΔP of the late rising phase gradually decreased. Tension decreased the slope of the early rising phase and increased the slope of the late rising phase. Stretching of the tubing decreased the slope of the early rising phase, but increased the slope of the late rising phase.

- A decrease in diameter of the tubing decreased the flow rate at which these three phases of the curves appeared.
- Pressure-flow relationships measured during perfusion with high viscosity solutions to simulate the microcirculation demonstrate a trend toward closer agreement with the waterfall model.
- 4. Oscillations of the tubing appeared at the beginning of the plateau phase and increased in pressure amplitude as flow was increased. The magnitude of the late rising phase was directionally related to the pressure amplitude of the oscillations. Outflow resistance decreased the frequency and amplitude of the oscillations and thereby decreased the slope of the late rising phase.
- 5. For the equine jugular vein in vitro, the pressure-flow relationship demonstrated a positive pressure intercept at  $P_i \stackrel{\text{def}}{=} P_e$ , and a slightly higher slope than that predicted by the waterfall model. These pressure-flow relationships were most similar to those produced by water perfusion of dialysis tubing. The pressure-flow relationships of the equine cephalic vein in vitro were more similar to those of the Penrose Starling resistor model, demonstrating a zero pressure-flow intercept at low  $P_e$ - $P_o$ , an early rising phase and a plateau phase at moderate flow rates.



#### BIELIOGRAPHY

- Alexander, R. The peripheral venous system. Handbook of Physiology, Sec. 2: Circulation Vol. II. Edited by W. E. Hamilton. Washington, D. C.: Am. Physiol. Soc., 1963.
- Alexander, R. S. Critical closure reexamined. <u>Circ. Res.</u> 40:531-535, 1977.
- American Association of Blood Banks. <u>Technical Methods and Procedures</u> of the American Association of Blood Banks. 6th edition. Washington, D. C.: American Association of Blood Banks, 1974.
- Archie, J. P., D. Fixler, D. Ullyot, J. Hoffman, J. Utley, and E. Carlson. Measurement of cardiac output with and organ trapping of radioactive microspheres. J. Appl. Physiol. 35:148-155, 1973.
- Archie, J. P., and R. Brown. Effect of preload on the transmural distribution of diastolic coronary blood flow. J. of Surgical Research. 16:215-223, 1974.
- Archie, J. P. Intramyocardial pressure: effect of preload on transmural distribution of systolic coronary blood flow. <u>American J.</u> of Cardiology. 35:904-911, 1975.
- Armour, J. A., and W. C. Randall. Canine left ventricular intramyocardial pressures. Am. J. Physiol. 220:1833-1839, 1971.
- Attinger, E. O. Wall properties of veins. <u>I.E.E.E. Trans. on Biomedical Engineering</u>. Vol. BME-16:253-261, 1969.
- Baird, R. J., F. Dutka, M. Okumori, A. de la Rocha, M. M. Golbach, T. J. Hill, and D. C. MacGregor. Surgical aspects of regional myocardial blood flow and myocardial pressure. <u>J. Thor. Cardiovascular Surg.</u> 69:17-29, 1975.
- Bates, B. A guide to physical examination. Philadelphia: J. B. Lippincott, 1974.
- Berne, R.M., and M. N. Levy. <u>Cardiovascular Physiology</u>. St. Louis: C. V. Mosby, 1972.

- Bissonnette, J. M., and R. C. Farrell. Pressure-flow and pressure-volume relationships in the fetal placental circulation.

  J. Appl. Physiol. 35:355-360, 1973.
- Brandi, G., W. M. Fam, and M. McGregor. Measurement of coronary flow in local areas of myocardium using xenon 133. J. Appl. Physiol. 24:446-450, 1968.
- Brandi, G., and M. McGregor. Intramural pressure in the left ventricle of the dog. Cardiovasc. Res. 3:472-475, 1969.
- Brecher, G. A. Mechanism of venous flow under different degrees of aspiration. Am. J. Physiol. 169:423-433, 1952.
- Brecher, G. A., G. Mixter, and L. Share. Dynamics of venous collapse in superior vena cava system. Am. J. Physiol. 171:194-203, 1952.
- Brecher, G. A., and G. Mixter, Jr. Effect of respiratory movements on superior cava flow under normal and abnormal conditions.

  Am. J. Physiol. 172:457-461, 1953.
- Brecher, G. A. Venous Return. New York: Grune and Stratton, 1956.
- Brooks, C., and A. B. Luckhardt. The chief physical mechanisms concerned in clinical methods of measuring blood pressure. <u>Am. J. Physiol</u>. 40:49-74, 1916.
- Brower, R. W. Pressure-flow characteristics of collapsible tubes. Ph.D. Thesis. University of Pennsylvania. Ann Arbor: University Microfilms, 1970.
- Brower, R. W., and A. Noordergraaf. Pressure-flow characteristics in collapsible tubes: A reconciliation of seemingly contradictory results. Annals of Biomedical Engineering. 1:333-355, 1973.
- Brower, R., and C. Scholten. Experimental evidence on the mechanism for the instability of flow in collapsible vessels.

  <u>Biol. Engng.</u> 13:839-844, 1975.
- Buckberg, G. D., J. P. Archie, D. E. Fixler, and J. Hoffman. Experimental subendocardial ischemia during left ventricular hypertension. <a href="Surg. Forum">Surg. Forum</a>. 22:123, 1971.
- Buckberg, G. D., J. C. Luck, D. B. Payne, J. I. E. Hoffman, J. P. Archie, and D. E. Fixler. Some sources of error in measuring regional blood flow with radioactive microspheres. <u>J. Appl. Physiol</u>. 31:598-604, 1971.
- Buckberg, G. D., D. E. Fixler, J. P. Archie, and J. Hoffman. Experimental subendocardial ischemia in dogs with normal coronary arteries. <u>Circ. Res</u>. 30:67-76, 1972.

- Buckberg, G. D., and A. Kattus. Factors determining the distribution and adequacy of left ventricular myocardial blood flow. Advances in Experimental Medicine and Biology. 39:95-113, 1975.
- Burton, A. C. On the physical equilibrium of small blood vessels. Am. J. Physiol. 164:319-329, 1951.
- Burton, A. C. Physical principles of circulatory phenomena: the physical equilibria of the heart and blood vessels. Handbook of Physiology, Sec. 2: Circulation Vol. I. W. F. Hamilton, Ed. Washington, D. C.: Am. Physiol. Soc., 1962.
- Burton, A. C. <u>Physiology and Biophysics of the Circulation</u>. 2nd ed. Chicago: Year Book Medical Publishers, 1972.
- Chiu, C. J., W. A. Mersereau, and M. J. Scott. Subendocardial hemor-rhagic necrosis. J. Thor. Cardiovascular Surg. 64:66-73, 1972.
- Conrad, W. A. Pressure-flow relationships in collapsible tubes. I.E.E.E. Trans. B.M.E. BME-16:284-295, 1969.
- Conrad, W. A. Pulmonary alveolar blood flow: Letters to the editor. Circ. Research. 32:117-118, 1973.
- Conrad, W. A., M. L. Cohen, and D. M. McQueen. Note on the oscillations of collapsible tubes. Med. and Biol. Engng. and Comput. 16:211-214, 1978.
- Cutforth, R., J. Wiseman, and R. D. Sutherland. The genesis of the cervical venous hum. Am. Heart J. 80:488-492, 1970.
- Cutarelli, R. and M. Levy. Intraventricular pressure and the distribution of coronary blood flow. <u>Circ. Res.</u> 12:322-327, 1963.
- Dieudonné, J. M. Tissue-cavitary difference pressure of dog left ventricle. Am. J. Physiol. 213:101-106, 1967.
- Domenech, R. J., J. Hoffman, M. Noble, K. Saunders, J. Henson, and S. Subijanto. Total and regional coronary blood flow measured by radioactive microspheres in conscious and anesthetized dogs. Circ. Res. 25:581-595, 1969.
- Donders, F. C. Physiologie des Menschen. Leipzig: Hirzel, 1859.
- Doppman, J., R. M. Rubinson, S. D. Rockoff, J. S. Vasko, R. Shapiro, and A. G. Morrow. Mechanism of obstruction of the infradiaphragmatic portion of the inferior vena cava in the presence of increased intra-abdominal pressure. <u>Investigative Radiology</u>. I:37-52, 1966.

- Downey, J. M., and E. S. Kirk. Distribution of the coronary blood flow across the canine heart wall during systole. <u>Circ. Res.</u> 34:251-257, 1974.
- Downey, J. M. and E. Kirk. Inhibition of coronary blood flow by a vascular waterfall mechanism. Circ. Res. 36:753-760, 1975.
- Driscol, T. E., T. W. Moir, and R. W. Eckstein. Vascular effects of changes in perfusion pressure in the nonischemic and ischemic heart. Circ. Res. Supp. II. 14 and 15:I-94 to I-101, 1964.
- D'Silva, J. L., D. Mendel, and M. C. Winterton. Effect of sympathomimetic amines on intramyocardial pressure in the rabbit. Am. J. Physiol. 205:10-16, 1963.
- Duomarco, J. L., R. Rimini, and P. Recarte. La presion intraabdominal y la presion en la bana caba inferior. Rev. argent. ce cardiol. 11:273, 1944.
- Duomarco, J. L., and R. Rimini. Energy and hydraulic gradient along systemic veins. Am. J. Physiol. 178:215-219, 1954.
- Flaherty, J. E., J. B. Keller, and S. I. Rubinow. Post buckling behavior of elastic tubes and rings with opposite sides in contact. SIAM J. Appl. Math. 23:446-455, 1972.
- Fung, Y. C. and S. S. Sobin. Pulmonary alveolar blood flow. <u>Circ. Res.</u> 30:470-490, 1972.
- Fung, Y. C. Reply to: Conrad, W. A. Pulmonary alveolar blood flow: Letters to the editor. Circ. Res. 32:118, 1973.
- Gilmore, J. P. Influence of tissue pressure on renal blood flow autoregulation. Am. J. Physiol. 206:707-713, 1964.
- Gottschalk, C. A comparative study of renal interstitial pressure. Am. J. Physiol. 169:180-187, 1952.
- Gray, S. D., E. Carlsson, and N. C. Staub. Site of increased vascular resistance during isometric muscle contraction. Am. J. Physiol. 213:683-689, 1967.
- Green, J. G. Pressure-flow and volume-flow relationships of the systemic circulation of the dog. Am. J. Physiol. 229:761-769, 1975.
- Gregg, D. E., and R. W. Eckstein. Measurements of intramyocardial pressure. Am. J. Physiol. 132:781-790, 1941.
- Griffiths, D. Steady fluid flow through veins and collapsible tubes. Med. and Biol. Engng. 9:597-602, 1971.

- Guyton, A. C., and L. Adkins. Quantitative aspects of the collapse factor in relation to venous return. Am. J. Physiol. 177:523-527, 1954.
- Guyton, A. C. Decrease of venous return caused by right atrial pulsation. Circ. Res. 10:188-196, 1962.
- Guyton, A. C. A concept of negative interstitial pressure based on pressures in implanted perforated capsules. <u>Circ. Res.</u> 12:399-414, 1963a.
- Guyton, A. C. Venous return. Handbook of Physiology, Sec. 2: Circulation Vol. II. Edited by W. F. Hamilton. Washington, D. C.:

  Am. Physiol. Soc., 1963b.
- Guyton, A., H. Granger, and A. Taylor. Interstitial fluid pressure. Physiological Reviews. 51:527-563, 1971.
- Guyton, A. C. <u>Textbook of Medical Physiology</u>. 5th edition. Philadelphia: W. B. Saunders Company, 1976.
- Haddy, F. J., J. B. Scott, and G. J. Grega. Peripheral circulation: fluid transfer across the microvascular membrane. <u>International Review of Physiology II</u>, Vol. 9. Edited by A. C. Guyton and A. W. Cowley. Baltimore: University Park Press, 1976.
- Hardison, J. E. The cervical venous hum: a help or a hindrance. N.E.J.M. 292:1239-1240, 1975.
- Hekmatpanah, J. Cerebral circulation and perfusion in experimental increased intracranial pressure. J. Neurosurg. 32:21-29, 1970.
- Hinshaw, L., S. Day, and C. Carlson. Tissue pressure as a causal factor in the autoregulation of blood flow in the isolated perfused kidney. Am. J. Physiol. 197:309-312, 1959.
- Hinshaw, L., R. Flaig, R. Logemann and C. Carlson. Intrarenal venous and tissue pressure and autoregulation of blood flow in the perfused kidney. Am. J. Physiol. 198:891-894, 1960.
- Holt, J. P. The collapse factor in the measurement of venous pressure. Am. J. Physiol. 134:292-299, 1941.
- Holt, J. P. The effect of positive and negative intra-thoracic pressure on cardiac output and venous pressure in the dog. Am. J. Physiol. 142:594-603, 1944.
- Holt, J. P. Flow of liquids through collapsible tubes. <u>Circ. Res.</u> 7:342-353, 1959.

- Holt, J. P. Flow through collapsible tubes and through <u>in situ</u> veins. IEEE Trans. B.M.E. BME-16:274-283, 1969.
- Hughes, J. M. B., F. G. Hoppin, Jr., and J. Mead. Effect of lung inflation on bronchial length and diameter in excised lungs. J. Appl. Physiol. 32:25-35, 1972.
- Katz, A. I. A model for the dynamics of the inferior vena cava of the terrestrial mammalian cardiovascular system. Ph.D. dissertation. Rutgers University. Ann Arbor: University Microfilms, 1968.
- Katz, A., Y. Chen, and A. Moreno. Flow through a collapsible tube: Experimental analysis and mathematical model. Biophysical Journal. 9:1261-1279, 1969.
- Katz, A. I., and Y. Chen. Cross-sectional geometry changes of cylindrical vessels under uniform pressure. <u>Proc. Ann. Conf. Eng. Med.</u> Biol. 12:12, 1970.
- Kirk, E. and C. Honig. An experimental and theoretical analysis of myocardial tissue pressure. Am. J. Physiol. 207:361-367, 1964a.
- Kirk, E., and C. Honig. Nonuniform distribution of blood flow and gradients of oxygen tension within the heart. Am. J. Physiol. 207:661-668, 1964b.
- Kjellmer, I. An indirect method for estimating tissue pressure with special reference to tissue pressure in muscle during exercise. Acta Physiol. Scand. 62:31-40, 1964.
- Knowlton, F. P., and E. H. Starling. The influence of variations in temperature and blood-pressure on the performance of the isolated mammalian heart. J. of Physiol. 44:206-219, 1912.
- Kober, G. and J. Scholtholt. Continuous recording of local myocardial function in normal and ischemic myocardium. <u>Basic Res. Cardiol.</u> 71:150-159, 1976.
- Kresch, E., and A. Noordergraaf. A mathematical model for the pressure-flow relationship in a segment of vein. <u>IEEE Trans. B.M.E.</u> BME-16:296-307, 1969.
- Kresch, E., and A. Noordergraaf. Cross-sectional shape of collapsible tubes. <u>Biophysical Journal</u>. 12:274-294, 1972.
- L'Abbate, R. Mildenberger, L. Christie, M. McGregor, and G. Klassen. The role of coronary perfusion pressure and left ventricular intracavitary pressure as determinants of coronary blood flow. Fed. Proc. 33:414, 1974.

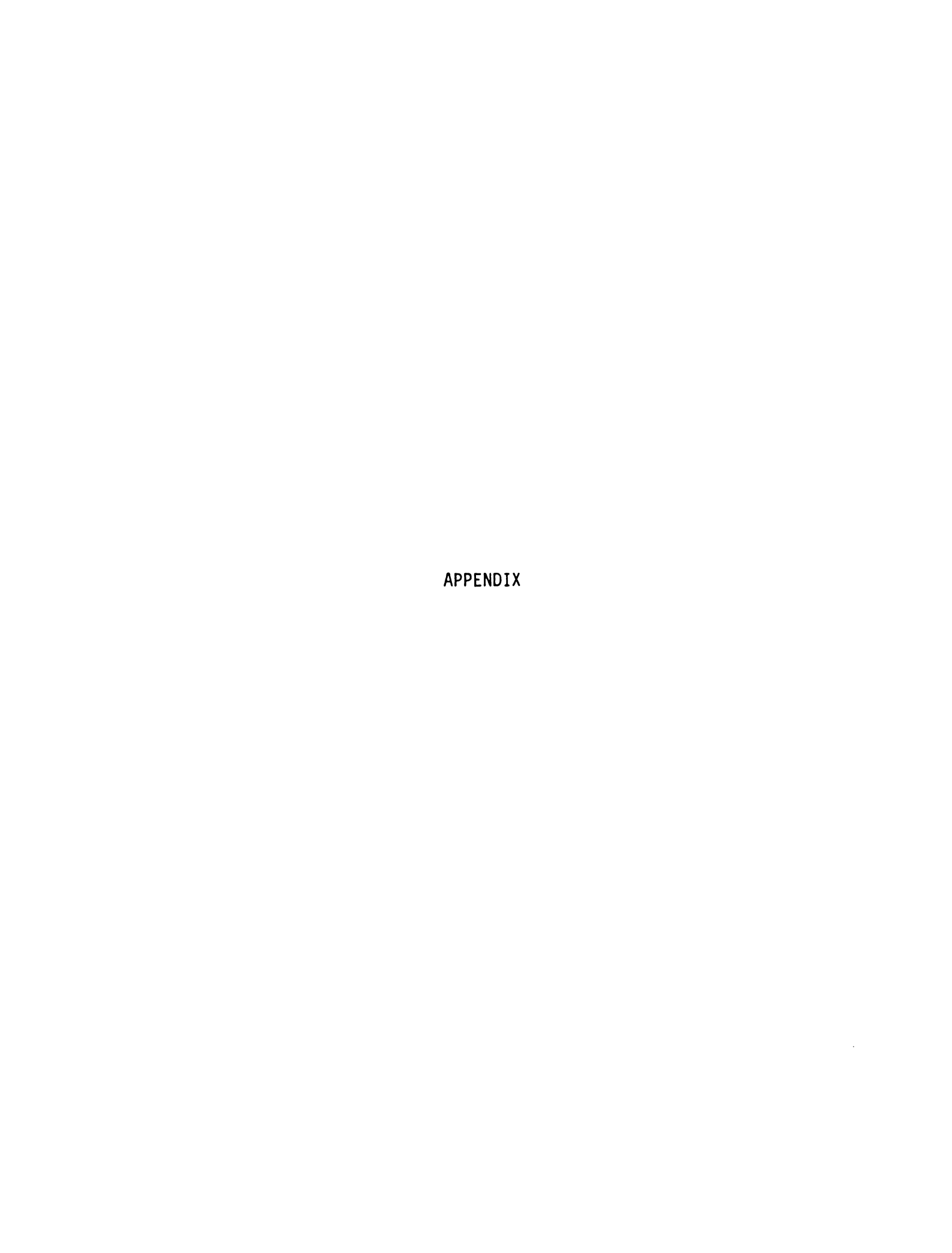
- Langlois, W. E. <u>Slow Viscous Flow</u>. New York: Macmillan Company, 1964.
- Lawrence, T., and R. M. Myerson. Functional vena caval obstruction in cirrhotics. Am. J. Gastroenterology. 60:135-141, 1973.
- Ledderhose, G. Studien über den blutlauf in den hautvenen unter physiologischen und pathologischen bedingungen. Mitteil. Grenzgeb. Med. and Chirurg. 15:355, 1906.
- Lenfant, C., and B. J. Howell. Cardiovascular adjustments in dogs during continuous pressure breathing. <u>J. Appl. Physiol</u>. 15:425-428, 1960.
- Lopez-Muniz, N. Stephens, B. Bromberger-Barnea, S. Permutt, and R. Riley. Critical closure of pulmonary vessels analyzed in terms of Starling resistor model. J. Appl. Physiol. 24:625-635, 1968.
- Mahrenholtz, V. O. Zur pumpwirkung kollabierfähiger ventilloser Schläuche. Ingenieur-Archiv. 43:173-182, 1974.
- Maloney, J. E., D. H. Bergel, J. B. Glazier, J. M. B. Hughes, and J. B. West. Transmission of pulsatile blood pressure and flow through the isolated lung. Circ. Res. 23:11-24, 1968.
- McDonald, D. Hemodynamics. <u>Annual Review of Physiology</u>. 30:525-556, 1968.
- Mitzner, W. Hepatic outflow resistance, sinusoid pressure, and the vascular waterfall. Am. J. Physiol. 227:513-519, 1974.
- Moir, T. W., and D. W. DeBra. Effect of left ventricular hypertension, ischemia, and vasoactive drugs on the myocardial distribution of coronary flow. Circ. Res. 21:65-74, 1967.
- Moreno, A. H., A. R. Burchell, R. van der Woude, and J. Burke.
  Respiratory regulation of spanchnic and systemic venous return.
  Am. J. Physiol. 213:455-462, 1967.
- Moreno, A., A. Katz, and L. Gold. An integrated approach to the study of the venous system with steps toward a detailed model of the dynamics of venous return to the right heart. <u>IEEE Trans. B.M.E.</u> BME-16:308-324, 1969.
- Moreno, A., A. Katz, L. Gold, and R. V. Reddy. Mechanics of distention of dog veins and other very thin-walled tubular structures. Circ. Res. 27:1069-1080, 1970.
- Morgan, B. C., F. Abel, G. L. Mullins, and W. G. Guntheroth. Flow patterns in cavae, pulmonary artery, pulmonary vein, and aorta in intact dogs. <u>Am. J. Physiol</u>. 210:903-908, 1966.

- Nakhjavan, F. K., W. H. Palmer, and M. McGregor. Influence of respiration on venous return in pulmonary emphysema. <u>Circulation</u>. 33:8-18, 1966.
- Nichol, J., F. Girling, W. Jerrard, E. Claxton, and A. Burton.
  Fundamental instability of the small blood vessels and critical closing pressures in vascular beds. <u>Am. J. Physiol</u>. 164:330-344, 1951.
- Ninomiya, I., and M. F. Wilson. Analysis of ventricular dimension in the unanesthetized dog. Circ. Res. 16:249-260, 1965.
- Nordenstrom, B., and A. Norhagen. Effect of respiration on venous return to the heart. Am. J. Roentgenology. 95:655-661, 1965.
- Norhagen, A. Selective angiography of the hepatic veins. <u>Acta Radiol</u>. Supplementum. 221:1-21, 1963.
- Oates, G. C. Fluid flow in soft-walled tubes. Part 1: Steady flow. Med. and Biol. Eng. 13:773-779, 1975a.
- Oates, G. C. Fluid flow in soft-walled tubes. Part 2: Behaviour of finite waves. Med. and Biol. Eng. 13:780-784, 1975b.
- Permutt, S., B. Bromberger-Barnea, and H. Bane. Alveolar pressure, pulmonary venous pressure, and vascular waterfall. Med. Thorac. 19:239-260, 1962.
- Permutt, S. and R. Riley. Hemodynamics of collapsible vessels with tone: the vascular waterfall. <u>J. Appl. Physiol</u>. 18:924-932, 1963.
- Phibbs, R. H., and L. Dong. Nonuniform distribution of microspheres in blood flowing through a medium-size artery. <u>Canad. J. Physiol. Pharmacol.</u> 48:415-421, 1970.
- Pifarré, R. Intramyocardial pressure during systole and diastole.
  Annals of Surgery. 168:871-875, 1968.
- Ranniger, K., and D. M. Switz. Local obstruction of the inferior vena cava by massive ascites. Am. J. Roentgenology, Radium Therapy and Nuclear Medicine. 93:935-939, 1965.
- Reddy, R. V., A. Noordergraaf, and A. Moreno. <u>In vitro</u> changes of shapes of veins under pressure. <u>Proc. Ann. Conf. Eng. Med. Biol.</u> 12:15, 1970.
- Rodbard, S., and Saiki, H. Flow through collapsible tubes. <u>American</u> Heart Journal. 46:715-725, 1953.

- Rodbard, S. Flow through collapsible tubes: augmented flow produced by resistance at the outlet. <u>Circulation</u>. 11:280-287, 1955.
- Rodbard, S. Autoregulation of encapsulated, passive, soft-walled vessels. American Heart Journal. 65:648-655, 1963.
- Rodbard, S., N. Handel, and L. Sadja. Flow patterns in a model of a contracting muscle. <u>Cardiovasc</u>. Res. 5:396-404, 1971.
- Rudolph, A. M., and M. Heymann. Circulation of the fetus in utero: methods for studying distribution of blood flow, cardiac output and organ blood flow. Circ. Res. 21:163, 1967.
- Scharf, S. M., B. Bromberger-Barnea, and S. Permutt. Distribution of coronary venous flow. J. Appl. Physiol. 30:657-662, 1971.
- Scholander, P. F., A. R. Hargens, and S. Miller. Negative pressure in the interstitial fluid of animals. Science. 161:323-328, 1968.
- Snashall, P. D., J. Lucas, A. Guz, and M. Floyer. Measurement of interstitial "fluid" pressure by means of a cotton wick in man and animals: an analysis of the origin of the pressure. <u>Clin Sci</u>. 41:35-39, 1971.
- Strandness, D. E., and D. S. Sumner. <u>Hemodynamics for Surgeons</u>. New York: Grune and Stratton, 1975.
- Stromberg, D. D., and C. Wiederhielm. Effects of oncotic gradients and enzymes on negative pressures in implanted capsules. Am. J. Physiol. 219:928-932, 1970.
- Stromme, S. B., J. E. Maggert, and P. F. Scholander. Interstitial fluid pressure in terrestrial and semiterrestrial animals. <u>J. Appl. Physiol</u>. 27:123-126, 1969.
- Swann, H. G., B. W. Hink, H. Koester, V. Moore, and J. M. Prine. The intra-renal venous pressure. <u>Science</u>. 115:64-65, 1952.
- Tafur, E., and W. G. Guntheroth. Simultaneous pressure, flow and diameter of the vena cava with fright and exercise. Circ. Res. 19:42-50, 1966.
- Utley, J., E. Carlson, J. Hoffman, H. M. Martinez, and G. D. Buckberg. Total and regional myocardial blood flow measurements with  $25\mu$ ,  $15\mu$ ,  $9\mu$ , and filtered 1 to  $10\mu$  diameter microspheres and antipyrine in dogs and sheep. Circ. Res. 34:391-404, 1974.
- Van der Meer, J. J., R. S. Reneman, H. Schneider, and J. Wieberdink.

  A technique for estimation of intramyocardial pressure in acute
  and chronic experiments. Cardiovasc. Res. 4:132-140, 1970.

- Vix, V. A., and T. K. Payne. Elevated inferior vena cava pressure in ascites. Am. J. Surgery. 123:721-723, 1972.
- Volkmann, A. W., <u>Die Hämodynamik</u>. Leipzig: Breitkopf and Haertel, 1850.
- West, J. B., C. T. Dollery, and A. Naimark. Distribution of blood flow in isolated lung: relation to vascular and alveolar pressures. J. Appl. Physiol. 19:713-724, 1964.
- West, J. B. Respiratory Physiology: the Essentials. Baltimore: Williams and Wilkins, 1974.
- West, J. B., and C. T. Dollery. Distribution of blood flow and the pressure-flow relations of the whole lung. <u>J. Appl. Physiol.</u> 20:175-183, 1965.
- Wexler, L., D. H. Bergel, I. T. Gabe, G. S. Makin, and C. J. Mills. Velocity of blood flow in normal human venae cavae. <u>Circ. Res.</u> 23:349-359, 1968.
- White, D. C. S. Biological Physics. London: Chapman and Hall, 1974.
- Yates, W. G. Experimental studies of the variation in the mechanical properties of the canine abdominal vena cava. Ph.D. dissertation. Stanford University. Dissertation Abstracts. 31(4B):1914, 1970.
- Yokota, H., and F. Kreuzer. Influence of body position and pneumoperitoneum on respiratory variation of venous return in anesthetized dogs. Pflugers Arch. 340:307-324, 1973.



#### APPENDIX

# SIMULTANEOUS MEASUREMENT OF REGIONAL INTRAMYOCARDIAL PRESSURE AND BLOOD FLOW

#### Introduction

The study of the physiology of transmural myocardial pressure and blood flow distribution has gained momentum because changes in these parameters may be related to the pathogenesis of a number of clinical conditions. For example, myocardial ischemia and necrosis have been reported after cardio-pulmonary bypass and hypovolemic shock in patients (Buckberg et al., 1971a, 1972) and experimental animals (Buckberg et al., 1972; Chiu et al., 1972). This injury is usually located in the inner half of the ventricular wall and is not in the anatomic distribution of any major coronary artery. One possible mechanism of inadequate subendocardial blood flow when aortic pressure is low may be that intramyocardial blood flow then becomes dependent on intramyocardial tissue pressure (L'Abbote et al., 1974). This possibility is further substantiated by the finding of a disproportionate decrease in flow distribution to the subendocardium during myocardial ischemia (Moir and DeBra, 1967; Cutarelli and Levy, 1963).

#### Intramyocardial Pressure Measurements

Brandi and McGregor (1969) reported that the ratio of peak systolic intra-mural to ventricular cavity pressure varies between zero and unity and is approximately equal to depth within the myocardium. However, a number of investigators have shown that the deeper myocardial layers generate higher pressures than the intraventricular pressure (D'Silva et al., 1963; Gregg and Eckstein, 1941; Kirk and Honig, 1964a). Criticisms of the validity of the techniques employed has created doubts about the absolute values of the intramyocardial pressures. A brief review of these techniques will help to point out their inaccuracies.

Tissue pressure is the pressure exerted against the outside of blood and lymphatic vessels. It is influenced by the geometrical dimensions of the interstitial spaces, the physical characteristics of surrounding tissues, and the amount of fluid and gel in the interstitial spaces. The pressure in the myocardium, the intramyocardial pressure, is influenced by transferred ventricular pressure and generated muscle tension (Driscol et al., 1964a). There are basically three indirect methods of measuring intramyocardial pressure: the open method, in which a small pocket of fluid is introduced into the myocardium and pressure within the fluid pocket is measured; the closed method, by which pressures are recorded from fluid which is contained within a membrane inserted within the myocardium; and the perfusion method, in which flow is directed through a collapsible vessel inserted into the myocardium; the pressure at which flow is interrupted is taken to be the intramyocardial pressure.

#### Open Method

Driscol et al. (1964) used a 16 gauge needle with a 1 mm diameter side opening inserted at right angles to the epicardial surface to a depth of 0.5 to 1.0 cm, and found this system suitable only for measurement of directional pressure changes. Brandi and McGregor (1969) introduced a polyethylene catheter (1 mm internal diameter) into the left ventricular wall through which saline was infused at various flow rates, while pressure was observed. The recorded pressure increased with increasing flow rates, and by extrapolation to zero flow, the intramyocardial pressure was estimated. They concluded that pressure recorded at any depth within the myocardium varies with the anatomical distortion caused by the fluid pocket from which it is recorded, so that high systolic intramyocardial pressure values recorded by the fluid pocket method are probably artifactual. This finding agrees with those of Gregg and Eckstein (1941), and van der Meer et al. (1970). Van der Meer et al. (1970), in testing the needle method, also found that the movements of the heart during contraction cause enlargement of the needle track, tending to lower the measured value of intramyocardial pressure, and that changes in needle position caused by manipulation of the heart also alter the intramyocardial pressure measurements. The method of Kirk and Honig (1964a) has been subject to the same criticism on the grounds that it is merely a modified open technique and can also cause pockets of liquid inside the myocardium.

#### Closed Method

Gregg and Eckstein (1941) drew a length of tied off carotid artery through a prepared tunnel in the myocardium and recorded pressures from it by means of a polyethylene cannula. The pressures recorded never exceeded systolic ventricular pressure. It was their conclusion that there was incomplete pressure transference through the walls of the artery so that the system was indicative only of directional changes of intramyocardial pressure. Further refinement of this closed system were provided by D'Silva et al. (1963) using tied off venous segments.

For the balloon method, a small cylindrical portion of latex tubing (1 mm internal diameter, 0.04 mm wall thickness) was tied to an 18 gauge needle with a closed end. The lumen of the needle was open to the latex balloon and filled with fluid to a pre-determined pressure range. The intramyocardial pressure is superimposed upon this initial balloon pressure. D'Silva et al. (1963) started with a balloon pressure of 20 mm Hg. and calibrated the system for further pressure changes. Dieudonné (1967) found that at an initial pressure of approximately 150 to 250 mm Hg, the balloon he was using became spherical, and then additional pressures were linearly additive, but that pressure transmission was extremely dependent upon initial inflation pressure. It would appear then, that this system has disadvantages similar to those of the open system: movement of the needle, creation of an excessively large track, and pressure dependence on volume displacement.

Van der Meer <u>et al</u>. (1970) tested a segment of closed saphenous vein inserted into a myocardial tunnel, and they found this method to be inaccurate because of the superimposition of the diastolic and systolic intramyocardial pressure upon the unknown distending pressure of the venous segment, and also because the slightest leakage in the system such as might occur through the vasa venarum could cause artifactually low measurements.

### Perfusion Method

Pifarré (1968) anastomosed jugular vein segments onto the descending aorta and then he tunneled them through the myocardium. One to six months later, the dogs were found to have new anastomoses between the graft and the coronary arteries. At the peak of contraction, pressure in the intraluminal segment of the graft was 60 to 100 mm Hg. higher than aortic pressure, as measured by a polyethylene cannula. During diastole, the pressure was 20 to 75 mm Hg. lower than the aorta. The diastolic pressure tended to be lower the longer the graft had been implanted, and may have reflected enlarging anastomoses which improved runoff.

However, when van der Meer et al. (1970) perfused chronic venous implants via silastic catheters connected at each end, they found that eight days after implant, connective tissue developed around the graft, decreasing the compliance of the system, and giving rise to an increase in diastolic intramyocardial pressure measurements. In a review of available methods, these investigators concluded that the venous graft perfusion method was the method of choice for chronic experiments, but

that there still was no reliable indirect technique for measurement of the actual extravascular pressure within the ventricular walls.

### Catheter-tip Micro-transducer Method

Very recently, the catheter-tip micro-transducer has been used for the measurement of intramyocardial pressures (Armour and Randall, 1971; Kober and Scholtholt, 1976; Baird et al., 1975). The micro-tip transducers were developed to overcome the errors associated with fluid filled catheter systems. The sensor is an ultraminiature silicon semi-conductor designed specifically for catheter tip applications. This transducer can be precisely calibrated and its location can be measured accurately at autopsy. The diaphragm of the manometer is located laterally near the tip of the catheter.

Local intramyocardial pressure measurements with catheter-tip subminiature pressure transducers were first published by Armour and Randall (1971). The pressure detecting elements which they used were relatively large (7x10x2.5 mm and 2.5x3x 1 mm) and they required surgical separation of myocardial fibers and creation of a tunnel in order to introduce the sensor into its location with the lateral sensing surface parallel to the regional fiber orientation. After a tunnel was created, they were able to record a gradient as the transducer was slipped diagonally through the myocardial wall from epicardial to endocardial layers. When the transducer entered the ventricular chamber, the pressure dropped to equal that of the intraventricular water filled catheter system.

Kober and Scholtholt (1976) incised the epicardium and then bluntly advanced their smaller diameter (1.67 mm outer diameter) catheter into the myocardium. Although postmortem examination showed that injury to the myocardium was minimal, the method does induce trauma around the catheter at the site of measurement.

Armour and Randall (1971) measured intramyocardial pressure simultaneously from the subepicardium and subendocardium of the anterior wall of the left ventricle, and compared these measurements with intraventricular pressures. A transmural systolic pressure gradient was consistently observed; the mean pressures were 93±7 to 121±10 mm Hg., respectively, while concurrent intraventricular pressure was 101±4 mm Hg.

# Myocardial Blood Flow

When myocardial blood flow is measured over a period of time, so that both systolic and diastolic flow are taken into account, myocardial blood flow to the beating heart is generally found to be uniform transmurally, although the findings seem to depend upon the method used to determine blood flow. Using the method of externally monitored clearance of diffusible radio-isotopes, Kirk and Honig (1964b) and Brandi et al. (1968) found a slower clearance rate in the subendocardium than the outer layers of the ventricle. Brandi et al. (1968) decided that accurate estimations of myocardial blood flow could not be determined by this technique on the basis of local conditions created by the injections. Intravascular administration of diffusible isotopes in the

beating heart demonstrate an equal distribution of flow to the subendocardium and subepicardium under normal coronary perfusion pressures and flow (Moir and DeBra, 1967; Cutarelli and Levy, 1963).

The use of small radioactive microspheres confirms this flow distribution (Buckberg, 1971b; Moir, 1967). The validity of the radioactive microsphere method as an estimate of flow to small areas of the left ventricular myocardium is dependent on microsphere size (Utley et al., 1974). It has been shown that the larger spheres undergo axial streaming (Phibbs and Dong, 1970) and therefore overestimate subendocardial blood flow (Domenech, 1969). In the beating heart, the endocardial to epicardial flow ratio was found to be 2.5, by the use of  $51-60~\mu$  spheres, but when smaller microspheres are used, the ratio approaches one (Buckberg, 1971b; Moir and DeBra, 1967).

If there is an equal distribution of blood flow across the myocardium, in combination with a systolic transmural pressure gradient, what effect does systole have upon the transmural distribution of blood flow? To measure this, Downey and Kirk (1974) used a bolus intracoronary injection of <sup>86</sup>Rb, and limited perfusion to periods of systole only. Their measurement revealed a transmural gradient of systolic blood flow with a flow rate in the outer fourth of the left ventricle about twice that in the inner fourth. Kirk and Honig (1964b) further showed that under conditions of constant coronary flow, vagal arrest causes the blood flow in the subepicardium to be redistributed to the deeper layers. It therefore appears that systole inhibits blood flow in the layers nearer to the endocardium more than in the epicardial layers.

If, under normal hemodynamic conditions, the distribution of coronary blood flow across the heart wall is uniform, then apparently the gradient in the distribution of flow during systole must be compensated for by a reverse gradient during diastole. It follows then that subendocardial muscle must have a lower vascular resistance in order to receive the same amount of flow per gram as subepicardial tissue during a shorter time period. This lowered resistance may be accomplished by way of a lowered vascular tone (Moir and DeBra, 1967). This possibility leads to the view that maximal vasodilation may occur earlier in the subendocardium under conditions of ischemia, and that when coronary vessels maximally dilate, further compensatory vasodilation of subendocardial vessels may no longer be possible. If only subepicardial vasodilation can occur, this may lead to subendocardial underperfusion. Under these conditions, when the coronary vessels are maximally dilated, intramyocardial pressure may play a decisive role in determining coronary vascular resistance. Several small microsphere studies support this conclusion (Buckberg and Kattus, 1975; L'Abbotte et al., 1974; Archie and Brown, 1974).

Buckberg and Kattus (1975) have shown that left ventricular diastolic blood pressure impedes subendocardial blood flow during cardiac failure secondary to aortic stenosis. Opening of a left atrial to right atrial shunt in a dog with this condition resulted in a marked increase in diastolic and subendocardial flow. L'Abbotte et al. (1974) found a decreased subendocardial to subepicardial flow ratio when left ventricular diastolic pressure was increased, even when coronary blood flow was constant.

Archie and Brown (1974) found that at high perfusion pressure, high pre-loads (15-26 mm Hg.) did not significantly decrease diastolic left subendocardial flow, but they suggested that the effects of increased diastolic intramyocardial pressure resulting from increased left ventricular intraluminal pressures would be more detectable at lower flow rates.

This following experiment was an attempt to correlate diastolic intraventricular pressures with intramyocardial pressures and to test whether or not elevated intraventricular pressures inhibit subendocardial blood flow by the mechanism of vascular collapse, as predicted by the Starling resistor model. The purpose of the following experiment was not to gather data upon which to base conclusions about the tested parameters, rather it was intended to be a pilot to study the feasibility of such research.

#### Methods

A dog weighing approximately 20 kg was anesthetized with sodium pentobarbital (30 mg/kg) intravenously and ventilated with a positive pressure Harvard Respirator (Model 607, Dover, Mass.) through an endotrachael tube with room air. The heart was exposed via a thoracotomy through the fourth intercostal space and a pericardotomy was performed. After systemic heparinization (300 u/kg intravenously), the coronary sinus was cannulated with a glass cannula of 0.7 cm. diameter, inserted through the right atrial appendage and right A-V valve. Coronary sinus blood was directed into a reservoir initially containing 500 ml 6%

Dextran in solution with normal saline. The sinus blood was returned via a Sigmamotor pump (Minneapolis, Minn.) to the left jugular vein. The left anterior descending coronary artery was cannulated at its origin with a 3 cm length of PE 240 tubing connected by siliconized latex tubing to the Holter roller pump (Extracorporeal Med. Spec., Mt. Laurel, N.J.), that led from a stirred reservoir of arterial blood obtained from the left carotid artery. After infusion of the Dextran solution, the animal was slowly hemorrhaged of 800 ml. blood from the carotid artery cannula into the arterial reservoir, and a slow infusion of blood bank Acid-Citrate-Dextrose solution\* was injected at 1 cc per minute into the perfusion line by a Harvard Apparatus Infusion Pump (Dover, Mass.).

When the heart stopped in diastolic arrest, the respirator was discontinued. A glass tube, 6 in long and 0.5 cm diameter was directed into the left ventricular cavity through an opening in the left atrial appendage. The glass tubing served as a guide for the insertion of a 60 cc capacity latex balloon on a stiff polyethylene catheter (for pressure measurement), after which it was removed. Sufficient distilled water was injected into the balloon through the catheter to create 40 mm Hg. pressure within the ventricle as measured by the catheter.

<sup>\*</sup>Formula for blood bank Acid-Citrate-Dextrose solution (American Association of Blood Banks, 1974). Tri-Sodium Citrate 22.0 Gm; Citric Acid 8.0 Gm; Dextrose 24.5 Gm. Water for injection sufficient to make 1000 ml. (The formula was modified for our purpose by adding only enough water to make 150 ml.)

A Millar 1.33 mm diameter micro-tip pressure transducer (Model pc-340, Houston, Texas) was placed perpendicular to the epicardial surface one centimeter deep into the left anterior myocardium in an area perfused by the coronary cannula, using the following method. A site was carefully selected in order to avoid trauma to blood vessels, and a #17 Argyle Medicut (Aloe Medical, St. Louis, Mo.) needle was inserted one centimeter deep into the myocardium. The needle was then removed, leaving its plastic sheath in the needle track within the myocardium. The micro-tip transducer was placed in the myocardium through this sheath, after which the sheath was removed. This method assured minimal trauma to the myocardium and protection for the transducer during insertion. A clamp was placed on the transducer catheter to prevent its movement. The transducer was connected to a six channel Hewlett-Packard (7796 Model 1065C, Waltham, Mass.) direct writing oscillograph, and intramyocardial pressure (Pp) was continuously monitored.

Coronary artery perfusion pressure  $(P_i)$  was monitored through a #20 needle on a PE 60 catheter inserted into the rubber tubing leading from the pump, at its junction with the cannulating polyethylene tubing. Resistance in the polyethylene cannula downstream from the pressure monitoring needle was tested and found to be less than 1 mm Hg/80 cc/min blood flow. Coronary sinus outflow pressure  $(P_0)$  was monitored via a PE 60 catheter inserted into the coronary sinus through the coronary sinus cannula. All pressure cannulae were connected to Statham pressure transducers (Model P23 Gb, Hato Rey, Puerto Rico) and recorded on the oscillograph. Blood flow rate was monitored upstream from the pump by a

flow-through flow probe (BLC-2024-F10, 3/32" diameter) connected to a BL-610 Pulsed Logic Flowmeter (Biotronex Laboratory, Inc., Silver Spring, Md.), also coupled to the oscillograph.

Regional myocardial blood flow was measured by the radioactive microsphere method (Archie et al., 1973; Buckberg et al., 1971b; Domenech et al., 1969; and Rudolph and Heymann, 1967). Radioactive microspheres,  $15\mu$  diameter, labeled with  $^{46}$ Sc,  $^{85}$ Sr, and  $^{141}$ Ce were injected into the arterial line upstream from the pump, using special needles constructed to assure adequate mixing of microspheres. These needles were #20 size with closed tips and eight  $200\mu$  diameter side openings dispersed around the lower half of the needle. The steady state was maintained for 12 minutes following each injection. Injections were made at a low flow rate with  $P_e-P_o$  less than zero, and at a low and high flow rate with  $P_e-P_o$  greater than zero.

At the completion of the protocol, the tissue surrounding the micro-transducer was removed and depth of the micro-transducer verified. A one centimeter diameter cylinder of myocardium surrounding the micro-transducer was removed, sliced into three near equal thickness layers parallel to the epicardial surface, and each slice was cut in half across its diameter. The tissue samples were weighed, and the radio-activity of the samples was measured using the Searle 1185 series gamma counter. The energy windows used were <sup>46</sup>Sc, 700-1150 keV; <sup>85</sup>Sr, 464-564 keV; <sup>141</sup>Ce, 95-195 keV. Separation of the isotope peaks was accomplished using a preprogrammed Wang 800 series computer in the manner of Rudolf and Heymann (1967). Radioactivity was expressed as counts per minute

and blood flow was calculated from the following formula:

This generated a flow rate in ml/min/gm tissue. The total counts injected were determined by a pre-injection one minute count of the syringes. Following injection all waste (needle, syringes, centrifuge probe, and tubes) was counted and subtracted from the pre-injection count.

## Results and Discussion

This experiment is the first attempt to correlate diastolic intraventricular pressures with flow to a specific region of the myocardium where intramyocardial pressure is measured directly. Previously calculations of intramyocardial pressure have been made using data about the flow rate to concentric layers of the myocardium (Archie, 1975).

This heart preparation was accomplished without coronary air embolism nor ischemia. The rate of ACD perfusion was sufficient to stop the heart in hypocalcemic arrest and maximally dilate the perfused coronary vascular bed, as tested by a 30 second occlusion and the absence of a further fall in perfusion pressure. It was not enough to cause any detectable myocardial edema, as was reported by Archie and Brown (1974) in pilot experiments. Temporary discontinuation of the ACD solution before, during, and after the experimental protocol was completed resulted in ventricular fibrillation, and a rise in perfusion,

intramyocardial, and interventricular pressures. This was indicative of continued viability of the myocardium.

The catheter-tip micro-transducer used for the measurement of intramyocardial pressures is the smallest available commercially. Its use has not been recorded previously. It was developed to overcome the errors associated with fluid filled catheter systems. As such its response is rapid; it has a frequency response of 0 (dc) to 20 kHz and a natural frequency of 25 to 40 kHz. It can be easily calibrated to atmospheric pressure so that the pressures measured are not superimposed on any unknown diastolic intramyocardial pressure, as with the indirect methods. It is a linear device, accurate to within 0.5% of any range from -300 to +400 mm Hg., and is insensitive to catheter movement type artifacts. Placement of the transducer through the Medicut sheath was satisfactory to locate the micro-tip intramyocardial pressure transducer midway through the myocardium with minimal trauma to the tissue. We were unable to insert the transducer bluntly, without a prepared tunnel, as Kober and Scholtholt (1976) seemed to have done. Perhaps, in their technique, the transducer was inserted bluntly into the already prepared incision. Indentation of the epicardium upon such attempted blunt insertion significantly altered readings. In trying to draw the transducer across the myocardial wall from within the ventricular cavity, a transmural gradient was impossible to obtain. Apparently the indentation in the wall of the catheter for the sensor surface was catching on myocardial fibers and causing "tenting" of the surface of the myocardium, and high readings resulted. A larger surgical tunnel as used by Armour

and Randall (1971) would be necessary, but this technique may cause excessive trauma to the myocardial tissues.

Coronary sinus pressure ( $P_0$ ) remained stable at 7 mm Hg. throughout the experiment. Intramyocardial pressures ( $P_e$ ), although very low (10 mm Hg.), were responsive to changes in intraventricular pressures. Even at very low flow rates (3 cc/min) and zero intramyocardial pressure, perfusion pressure ( $P_i$ ) remained above 15 mm Hg.

Two microsphere injections were made at  $P_e^-P_0$  (intramyocardial pressure - coronary sinus pressure) = 3 mm Hg., and one injection was made at  $P_e^-P_0^-$  = -5 mm Hg. (Figure 14). At the lower pressure, the model predicts that coronary vessels should be maximally distended by blood flow, but at the higher pressure, the model predicts increased resistance to flow due to vascular collapse.

Since data is available for only one dog (Table 10), the data from this experiment cannot be generalized. The validity of the microsphere method for determination of blood flow is dependent upon statistical interpretation. However, these limited data indicate at very low flow rates (0.1 ml/min/gm of tissue)  $P_i$ - $P_o$ , and therefore, resistance, is increased in the presence of high pre-load during diastole. At higher pressures and flow rates, the sub-endocardium shows the highest blood flow to weight ratio and the ratio declines across the wall of the myocardium. Since the microvasculature here investigated was maximally dilated, a greater blood flow to weight ratio in the sub-endocardium indicates an increase in vascularity of that tissue as the mechanism of increased flow during diastole. This finding is in conflict with the

Figure 16. Simultaneously recorded intramyocardial pressure and regional blood flow of the maximally dilated left anterior descending coronary vascular bed during diastolic arrest.

∇ represents the sub-epicardial layer.

 $\Delta$  represents the middle layer.

Orepresents the sub-endocardial layer.

The dashed line represents the pressure-flow relationships as predicted by the waterfall model for  $P_e-P_o<0$ .

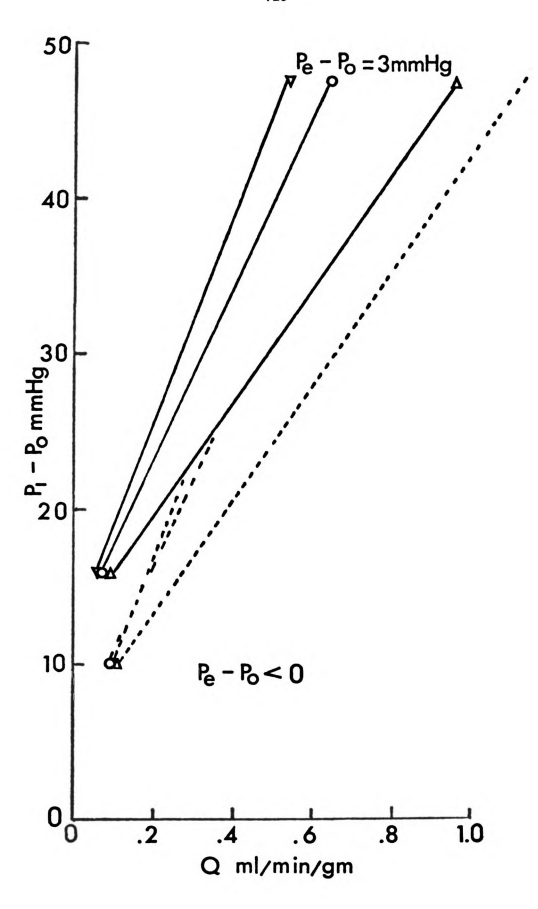


Table 10. Regional Intramyocardial Blood Flow and Simultaneously Recorded Intramyocardial Pressure

					Flow rate cc/sec/gm		
Pe-Po mm Hg	P <sub>i</sub> -P <sub>o</sub> mm Hg	P <sub>i</sub> mm Hg	P <sub>o</sub> mm Hg	P <sub>e</sub> mm Hg	Sub- epicardium	Middle layer	Sub- endocardium
3	48	55	7	10	0.54	0.65	0.98
3	16	23	7	10	0.09	0.05	0.05
-5	10	17	7	2	0.10	0.09	0.11

view of Moir and DeBra that increased flow during diastole is the result of lowered vascular tone. The dashed lines of the graph indicate the pressure-flow relationships when the intramyocardial pressure ( $P_e$ ) is less than coronary sinus pressure ( $P_o$ ), as the waterfall model predicts them. It can be seen that this model does not predict a decrease in sub-endocardial to sub-epicardial flow ratio when left ventricular pressure is increased, as L'Abbote et al. (1974) found. Nor is this prediction consistent with the findings of Archie and Brown (1974), that at high perfusion pressures, high pre-loads do not significantly decrease diastolic blood flow. Whether or not the predictions of the waterfall model are accurate for the myocardial microcirculation remains to be more thoroughly tested.

It is encouraging to note the internal consistency of the data from this experiment. The data points are reasonably close and do not reflect random scattering. In addition, they represent a reasonable approximation to generally accepted myocardial flow rates. The data of this experiment indicate that this experimental technique may be used for further quantification of pressure-flow relationships of the myocardial microcirculation.

